

# **Molecular Characterization of the Postsynaptic Density**

**Thesis by**

**Michelle Louise Apperson**

**In Partial Fulfillment of the Requirements**

**for the Degree of**

**Doctor of Philosophy**

**California Institute of Technology**

**Pasadena, CA**

**1996**

**(Submitted May 21, 1996)**

**To Ken and Lindsay**

## ACKNOWLEDGEMENTS

I have many people to thank for giving me a thoroughly enjoyable time as a graduate student at Caltech. First, I would like to give special thanks to my advisor, Mary Kennedy, for supporting my personal and educational growth over the last six years. Mary has been very tolerant of the amount of time I've spent outside the lab performing R.A. duties, taking care of my family, and commuting from Laguna Beach. I also thank Mary for giving me the freedom to design and carry out my own experiments and for keeping me on the right path when I needed guidance. Mary has been an inspirational role model for me because she is such a talented, honest, and hardworking scientist. I also appreciate the sacrifices made by Mary and the female scientists of her generation who forged a path in a male-dominated profession and made it easier for women like me to follow. Lastly, the respect and encouragement I received from Mary has given me a sense of confidence in my abilities as a scientist that will be a great asset in the years ahead.

I would also like to thank the other members of my committee, Bill Dunphy, Henry Lester, Erin Schuman, and Kai Zinn. They not only provided valuable suggestions about my project, but also inspired me with their excellent research. Additionally, I thank people in the Biology Department at Caltech for the open flow of information that was crucial to the success of my project.

Mary Kennedy's lab seems to be a magnet for nice people. In particular, I would like to thank Leslie Schenker for creating a great atmosphere in the lab with her genuineness and warmth, for her excellent expert assistance with immunocytochemistry, and for doing the rat perfusions and cell culturing for me. I would also like to thank Il-Soo Moon for his help during the initial stages of the project. Frank Asuncion provided excellent technical assistance in the purification of fusion proteins and has been a fun

person to have around the lab. Thanks to Melinda Kiely for all of our talks about science, babies, and major life decisions. Also, Kathleen Branson was a great help in preparing this manuscript. Additionally, I thank the past and present members of the lab that I have worked with and learned from.

My Caltech experience was made complete by friendships and experiences gained as an R.A. in Blacker House. I would like to thank the undergraduates for providing me with “varied and interesting conversation” and reminding me how much I really care about people. I also thank Kim West and the great group of R.A.’s for all of the fun times we had together.

Lastly, I would like to thank members of my family for their support. My parents deserve great thanks for giving me so much love and for saying, “you can do anything you set your mind to” throughout my life. I thank Ken and Lindsay for the beach trips, singing, laughter, and love that fill me with such joy. I would not have been able to balance working toward my Ph.D., being an R.A., and first-time motherhood without the enormous amount of support I received from my husband, Ken. A special thanks to my wonderful daughter, Lindsay, who makes my life complete with her big hugs and kisses at the end of a long day.

## ABSTRACT

The postsynaptic density (PSD) is an electron dense structure just beneath the postsynaptic membrane. Several functions have been proposed for the PSD including regulating receptor number and clustering, anchoring signal transduction molecules at the synapse and mediating adhesion between the presynaptic and postsynaptic membranes. However, little was known about the proteins that make up the PSD until the biochemical purification of a PSD fraction from brain was established in 1974. Since then, several interesting proteins have been localized to the PSD fraction. The most abundant PSD protein is the  $\alpha$  subunit of the type II calcium/calmodulin dependent protein kinase ( $\alpha$ CaMKII). This protein is likely to play a role in the calcium-mediated signal transduction at the synapse that mediates certain forms of synaptic plasticity. Another major PSD protein is PSD-95, a member of the guanylate kinase family (GUK) of proteins.

Here, I describe the purification and identification of three additional PSD proteins that comigrate at a molecular weight of 180 kDa on SDS-polyacrylamide gels. First, PSD-gp180 is identified as the 2B subunit of the N-methyl-D-aspartate receptor (NR2B). NR2B is a major component of the PSD fraction and binds to PSD-95 *in vitro*. This interaction may anchor NMDA receptors at the synapse.

Next, I report the cloning and characterization of densin-180, a 180 kDa PSD protein with a novel adhesion molecule-like sequence. Densin-180 is a brain-specific sialomucin that is enriched in the PSD fraction and localized to the synapse by immunocytochemistry.

In order to study the assembly of PSD proteins at the synapse, I use antibodies against  $\alpha$ CaMKII, PSD-95 and densin-180 for double labeling cultured hippocampal

neurons. In these cultures, densin-180 protein is the first marker to be expressed and this early densin-180 expression is in a diffuse membrane pattern along dendrites. When synapse formation begins at about 5 days after plating, the densin-180 protein is clustered at synapses and PSD-95 expression is induced. PSD-95 colocalizes with densin-180 clusters. The  $\alpha$ CaMKII protein is expressed later in synapse formation (7 to 9 days *in vitro*) and may be a marker of mature excitatory neurons.

In the brain, densin-180 is localized to the neuropil regions in a punctate pattern likely to represent synaptic staining. In addition, anti-densin-180 is localized to a specific set of cells and that may represent undifferentiated neurons and small processes that may represent dendritic filopodia.

The third 180 kDa PSD protein is citron, a recently identified Rho/Rac binding protein. The citron sequence contains numerous motifs found in signal transduction proteins and a myosin-like coiled coil domain. Citron may be a target for Rho/Rac-dependent signal transduction at the synapse and may mediate physical stabilization of the postsynaptic density.

**TABLE OF CONTENTS**

DEDICATION .....	ii
ACKNOWLEDGEMENTS .....	iii
ABSTRACT .....	v
TABLE OF CONTENTS .....	vii
LIST OF FIGURES .....	xii
Chapter 1. Introduction .....	1
Overview .....	2
Methods for studying neuronal function .....	2
Molecular mechanisms and synaptic plasticity .....	3
Structure of the CNS synapse .....	6
Proteins of the PSD fraction .....	7
Evidence of adhesion molecules at the synapse .....	10
Evidence of adhesion molecules in the synaptosome and PSD fractions .....	12
The LRR family of proteins .....	12
The sialomucin family of proteins .....	14
Adhesion mediated by the platelet glycoprotein Ib-IX complex .....	16
Summary .....	17
References .....	19
Figure legends .....	28
 Chapter 2. The Major Tyrosine-Phosphorylated protein in the postsynaptic density fraction is N-methyl-D-aspartate receptor subunit 2B	
Published as an article in Proc. Natl. Acad. Sci. U.S.A. 91 3954-3958 (1994) .....	38

Abstract .....	40
Introduction .....	42
Materials and methods .....	44
Purification of PSD-gp180 .....	44
Preparation of antibodies against the C-terminus of NR2B .....	44
Immunoblots with anti-NR2B and anti-phosphotyrosine .....	45
Immunoprecipitation .....	45
Analytical methods .....	46
Results .....	47
Purification of PSD-gp180 .....	47
Sequencing and identification of NR2B .....	47
Identification of NR2B by antibody binding .....	47
Reaction of NR2B with anti-phosphotyrosine antibodies .....	48
Enrichment of NR2B in the PSD fraction .....	49
Discussion .....	50
References .....	53

Chapter 3. Characterization of densin-180, a new brain-specific synaptic protein of  
the O-sialoglycoprotein family

In preparation for submission to the Journal of Neuroscience (1996) .....	64
Abstract .....	66
Introduction .....	67
Materials and methods .....	69
Purification of densin-180 and sequencing of tryptic peptides .....	69

Molecular cloning of densin-180 .....	69
Preparation of antibodies against densin-180 .....	71
Immunoblots .....	73
Subcellular fractions of rat brain .....	73
Deglycosylation with neuraminidase .....	74
Digestion of densin-180 with O-sialoglycoprotease .....	75
Phosphorylation and immunoprecipitation of densin-180 .....	75
Isolation of mRNA and Northern blotting .....	76
Immunocytochemical labeling of dissociated hippocampal neurons ..	77
Results .....	79
PCR cloning based on tryptic peptide sequences .....	79
Cloning and sequencing of full length densin-180 cDNAs .....	80
Domain structure of densin-180 .....	81
Densin-180 associates with the particulate fraction .....	83
Densin-180 is a sialoglycoprotein .....	84
Densin-180 is phosphorylated by CaM Kinase II .....	86
Densin-180 mRNA is detected only in brain .....	87
Densin-180 is highly enriched in PSD fractions .....	87
Densin-180 is located at synapses in dissociated hippocampal neurons .....	88
Discussion .....	90
References .....	97
Figure Legends .....	107

Chapter 4. The expression of densin-180 and other synaptic markers reveals an ordered assembly of postsynaptic density proteins during synapse formation in culture .....	122
Introduction .....	123
Materials and methods .....	125
Immunoblots of rat brain fractions .....	125
Immunofluorescent staining of dissociated hippocampal neuronal cultures .....	125
Controls for brightness and contrast settings in younger cultures .....	125
Results .....	127
Expression of the densin-180 protein increases during synaptogenesis in the brain .....	127
Densin-180 is highly expressed before synaptogenesis, then becomes clustered during synaptogenesis in dissociated hippocampal neurons .....	127
Clusters of densin-180 appear at early synapses in cultured hippocampal neurons double-labeled with synapsin I .....	128
Clusters of densin-180 staining at early synapses colocalize with PSD-95 .....	128
Induction of $\alpha$ CaMKII expression is not required for densin-180 cluster formation .....	129
Discussion .....	131
References .....	134
Figure legends .....	136

Appendix I. Characterization of the specificity of mouse and rabbit anti-densin-180	
antibodies .....	145
Figure legends .....	147
Appendix II. Brain immunocytochemistry using mouse and rabbit anti-densin-180	
antibodies .....	151
References .....	155
Figure legends .....	156
Appendix III. Identification of citron in the PSD fraction .....	160
Discussion .....	164
References .....	165
Figure legends .....	167

**LIST OF FIGURES****CHAPTER 1**

Figure 1.1. Serial electron micrographs through a dendritic spine .....	31
Figure 1.2. Electron micrographs of synaptosome and postsynaptic density fractions at different stages in the purification . .....	32
Figure 1.3. Protein composition of detergent-extracted PSD fractions .....	33
Figure 1.4. Electron micrographs of non-lysed and lysed synaptosomes .....	34
Figure 1.5. Structure of leucine-rich repeats .....	35
Figure 1.6. Summary of O-glycosylated membrane proteins and their interactions with selectins .....	36
Figure 1.7. Structure of GPIb $\alpha$ .....	37

**CHAPTER 2**

Table I. Peptides .....	59
Figure 1. Purification of PSD-gp180 .....	60
Figure 2. Reactions of proteins in the PSD fraction with anti-NR2B and anti- phosphotyrosine antibodies .....	61
Figure 3. Reaction of immunoprecipitated PSD-gp180 with anti-phosphotyrosine antibodies .....	62
Figure 4. Enrichment of PSD-gp180 in the PSD fraction .....	63

**CHAPTER 3**

Figure 1. Tryptic peptide sequences and PCR cloning of densin-180 .....	114
---	-----

Figure 2. Densin-180 cDNA sequence and protein translation .....	115
Figure 3. Domain structure of densin-180 .....	116
Figure 4. Solubility of densin-180 in brain membrane fractions .....	117
Figure 5. Densin-180 is a sialomucin .....	118
Figure 6. Densin-180 is phosphorylated by endogenous $\alpha$ CaMKII in the PSD fraction .....	119
Figure 7. Densin-180 mRNA expression is brain-specific and densin-180 protein is enriched in detergent-extracted PSD fractions .....	120
Figure 8. Immunocytochemical localization of densin-180 at synapses in dissociated hippocampal neurons .....	121
 CHAPTER 4	
Figure 4.1. Densin-180 expression is induced during synaptogenesis in the brain ..	139
Figure 4.2. Clusters of densin-180 staining form during synaptogenesis in cultured hippocampal neurons .....	140
Figure 4.3. Densin-180 and synapsin I staining during early synapse formation in culture .....	141
Figure 4.4. Densin-180 and PSD-95 staining during early synapse formation in culture .....	142
Figure 4.5. Densin-180 and $\alpha$ CaMKII staining during early synapse formation in culture .....	143
Figure 4.6. $\alpha$ CaMKII staining is absent from some neurons even after 14 days <i>in vitro</i> .....	144

## APPENDIX I

Figure I.1. M2 staining and pre-absorbed M2 staining of cultured hippocampal neurons at 9 days <i>in vitro</i> .....	148
Figure I.2. CT245 and pre-absorbed CT245 staining of cultured hippocampal neurons at 9 days <i>in vitro</i> .....	149
Figure I.3. M2 and CT245 anti-densin-180 double-labeling of cultured hippocampal neurons that were fixed after 14 days <i>in vitro</i> .....	150

## APPENDIX II

Figure II.1. Densin-180 and PSD-95 double-labeling of the molecular layer in the CA3 region of the hippocampus .....	157
Figure II.2. Densin-180 and PSD-95 double-labeling of the molecular layer in the CA1 region of the hippocampus .....	158
Figure II.3. Montage of two 63X images of CT245 anti-densin-180 staining in the CA1 region of the hippocampus .....	159

## APPENDIX III

Figure III.1. Amino acid sequences of four PSD-up180 tryptic peptides are identical to citron .....	169
Figure III.2. Comparison of the domain structures of citron and ROK $\alpha$ .....	170
Figure III.3. Sequence comparisons of Rho binding domains .....	171

# **CHAPTER 1**

## **Introduction**

**Overview**

In this introduction, I discuss the structure of the CNS synapse, proposed functions of the postsynaptic density (PSD), and methods used for the study of PSD proteins. My review of molecules involved in long-term potentiation is not extensive and is simply used to illustrate some of our motivations in studying PSD proteins. I only briefly mention the characterization of densin-180 because this is described in detail in Chapter 3. In the second part of the introduction, I provide a general overview of adhesion mediated by molecules that are similar to densin-180 and suggest that densin-180 may mediate similar mechanisms of adhesion at the synapse.

**Methods for studying neuronal function**

The study of brain function has exploded over the last 50 years with the discovery of new cell biological techniques. First, the advent of microscopy allowed scientists to view the fine structure of neurons. Electron microscopy in particular revealed many aspects of mechanisms by which the brain is put together and has contributed to a number of hypotheses about how neurons communicate. Electrophysiology has enabled the study of the electrical properties of neurons, absolutely essential to their function. The recent advances in molecular biology and biochemistry have enabled us to determine protein structures, even at the atomic level. More recently, genetic engineering techniques have allowed us to test individual protein functions by generating mouse mutants in these proteins and assaying the effects of the mutations. These methods can be particularly powerful when used in combination to study the nervous system.

The first synapse studied in detail was the neuromuscular junction. Electron microscopists first identified vesicles in the nerve terminals at synapses on muscle fibers.

They speculated that these vesicles might contain neurotransmitter that was released by the nerve to activate muscle contraction. Physiologists confirmed this hypothesis by proving that the neurotransmitter (acetylcholine) was released in quanta to induce a depolarizing current in the muscle fiber (Fatt and Katz, 1954). Other electrophysiologists were able to show that the postsynaptic response was mediated by ion flow through a neurotransmitter receptor. Similar methods were also used to identify an acetylcholine receptor (AChR) at the synapse and to show that this receptor is sensitive to  $\alpha$ -bungarotoxin, a toxin that causes muscle paralysis. The AChR was purified based on tight binding to alpha bungarotoxin and the primary structure was determined by biochemical and molecular genetic methods. More recently, a large number of molecules of the pre and postsynaptic specializations have been discovered and are thought to be involved in the formation and functioning of the neuromuscular junction (Reviewed in Fallon and Hall, 1994 and Froehner and Fallon, 1995).

### **Molecular mechanisms and synaptic plasticity**

The research of synaptic transmission in the central nervous system has recently become focused on the study of synaptic plasticity, in particular the form of synaptic plasticity called long-term potentiation (LTP). LTP is a mechanism by which an excitatory response of a neuron can be strengthened by prior high frequency stimulation to increase subsequent responses to low frequency stimulations. It is thought that neurons use this memory of prior stimulation to encode memory formation by the hippocampus. Despite the large number of labs studying LTP, there is no “unified hypothesis” about how it works. Rather, there has been much recent controversy over whether maintenance of LTP is a presynaptic or postsynaptic phenomenon (reviewed in Madison and Schuman, 1991

and Edwards, 1991).

Despite the controversy, there are two very nice examples of proteins that have been proven to play an important role in the generation of LTP. The NMDA-type glutamate receptor (NMDAR) has been shown to be essential for LTP by several criteria (see Collingridge, 1995 for review). First, the induction of LTP can be blocked by treating neurons with APV, a specific inhibitor of NMDARs (Morris et al., 1986).

Electrophysiological experiments revealed an interesting aspect of NMDAR regulation that is likely to mediate its role in LTP. At or near resting membrane potentials, NMDARs are inactive because magnesium blocks the pore of the channel, but at elevated membrane potentials, the magnesium block is weakened and the channels can open in response to ligand binding. Molecular cloning of the NMDAR subunits, followed by study of the receptor expressed in heterologous cells, confirmed their ability to conduct calcium in a voltage-dependent manner similar to the native receptor. Lastly, in the brain, certain memory enhancing drugs act by directly binding to NMDARs.

The second protein implicated in the formation of LTP is the type II  $\text{Ca}^{2+}$ -calmodulin dependent protein kinase (CaMKII). This kinase has been implicated in the generation of LTP in response to calcium entry through the NMDARs by a number of different approaches. First, elegant biochemical studies of the regulation of CaMKII identified a molecular mechanism that might underlie memory formation. CaMKII is normally dependent on calcium/calmodulin for activity. However, the autophosphorylated form of CaMKII has a high level of calcium-independent activity. Thus, CaMKII has the potential to become autophosphorylated upon calcium entry at the synapse and to stay active even after the calcium concentration returns to resting levels (Kennedy et al., 1990). This finding motivated several labs to investigate the role of CaMKII further. Malinow et

al., 1989 showed that addition of specific pseudosubstrates that inhibit CaMKII also block LTP. As additional evidence, transgenic mice were generated that lack the alpha subunit of CaMKII. These mice do not exhibit LTP and have some memory defects (for review, see Stevens et al., 1994).

In an elegant set of experiments, nitric oxide (NO) was implicated as a retrograde messenger important in the formation and maintenance of LTP at synapses in area CA1 of the hippocampus (for review, see Schuman and Madison, 1994). The cloning of three forms of nitric oxide synthase (NOS) that are activated by  $\text{Ca}^{2+}$ /calmodulin suggested that a form of NOS might be located in the postsynaptic compartment and produce NO in response to calcium influx through glutamate receptors. However, the isoform of NOS first termed the “neuronal” NOS (nNOS) did not appear to be localized at synapses in area CA1 of the hippocampus by immunocytochemistry. Additionally, a mouse knockout mutant missing the neuronal NOS did not show a defect in LTP (Huang et al., 1993). More recently, the isoform of NOS first termed the “endothelial” NOS (eNOS) has been found to be expressed in high concentration in CA1 pyramidal neurons. However, the only defect reported in the mouse knockout mutant missing the “endothelial” form of NOS is high blood pressure (Huang et al., 1995). One possibility is that eNOS and nNOS have somewhat redundant functions in CA1 neurons. Another possibility is that the expression of one form of NOS is induced to compensate for the loss of the other isoform. Double mouse mutants that lack both forms of NOS may clarify these issues.

The above examples illustrate the power of structural studies of the synapse that complement pharmacological and physiological studies. My research has been motivated in part by the need to identify the full complement of proteins located at the synapse in order to more fully understand the mechanisms that underlie synaptic plasticity.

### **Structure of the CNS synapse**

Examination of the brain by electron microscopy resulted in the identification of a synaptic structure that is reminiscent of the synapse at the neuromuscular junction. A compact presynaptic terminal contains small, clear vesicles that have been shown to contain neurotransmitters. Neurotransmitter receptors are believed to be clustered in the postsynaptic membrane apposed to the presynaptic terminal and separated from the presynaptic membrane by a uniform synaptic cleft containing electron dense material. However, unlike the neuromuscular junction, the synapse in the central nervous system (CNS) has a unique postsynaptic specialization known as a spine. This synapse is characterized by a spiny postsynaptic protrusion from the dendritic shaft that meets the axon terminal. The spine has the potential to compartmentalize proteins and molecules necessary for synaptic transmission and/or regulation of the synapse structure (see Harris and Kater, 1994). Recent evidence suggests that differences in spine morphology may underlie the ability of neurons to exhibit LTP (Harris et al., 1992).

Excitatory synapses in the CNS are characterized by a particularly large, dense thickening just beneath the postsynaptic membrane, termed the postsynaptic density. Figure 1.1 shows an electron micrograph of serial thin sections through a single synapse in the hippocampus. This figure highlights the tight correlation between the presence of docked vesicles at the presynaptic membrane and the thick PSD underneath the postsynaptic membrane, suggesting a high degree of coordination between protein assemblies at the pre and postsynaptic membranes (Harris and Sultan, 1995). Based entirely on pictures like these, early electron microscopists proposed several functions for the PSD, including regulation of adhesion between the presynaptic and postsynaptic

membranes, anchoring of neurotransmitter receptors at the postsynaptic membrane, and maintenance of the structure of the synapse.

### **Proteins of the PSD fraction**

In 1974, Cotman et al. first developed a procedure for purifying a subcellular fraction termed the PSD fraction. Cohen et al. (1977) modified the original preparation by developing a protocol that used milder detergent extraction and resulted in higher recovery of PSD protein. Essentially, the PSD fraction is purified by centrifugation after detergent extraction of synaptosomes prepared from brain homogenates. During homogenization of brain tissue, the PSD remains attached to synaptosomes probably via adhesion molecules that cross the synaptic junction. The detergent Triton-X100 (0.5%) dissolves synaptosomal membranes and a subsequent pelleting of the insoluble fraction gives purified PSDs, relatively free of presynaptic membranes. The structures that are enriched by this purification have a morphology similar to that of intact brain PSDs viewed in the electron microscope (Figure 1.2). The remarkable similarity between the structures of the brain PSD and the PSD fraction suggests that this fraction is made up of the same set of protein components as the PSD in the brain. This biochemical purification has enabled our lab and others to identify individual proteins in the PSD.

The first labs to work with the PSD fraction used antibodies to characterize a number of major proteins such as fodrin, actin and tubulin. More recently, labs have used antibodies against known proteins to identify the AMPA-type glutamate receptor, GluR1, and an “A-kinase anchoring protein” as (albeit minor) components of the PSD fraction (Rogers et al., 1991 and Carr et al., 1992). There are many other proteins reported in the literature that are associated with the PSD fraction, but are not necessarily enriched in the

PSD fraction over other membrane fractions.

There have been two approaches used to identify novel proteins in the PSD fraction. In one approach, antibodies against the fraction are generated and cDNA clones are obtained by screening expression libraries. This method has been of limited use because it results in a high rate of false positives at several steps. For example, the immunization of mice with total PSD proteins selects for the most antigenic and not necessarily the most abundant proteins. Thus, it may target proteins that are minor contaminants of the PSD fraction. Also, expression library screening usually results in a number of false positives. Nonetheless, this approach does have the potential to identify relatively minor proteins in the PSD fraction that are associated with the synapse *in vivo* and have important functions. Proteins that have been identified in the PSD fraction using this method include SAP-97 (Muller et al., 1995) and dynamin (Walsh and Kuruc, 1992).

A second approach to identify novel PSD proteins involves direct microsequencing and cloning of proteins from the PSD fraction. A common criticism of the use of the PSD fraction to determine its structural components is that non-PSD proteins may adhere to the PSD during homogenization. Our lab has determined that many of these nonspecifically bound, non-PSD proteins are likely to be removed by additional detergent washes. For example, I identified a 110 kDa protein in the PSD fraction that is extracted by N-octyl glucoside as hexokinase, a mitochondrial enzyme and probably a contaminant of the PSD preparation (Apperson and Kennedy, 1993). Many proteins can be removed from the PSD fraction purified by one extraction with Triton-X100 followed by an extraction with the relatively harsh detergent N-lauroyl sarcosinate (sarcosyl), originally used by the Cotman lab in their purification of the PSD fraction. We refer to the proteins that remain in the insoluble pellet after sarcosyl extraction as “core” proteins. Our recent work suggests

that they are likely to be important structural components of the PSD (Figure 1.3). For example, the  $\alpha$  subunit of CaMKII is enriched in the “core” fraction and has also been localized to the PSD by immuno-electron microscopy (Kennedy et al., 1990). Because of results like these, we have decided that we would increase our chance of identifying “real” components of the PSD by directly sequencing proteins that remain in the PSD fraction after multiple detergent extractions.

Our laboratory has used this technique to identify two proteins that are tightly associated with the PSD fraction. The first is PSD-95 (Cho et al., 1992), a novel brain-specific protein with significant homology to the *Drosophila* discs-large protein (*dlg*, Woods and Bryant, 1991). The Cho et al. paper first identified three repeats in PSD-95 and *dlg* that are now called PDZ domains (Kennedy, 1995). Like the  $\alpha$  subunit of CaMKII, PSD-95 has been localized to the PSD by immuno-electron microscopy of synaptosomes (Hunt et al., 1996). The second protein we identified is the 2B subunit of the NMDA receptor, which we showed is the major tyrosine-phosphorylated protein in the PSD fraction (Moon et al., 1994). Both PSD-95 and NR2B remain associated with the sarcosyl-extracted PSD fraction. Recently, (Kornau et al., 1995) used a yeast two-hybrid screen to select proteins that associate with the unique C-terminal domains of the NMDA receptor type 2 subunits. This screen identified PSD-95 as a protein interacting with the “bait.” The interacting regions of the two proteins were identified as the second PDZ domain of PSD-95 and the terminal seven or so amino acids of the NR2 subunits, all of which are homologous and comprise a motif termed tSXV (terminal SXV). Additionally, we have shown that NR2B and PSD-95 colocalize at synapses in dissociated hippocampal neuronal cultures. This specific and tight association may reflect a mechanism for clustering NMDA receptors in the postsynaptic membrane, one of the initial proposed

functions of the PSD.

Thus, I decided to probe further the function of the PSD through the molecular characterization of proteins in the PSD fraction. Since the time that I began my thesis work, our lab and others have identified likely candidates in the PSD fraction for receptor clustering (NR2B/PSD-95), signal transduction (CaMKII) and structural elements (dystrophin, fodrin, tubulin and actin), but no strong candidates for adhesion molecules.

### **Evidence of adhesion molecules at the synapse**

Adhesion between presynaptic and postsynaptic membranes is another proposed function of the PSD that remains to be tested. Most of what we know about adhesion molecules in the nervous system comes from studies of neurite outgrowth and axon pathfinding during development. The majority of adhesion molecules involved in these processes fall into three classes: the immunoglobulin (Ig) superfamily, the cadherin family, and the integrin family of proteins. The Ig and cadherin families are thought to promote adhesion between neurons by homophilic interactions whereas the integrin family promotes adhesion by binding to extracellular matrix molecules.

At the synapse, a dense-staining material fills the synaptic cleft and has been proposed to contain adhesion and extracellular matrix molecules. There is a very tight correlation between sites of vesicle docking at the presynaptic membrane and sites of thick postsynaptic densities beneath the postsynaptic membrane. This specificity of interaction between axon terminal and dendritic spine suggests a heterophilic recognition between a presynaptically expressed adhesion molecule and a postsynaptic partner. However, despite the considerable indirect evidence for adhesion molecules in the synaptic cleft, little is known about the primary structure of proteins that reside there.

One possible protein pair located in the synaptic cleft is the neurexin/neuroligin binding pair. Neurexins are a large family of related proteins that were identified as receptors for  $\alpha$ -latrotoxin, a toxin that binds to presynaptic nerve terminals and triggers massive transmitter release (Ushkaryov et al., 1992). Neurexins contain extracellular EGF repeats and laminin A-like domains as well as a single serine/threonine-rich domain that may serve as an attachment site for O-linked sugars. Immunofluorescent labeling of neurexin in the brain has shown that it colocalizes with the synaptic marker synaptophysin. The neuroligins have been identified as specific binding partners for some forms of neurexins and are enriched in brain synaptic membrane fractions (Ichtchenko et al., 1995, and Ichtchenko et al., 1996). Neuroligins are transmembrane proteins that contain an esterase domain and a potential O-linked sugar attachment site in the extracellular region of the protein.

At least two other adhesion molecules have been reported to be localized at synapses by electron microscopy. First, a monoclonal antibody to the extracellular domain of N-cadherin densely stains the synaptic cleft in the developing optic tectum (Yamagata et al., 1995). However, poor tissue preservation in these sections raises the possibility of nonspecific staining. Second, an antibody specific for the 180 kDa form of N-CAM (N-CAM 180) has been reported to stain approximately 30 to 40 % of all postsynaptic densities in fixed brain tissue (Persohn et al., 1989). However, the N-CAM 180 protein is not enriched in PSD fractions, indicating that the synaptic N-CAM may not form detergent-resistant bonds with proteins of the PSD fraction. In both of these studies, bound antibodies were detected with a horseradish peroxidase reaction product that can precipitate artifactually on the postsynaptic density and membranes, and is very similar to the normal electron-dense appearance of PSDs.

### **Evidence of adhesion molecules in the synaptosome and PSD fractions**

Electron micrographs of non-lysed and lysed synaptosomes show a loss of some of the densely staining cleft material present in the intact brain, suggesting that some of the extracellular matrix or adhesion molecules spanning the cleft may be lost during homogenization of the brain. In certain sections it is possible to discern thin “threads” of electron-dense material joining the pre and postsynaptic membranes (highlighted in Figure 1.4 with transparent yellow lines). In Chapter 3, I describe the cloning of a novel adhesion molecule-like protein from the PSD fraction that we have named densin-180. Densin-180 contains an arrangement of domains found in other adhesion molecules, most notably, leucine rich repeats (LRRs) and an O-sialomucin domain. Not only is this the first molecule of its kind cloned from mammalian brain, it is also the first potential adhesion molecule directly identified as enriched in the PSD fraction. Perhaps proteins in other systems that contain similar adhesion motifs can provide clues about a mechanism of adhesion mediated by densin-180 at the synapse.

### **The LRR family of proteins**

The leucine-rich-repeat family contains a large number of proteins with a wide range of functions, including cell adhesion, signal transduction, and gene expression. The leucine-rich repeats (LRRs) of different proteins vary in length from 20 to 29 amino acids, with 24 the most common. The only generalization that can be made about the function of LRRs in this family of proteins is that the LRR region forms specific, tight interactions with binding partners. The recent crystal structure of ribonuclease inhibitor (RI) bound to ribonuclease A provides a structural basis for this general function of LRR domains (Kobe

and Deisenhofer, 1995). Ribonuclease inhibitor is made up almost entirely of leucine-rich repeat units that form a  $\beta$ - $\alpha$  structure. This structure is horseshoe-shaped and binds RNase along the concave surface formed by the  $\beta$ -sheets of the LRR (see Figure 1.5A). When the inhibitor is bound to it, the RNase surface is no longer accessible to the solvent. RI changes its conformation upon binding RNase by an elastic alteration of the entire structure that appears to rely on the flexibility of the LRR repeats. This flexibility is likely to be important for the tight protein-protein binding between RI and RNase ( $K_i$  of  $6.7 \times 10^{-14}$  M).

The LRRs of RI are among the longest in the family (28-29 residues). Nevertheless, based upon the crystal structure of RI, Kajava et al., 1995, generated a model of the three-dimensional structure of the more typical 24 residue LRRs of the ligand binding domain of the thyrotropin receptor (TSHR). They constructed their model based upon a consensus sequence generated from proteins with more typical 20-24 amino acid LRRs. The predicted structure of the 8 LRRs in TSHR has a less curved structure than the LRRs of RI due to the shorter  $\alpha$  helices and slightly different conformations of the  $\alpha$ - $\beta$  and  $\beta$ - $\alpha$  connecting loops (Figure 1.5B). This confirmation also predicts a larger surface area available for ligand binding.

Cell surface proteins make up the largest subfamily of LRR proteins. Some LRR-receptors are thought to bind ligand via their LRR domains to mediate signal transduction in the cytosol. Examples include the trophic factor receptors trk and trk B (Schneider and Schweiger, 1991), as well as the plant receptor serine/threonine kinase protein TMK1 (Chang et al., 1992). Other LRR glycoproteins are involved in adhesion. For example, chaoptin is a PI linked protein that was identified as a surface protein in the

developing imaginal eye disc and adult eye of *Drosophila*. Choptin mediates homophilic adhesion *in vitro* (Krantz and Zipursky, 1990). Lastly, some of the LRR glycoproteins have potential roles in both adhesion and signal transduction. The transmembrane receptor, toll, was identified as a *Drosophila* gene involved in establishing the dorsal-ventral body axis (Hashimoto et al., 1988). The extracellular domain of toll contains a large number of LRRs and the cytoplasmic region contains an interleukin-1 (IL-1) domain. Toll has been shown to promote heterotypic cell adhesion (Keith and Gay, 1990) and may mediate signal transduction through the IL-1 domain.

There is some evidence that LRR molecules are important in the development of the nervous system. Most of this evidence comes from genetic studies of *Drosophila* development in which several LRR-containing proteins have been implicated in axon pathfinding and target specificity (reviewed in Hortsch and Goodman, 1991). Connectin is a PI-linked adhesion molecule that mediates homotypic adhesion *in vitro* and is expressed both on motoneuron axons and on the target muscles they innervate (Meadows et al., 1994). Only a few LRR-containing proteins have been identified in mammalian neurons. They include the oligodendrocyte-myelin glycoprotein (Mikol et al., 1990) and a new protein, NLRR-3 (Taniguchi et al., 1996). However, a role for these proteins in adhesion has not been established.

### **The sialomucin family of proteins**

A new subfamily of glycoproteins has been recognized that contains mucin-like regions in the extracellular domains (reviewed in Strous and Dekker, 1992). The O-linked glycosyl groups attached to these domains often contain large amounts of sulfates or sialic acid that are necessary for protein function. These mucins are either secreted or

membrane-bound. Secreted mucins can form a protective gel on the surface of some cell types. For example, the mucous layer in the intestine is composed largely of secreted mucins that act as a selective barrier to diffusion.

Membrane proteins that contain mucin domains have also been well characterized. CD34 and CD43 are examples of sialoglycoproteins that are involved in cell signaling in the immune system. These proteins have a role in the normal growth and differentiation of stem cells into mature leukocytes. In carcinoma cells, epiglycanin, epitectin and ascites sialoglycoprotein-1 are sialomucins that may be involved in the progression of cancer.

In the nervous system, a number of proteins have been described with mucin-like serine/threonine rich domains that are potential sites of O-glycosylation. Indirect evidence indicates that neurexins are sialomucins because they contain a mucin-like sequence and are sensitive to neuraminidase and O-glycanase digestion. Neuroligins also have a number of clustered serines and threonines, but their glycosylation has not been studied.

Sialoglycoproteins that are expressed in the brain include the cellular prion protein (Oesch et al., 1985) and cranin, a brain form of alpha-dystroglycan (Smalheiser and Kim, 1995).

The O-linked sugar domains in these and other proteins have been proposed to mediate several different functions. First, mucins contribute to the formation of a protective layer on the surface of cells that repels other proteins and cells. For example, the glycocalyx is composed entirely of mucins that form a protective surface extending 100 Angstroms from the erythrocyte membrane (Viitala and Jarnefelt, 1985). Next, the mucin domain of CD43 has been shown to form an extended rod-like structure and similar domains in other proteins have been proposed to function by extending a binding domain into the extracellular space (reviewed in Jentoft, 1990). Lastly, the O-linked sugars serve as a site for specific transient binding by a new family of adhesion proteins, the selectins

(summarized in Figure 1.6).

Selectins specifically interact with carbohydrates in a calcium-dependent manner through a C-type lectin domain (reviewed in Cummings and Smith, 1992). There are three known members of this family, P-selectin, E-selectin, and L-selectin (found in platelets, endothelial cells and leukocytes, respectively). Selectins mediate the adhesion responsible for cell rolling during the inflammation response. During inflammation, leukocytes are recruited from the circulating blood by binding to the surface of the blood vessel wall. The phenomenon of rolling occurs in conditions of high shear force because transient contacts are made with endothelial cells of the blood vessel. The selectins are thought to mediate these transient contacts by the rapid formation and dissociation of bonds with a specific ligand on the blood vessel. The high on and off rates of these interactions are not only important for function of these molecules in transient adhesion, but are also responsible for the overall low affinities reported for selectin interactions ( $K_d$  of  $10^{-4}$  M has been reported for E-selectin binding to carbohydrate in van der Merwe and Barclay, 1994).

### **Adhesion mediated by the platelet glycoprotein Ib-IX complex**

The platelet glycoprotein Ib-IX complex also mediates adhesion in conditions of high shear forces generated in the blood (reviewed in Williams et al., 1995 and Roth, 1991). GPIb $\alpha$  is the largest member of this complex and binds to von Willebrand factor to mediate adhesion of platelets to the blood vessel wall. Ligand binding is mediated through an extracellular N-terminal LRR domain (Figure 1.7A). The LRR domain is followed by a sialomucin domain that extends the ligand binding domain from the cell surface. On the cytoplasmic side, GPIb $\alpha$  binds to actin binding protein (ABP) and may mediate

cytoskeletal rearrangement in response to ligand binding on the surface. Von Willebrand factor (vWF) binding to GPIIb $\alpha$  initiates a series of signal transduction events such as phospholipid metabolism, activation of protein kinases, and elevation of cytoplasmic calcium. The binding of vWF to GPIIb $\alpha$  ( $K_d$  of 1.2 nM; from Meyer et al., 1993) is likely to involve high rates of association and dissociation and be resistant to tensile stress. Interestingly, platelets move slowly along the surface of immobilized von Willebrand factor in the presence of high shear forces in a manner reminiscent of leukocyte cell rolling on the endothelium (Savage et al., 1996).

Analysis of the GPIIb complex by electron microscopy reveals a rod-like structure corresponding to the mucin domain of GPIIb $\alpha$  that connects the globular ligand binding and cytoplasmic domains (Figure 1.7B) (Fox et al., 1988). This domain is similar to the mucin domain of CD43 that extends to 2.5 Angstroms per residue (Cyster et al., 1991).

## **Summary**

In this thesis, I describe the characterization of densin-180, a brain protein that contains both leucine-rich and sialomucin domains and may mediate adhesion at the synapse via mechanisms that are similar to GPIIb $\alpha$  adhesion. Based on the structure of CD43, the 80 amino acid mucin domain of densin-180 has the potential to extend 20 nm from the surface of the cell. At the synapse, the filamentous structures that extend the 10 to 20 nm between the pre and postsynaptic membranes may correspond to the sialomucin domain of densin-180. By analogy with the adhesion mediated by GPIIb $\alpha$ , the adhesion mediated by densin-180 might be expected to withstand the shear forces generated during the brain homogenization used to make synaptosome and PSD fractions. Additionally, the

type of transient and specific adhesion that has been described for GPIb $\alpha$  could be used by densin-180 to mediate the dynamics of neurite outgrowth, synapse formation and synaptic plasticity in the brain.

**REFERENCES**

- Apperson, M. L., and Kennedy, M. B. (1993). The detergent-extractable portion of the postsynaptic density fraction contains a rat brain hexokinase. *Caltech Biology Annual Report*, 215.
- Carr, D. W., Stofdo-Hahn, R. E., Fraser, I. D. C., Cone, R. D., and Scott, J. D. (1992). Localization of the cAMP-dependent protein kinase to the postsynaptic densities by A-Kinase Anchoring Proteins. *J. Biol. Chem.* 267, 16816-16823.
- Chang, C., Schaller, G. E., Patterson, S. E., Kwok, S. F., Meyerowitz, E. M., and Bleecker, A. B. (1992). The TMK1-gene from arabidopsis codes for a protein with structural and biochemical characteristics of a receptor protein-kinase. *Plant Cell* 4, 1263-1271.
- Cho, K.-O., Hunt, C. A., and Kennedy, M. B. (1992). The rat brain postsynaptic density fraction contains a homolog of the *Drosophila* discs-large tumor suppressor protein. *Neuron* 9, 929-942.
- Cohen, R. S., Blomberg, F., Berzins, K., and Siekevitz, P. (1977). The structure of postsynaptic densities isolated from dog cerebral cortex I. overall morphology and protein composition. *J. Cell Biol.* 74, 181-203.
- Collingridge, G. L. (1995). Memories of NMDA receptors and LTP. *TINS* 18, 54-56.

Cotman, C. W., Banker, B., Churchill, L., and Taylor, D. (1974). Isolation of postsynaptic densities from rat brain. *J. Cell Biol.* *63*, 441-455.

Cummings, R. D., and Smith, D. F. (1992). The selectin family of carbohydrate-binding proteins: structure and importance of carbohydrate ligands for cell adhesion. *BioEssays* *14*, 849-856.

Cyster, J. G., Shotton, D. M., and Williams, A. F. (1991). The dimensions of the lymphocyte-T glycoprotein leukosialin and identification of linear protein epitopes that can be modified by glycosylation. *EMBO J.* *10*, 893-902.

Edwards, F. (1991). Neurobiology - LTP is a long-term problem. *Nature* *350*, 271-272.

Fallon, J. R., and Hall, Z. W. (1994). Building synapses: agrin and dystroglycan stick together. *TINS* *17*, 469-473.

Fatt, P., and Katz, B. (1954). Spontaneous subthreshold activity at motor nerve endings. *J. Physiol.* *117*, 109-128.

Fox, J. E. B., Aggerbeck, L. P., and Berndt, M. C. (1988). Structure of the glycoprotein Ib-IX complex from platelet membranes. *J. Biol. Chem.* *263*, 4882-4890.

Froehner, S. C., and Fallon, J. R. (1995). Synapses take the rap. *Nature* *377*, 195-196.

Harris, K. M., Jensen, F. E., and Tsao, B. (1992). Three-dimensional structure of dendritic spines and synapses in rat hippocampus (CA1) at postnatal day 15 and adult ages: implications for the maturation of synaptic physiology and long-term potentiation. *J. Neurosci.* *12*, 2685-2705.

Harris, K. M., and Kater, S. B. (1994). Dendritic spines: cellular specializations imparting both stability and flexibility to synaptic function. *Ann. Rev. Neurosci.* *17*, 341-371.

Harris, K. M., and Sultan, B. (1995). Variation in the number, location and size of synaptic vesicles provides an anatomical basis for the nonuniform probability of release at hippocampal CA1 neurons. *Neuropharm.* *34*, 1387-1395.

Hashimoto, C., Hudson, K. L., and Anderson, K. V. (1988). The Toll gene of drosophila, required for dorsal-ventral embryonic polarity, appears to encode a transmembrane protein. *Cell* *52*, 269-279.

Hortsch, M., and Goodman, C. S. (1991). Cell and substrate adhesion molecules in drosophila. *Annu. Rev. Cell Biol.* *7*, 505-557.

Huang, P. L., Dawson, T. M., Bredt, D. S., Snyder, S. H., and Fishman, M. C. (1993). Targeted disruption of the neuronal nitric oxide synthase gene. *Cell* *75*, 1273-1286.

Huang, P. L., Huang, Z. H., Mashimo, H., Bloch, K. D., Moskowitz, M. A., Bevan, J. A.,

and Fishman, M. C. (1995). Hypertension in mice lacking the gene for endothelial nitric-oxide synthase. *Nature* 377, 239-242.

Hunt, C. A., Schenker, L. J., and Kennedy, M. B. (1996). PSD-95 is associated with the postsynaptic density and not with the presynaptic membrane at forebrain synapses. *J. Neurosci* 16, 1380-1388.

Ichtkenko, K., Hata, Y., Nguyen, T., Ullrich, B., Missler, M., Moomaw, C., and Südhof, T. C. (1995). Neuroligin 1: a splice site-specific ligand for  $\beta$ -Neurexins. *Cell* 81, 435-443.

Ichtkenko, K., Nguyen, T., and Südhof, T. C. (1996). Structures, alternative splicing, and neurexin binding of multiple neuroligins. *J. Biol. Chem.* 271, 2676-2682.

Jentoft, N. (1990). Why are proteins O-glycosylated? *TIBS* 15, 291-294.

Kajava, A. V., Vassart, G., and Wodak, S. J. (1995). Modeling of the three-dimensional structure of proteins with the typical leucine-rich repeats. *Structure* 3, 867-877.

Keith, F. J., and Gay, N. J. (1990). The drosophila membrane-receptor toll can function to promote cellular adhesion. *EMBO J.* 9, 4299-4306.

Kennedy, M. B., Bennett, M. K., Bulleit, R. F., Erondy, N. E., Jennings, V. R., Miller, S. M., Molloy, S. S., Patton, B. L., and Schenker, L. J. (1990). Structure and regulation of type II calcium/calmodulin-dependent protein kinase in central nervous system neurons. *C.*

S. H. S. Q. B. 55, 101-110.

Kennedy, M. B. (1995). Origin of PDZ (DHR, GLGF) domains. *TIBS* 20, 350.

Kobe, B., and Deisenhofer, J. (1995). A structural basis of the interactions between leucine-rich repeats and protein ligands. *Nature* 374, 183-186.

Kornau, H.-C., Schenker, L. T., Kennedy, M. B., and Seeburg, P. H. (1995). Domain interaction between NMDA receptor subunits and the postsynaptic density protein PSD-95. *Science* 269, 1737-1740.

Krantz, D. E., and Zipursky, S. L. (1990). *Drosophila* chaoptin, a member of the leucine-rich repeat family, is a photoreceptor cell-specific adhesion molecule. *EMBO J.* 9, 1969-1977.

Madison, D. V., and Schuman, E. M. (1991). LTP, Post or Pre - a look at the evidence for the locus of long-term potentiation. *New Biologist* 3, 549-557.

Malinow, R., Schulman, H., and Tsien, R. W. (1989). Inhibition of post-synaptic PKC or CaMKII blocks induction but not expression of LTP. *Science* 245, 862-866.

Meadows, L. A., Gell, D., Broadie, K., Gould, A. P., and White, R. A. H. (1994). The cell adhesion molecule, connectin, and the development of the *drosophila* neuromuscular system. *J. Cell Sci.* 107, 321-328.

Meyer, S., Gundula, K., Haring, P., Schumpp-Vonach, B., Clemetson, K. J., Hadvary, P., and Steiner, B. (1993). Expression and characterization of functionally active fragments of the platelet glycoprotein (GP) Ib-IX complex in mammalian cells. *J. Biol. Chem.* 268, 20555-20562.

Mikol, D. D., Gulcher, J. R., and Stefansson, K. (1990). The oligodendrocyte myelin glycoprotein belongs to a distinct family of proteins and contains the HNK-1 carbohydrate. *J. Cell Biol.* 110, 471-479.

Moon, I. S., Apperson, M. L., and Kennedy, M. B. (1994). The major tyrosine-phosphorylated protein in the postsynaptic density fraction is N-methyl-D-aspartate receptor subunit 2B. *Proc. Natl. Acad. Sci. USA* 91, 3954-3958.

Morris, R. G. M., Anderson, E., Lynch, G. S., and Baudry, M. (1986). Selective impairment of learning and blockade of long-term potentiation by an N-methyl-D-aspartate receptor antagonist AP5. *Nature* 319, 774-776.

Muller, B. M., Kistner, U., Veh, R. W., Caseslanghoff, C., Becker, B., Gundelfinger, E. D., and Garner, C. C. (1995). Molecular characterization and spatial-distribution of SAP97, a novel presynaptic protein homologous to SAP90 and the drosophila disks-large tumor-suppressor protein. *J. Neurosci.* 15, 2354-2366.

Oesch, B., Westaway, D., Walchli, M., McKinley, M. P., Kent, S. B. H., and Aebersold,

R. (1985). A cellular gene encodes scrapie PrP 27-30 protein. *Cell* 40, 735-746.

Persohn, E., Pollerberg, G. E., and Schachner, M. (1989). Immunoelectron-microscopic localization of the 180 kD component of the neural cell adhesion molecule N-CAM in postsynaptic membranes. *J. Comp. Neurol.* 288, 92-100.

Rogers, S. W., Hughes, T. E., Hollmann, M., Gasic, G. P., Deneris, E. S., and Heinemann, S. (1991). The characterization and localization of the glutamate receptor subunit GluR1 in the rat brain. *J. Neurosci.* 11, 2713-2724.

Roth, G. J. (1991). Developing relationships: arterial platelet adhesion, glycoprotein Ib, and leucine-rich glycoproteins. *Blood* 77, 5-19.

Savage, B., Saldívar, E., and Ruggeri, Z. M. (1996). Initiation of platelet adhesion by arrest onto fibrinogen or translocation on von Willebrand factor. *Cell* 84, 289-297.

Schneider, R., and Schweiger, M. (1991). A novel modular mosaic of cell adhesion motifs in the extracellular domains of the neurogenic trk and trkB tyrosine kinase receptors. *Oncogene* 6, 1807-1811.

Schuman, E. M., and Madison, D. V. (1994). Nitric oxide and synaptic function. *Annu. Rev. Neurosci.* 17, in the press.

Smalheiser, N. R., and Kim, E. (1995). Purification of cranin, a laminin binding

membrane protein. *J. Biol. Chem.* 270, 15425-15433.

Springer, T. A. (1994). Traffic signals for lymphocyte recirculation and leukocyte emigration - the multistep paradigm. *Cell* 76, 301-314.

Stevens, C. F., Tonegawa, S., and Wang, Y. (1994). The role of calcium-calmodulin kinase II in 3 forms of synaptic plasticity. *Current Biol.* 4, 687-693.

Strous, G. J., and Dekker, J. (1992). Mucin-type glycoproteins. *Crit. Rev. Biochem.* 27, 57-92.

Taniguchi, H., Tohyama, M., and Takagi, T. (1996). Cloning and expression of a novel gene for a protein with leucine-rich repeats in the developing mouse nervous system. *Molec. Brain. Res.* 36, 45-52.

Ushkaryov, Y. A., Petrenko, A. G., Geppert, M., and Südhof, T. C. (1992). Neurexins: synaptic cell surface proteins related to the  $\alpha$ -latrotoxin receptor and laminin. *Science* 257, 50-55.

van der Merwe, P. A., and Barclay, A. N. (1994). Transient intercellular adhesion: the importance of weak protein-protein interactions. *TIBS* 19, 354-358.

Viitala, J., and Jarnefelt, J. (1985). The red-cell surface revisited. *TIBS* 10, 392-395.

Walsh, M. J., and Kuruc, N. (1992). The postsynaptic density: constituent and associated proteins characterized by electrophoresis, immunoblotting, and peptide sequencing. *J. Neurochem.* *59*, 667-678.

Williams, M. J., Du, X., Loftus, J. C., and Ginsberg, M. H. (1995). Platelet adhesion receptors. *Sem. Cell Biol.* *6*, 305-314.

Woods, D. F., and Bryant, P. J. (1991). The discs-large tumor suppressor gene of *Drosophila* encodes a guanylate kinase homolog localized at septate junctions. *Cell* *66*, 451-464.

Yamagata, M., Herman, J.-P., and Sanes, J. R. (1995). Lamina-specific expression of adhesion molecules in developing chick optic tectum. *J. Neurosci.* *15*, 4556-4571.

**FIGURE LEGENDS**

Figure 1.1. Serial electron micrographs through a dendritic spine. Each of the eight micrographs contains a section through the dendritic spine and its corresponding presynaptic bouton. A non-docked vesicle (arrow) in the presynaptic bouton is shown in (A). Characteristic docked vesicles (curved arrows) across from the PSD (arrowhead) are shown in (B), (E) and (G). The synaptic cleft (wiggly arrow) contains dense staining material (C). Extracellular space that does not have dense staining material is shown with an arrow in (F). Arrowhead in (H) denotes the gray edge of the plasma membrane. Astrocytic processes are shown in consecutive sections (B) through (H) with a star. From Harris and Sultan, 1995.

Figure 1.2. Electron micrographs of synaptosome and postsynaptic density fractions at different stages in the purification. A single synaptosome (A), lysed synaptosome (B), and postsynaptic density after sarcosyl extraction (C) from each fraction is shown. From Cotman et al., 1974.

Figure 1.3. Protein composition of detergent-extracted PSD fractions. PSD fractions were obtained after extraction of synaptosomes once with Triton X-100 (One Triton), twice with Triton X-100 (Two Triton) or once with Triton X-100 and once with sarcosyl (One Triton + Sarcosyl) and pelleting at 201,800 x g for 1 hour. Synaptosome and PSD fractions were separated by SDS-PAGE and stained with Coomassie blue. The location of actin, tubulin, fodrin, PSD-95, hexokinase and the  $\alpha$  and  $\beta$  subunits of the CaMKII are identified on the right. Molecular weight markers are shown at the left. From Cho et al., 1992.

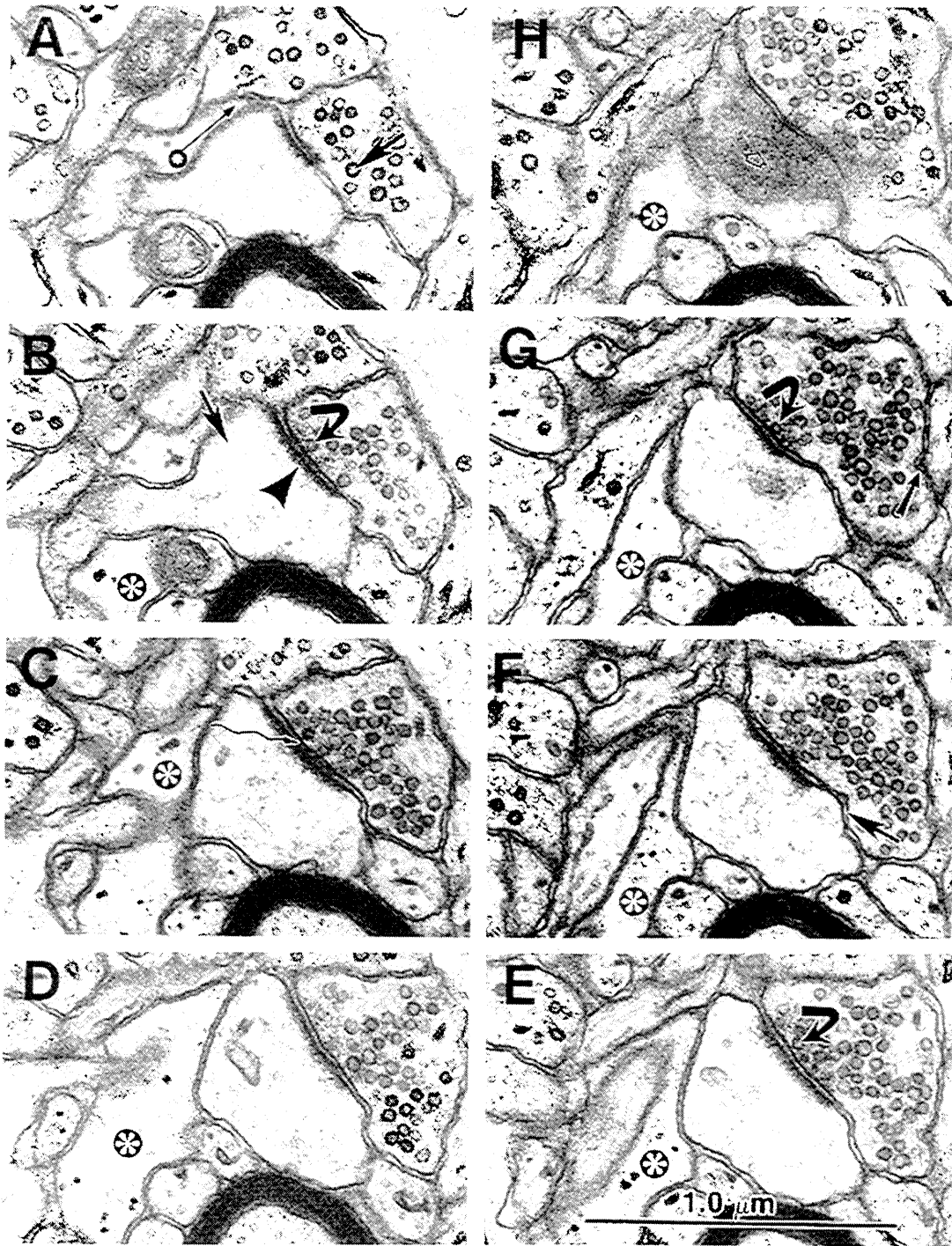
Figure 1.4. Electron micrographs of non-lysed and lysed synaptosomes. Non-lysed synaptosomes stained for PSD-95 are shown in (a). Lysed synaptosomes stained for synapsin I are shown in (b). In both cases, there are several examples of thin electron dense "lines" connecting the presynaptic and postsynaptic membranes (indicated with transparent yellow lines in right panels). Scale bar represents 100 nm. Adapted from Hunt et al., 1996.

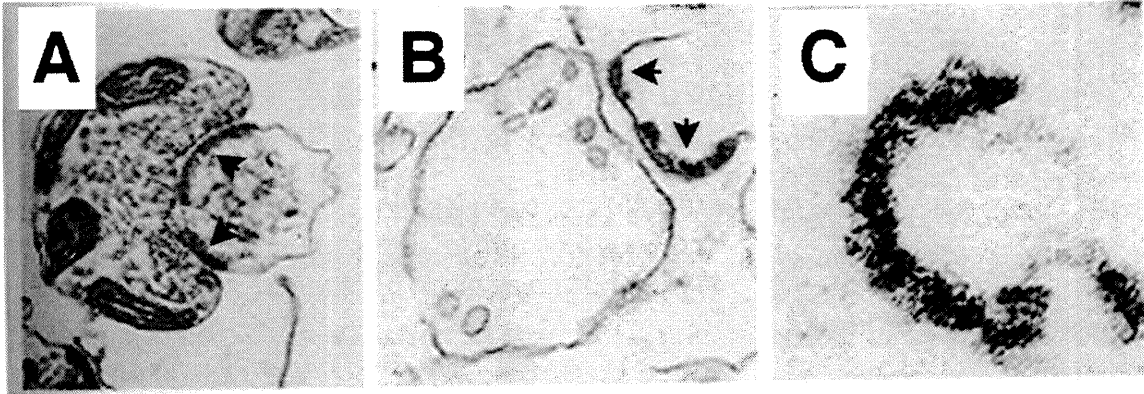
Figure 1.5. Structures of leucine-rich repeats. Two projections of the crystal structure of ribonuclease-bound ribonuclease inhibitor (RI) is shown in (A) and (B). The RI is green and the RNaseA is yellow. (B) is rotated 90° along the horizontal axis compared to (A). From Kobe and Deisenhofer, 1995. A model of the more typical 24 amino-acid leucine-rich repeats of thyrotropin receptor (TSHR) is shown in (C). The part of the structure that is conserved between RI and TSHR is shown in green and the modeled part of the structure is in blue. From Kajava et al., 1995.

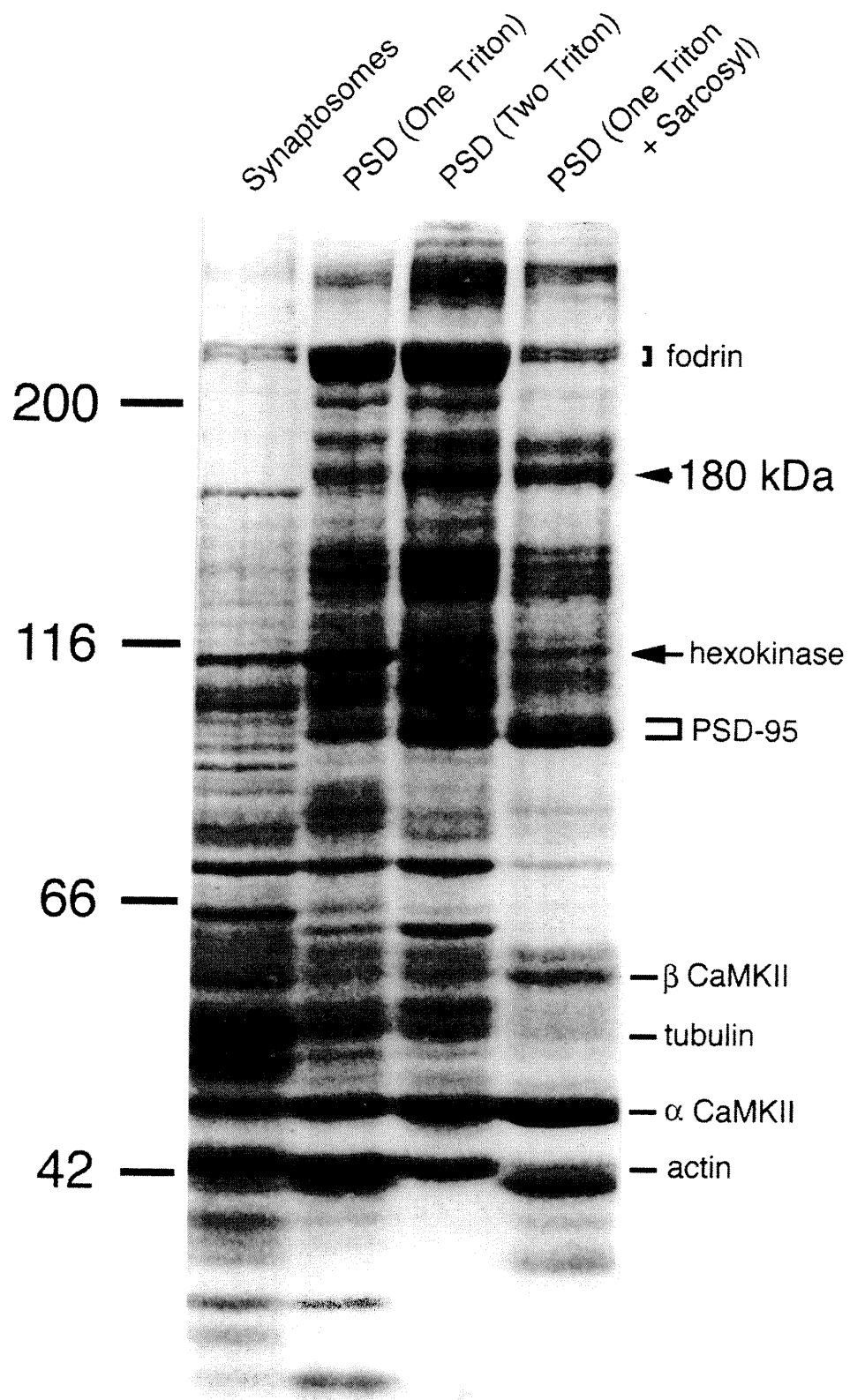
Figure 1.6. Summary of O-glycosylated membrane proteins and their interactions with selectins. Several membrane glycoproteins drawn to scale are shown in (A). The O-glycosylated regions of these proteins are represented as stiff, extended structures with a length of 2.5 Angstroms per amino acid residue. Globular regions are represented as spheres and the dotted line represents the extension of the erythrocyte glycocalyx as estimated by Viitala and Jarnefelt, 1985. The low-density lipoprotein (LDL) receptor contains a total of 840 amino acids of which 48 are present in the O-glycosylated regions. Decay accelerating factor (DAF, 347 amino acids in length) contains 70 amino acids in the

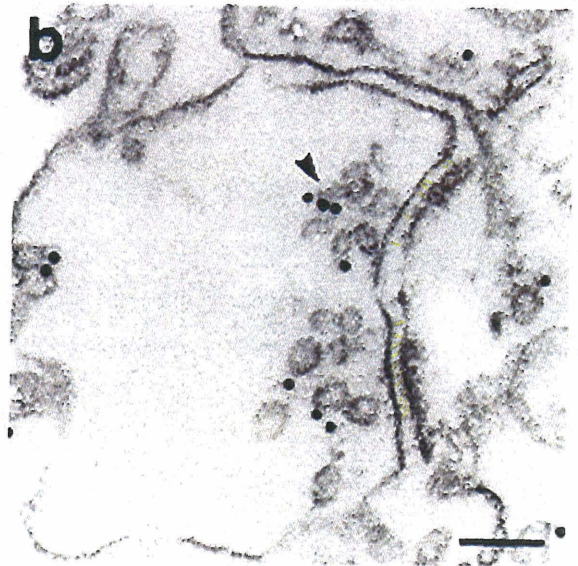
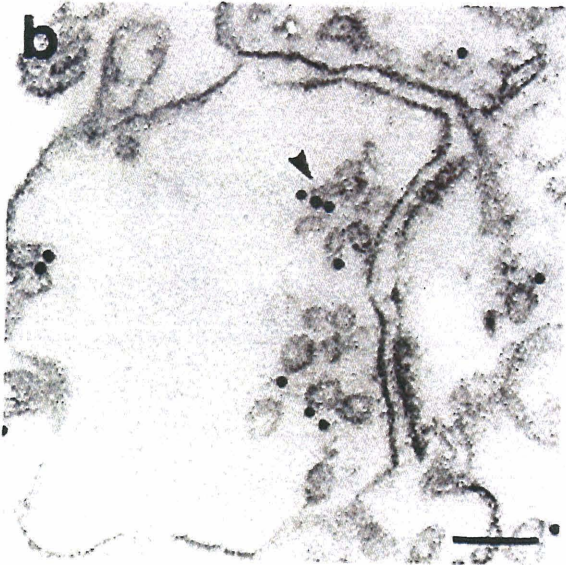
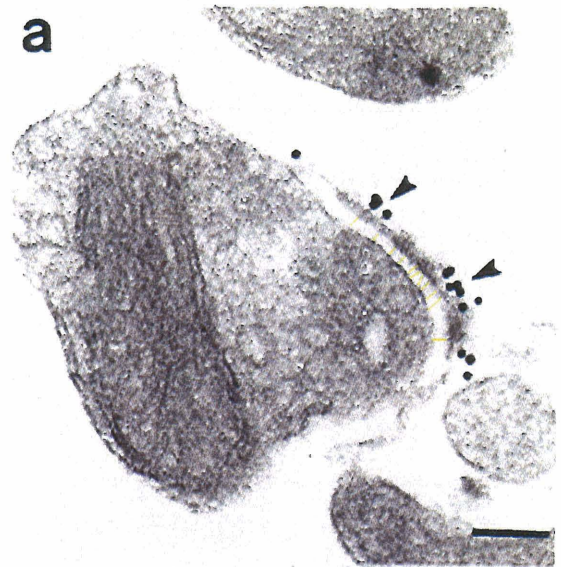
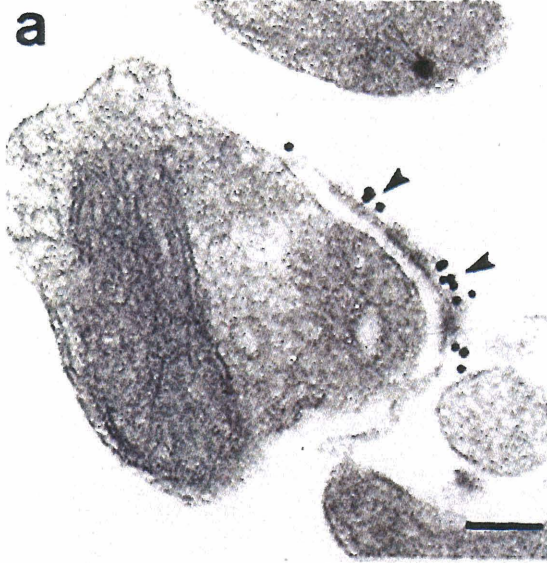
O-glycosylated domain. Leukosialin is a transmembrane sialoglycoprotein in which most of the extracellular domain is glycosylated. From Jentoft, 1990. A schematic of the interaction of selectins with mucins is shown in (B) drawn to scale. The dimensions of the PSGL-1 (P-selectin glycoprotein ligand-1) and CD34 are based on CD43 structure (Springer, 1994). The neutrophil membrane projection represents a microvillus, is not drawn to scale, and is actually larger than shown. From van der Merwe and Barclay, 1994.

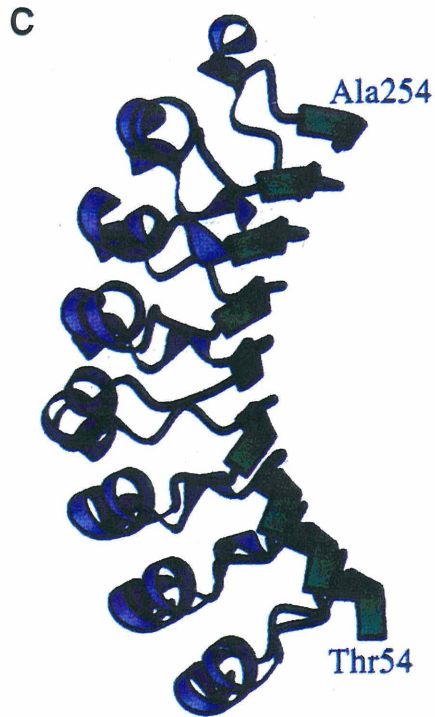
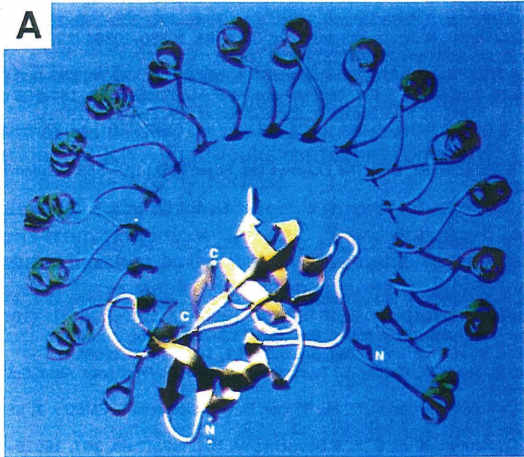
Figure 1.7. Structure of GPIb $\alpha$ . (A) shows a schematic diagram of proteins in the GPIb-IX complex (from Williams et al., 1995). Disulphide linked GPIb $\alpha$  and GPIb $\beta$  associate non-covalently with a third subunit, GPIX. The extracellular domains of GPIb $\beta$  and GPIX contain a single leucine-rich repeat (LRR) and the extracellular domain of GPIb $\alpha$  contains seven LRRs (shaded disks). The disulphide looped C-terminal cysteine rich domain is represented by a shaded block). The N-terminal von Willebrand factor binding domain of GPIb $\alpha$  is extended from the membrane via the rod-like sialomucin domain which is extensively glycosylated (represented by black dots). Part (B) shows an electron micrograph of purified GPIb complex visualized using rotary shadowing (from Fox et al., 1988). The globular portions of the dumbbell-shaped structure correspond to the cytoplasmic and vWF-binding domains of GPIb. The extended part of the structure corresponds to the mucin homology domain of GPIb $\alpha$ .



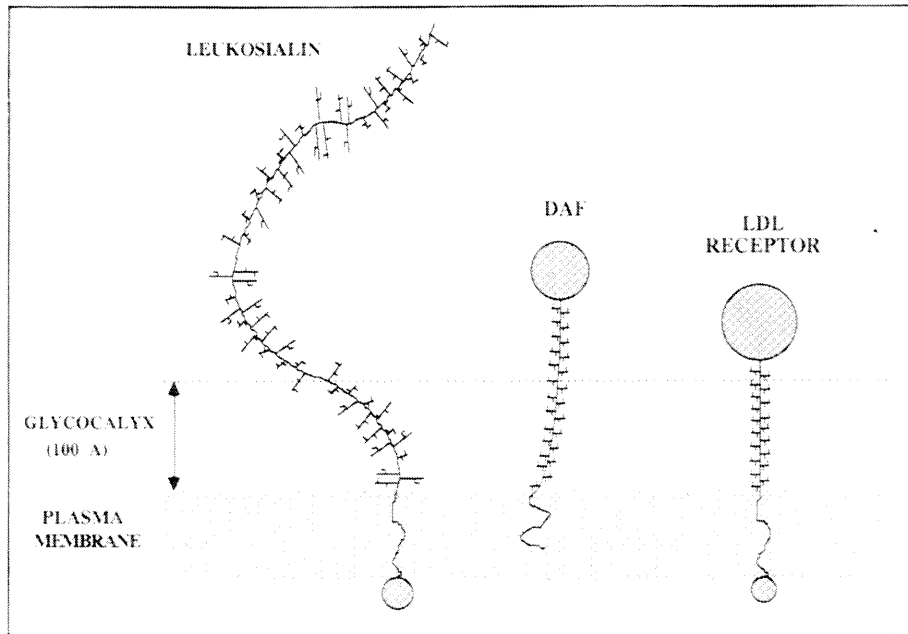




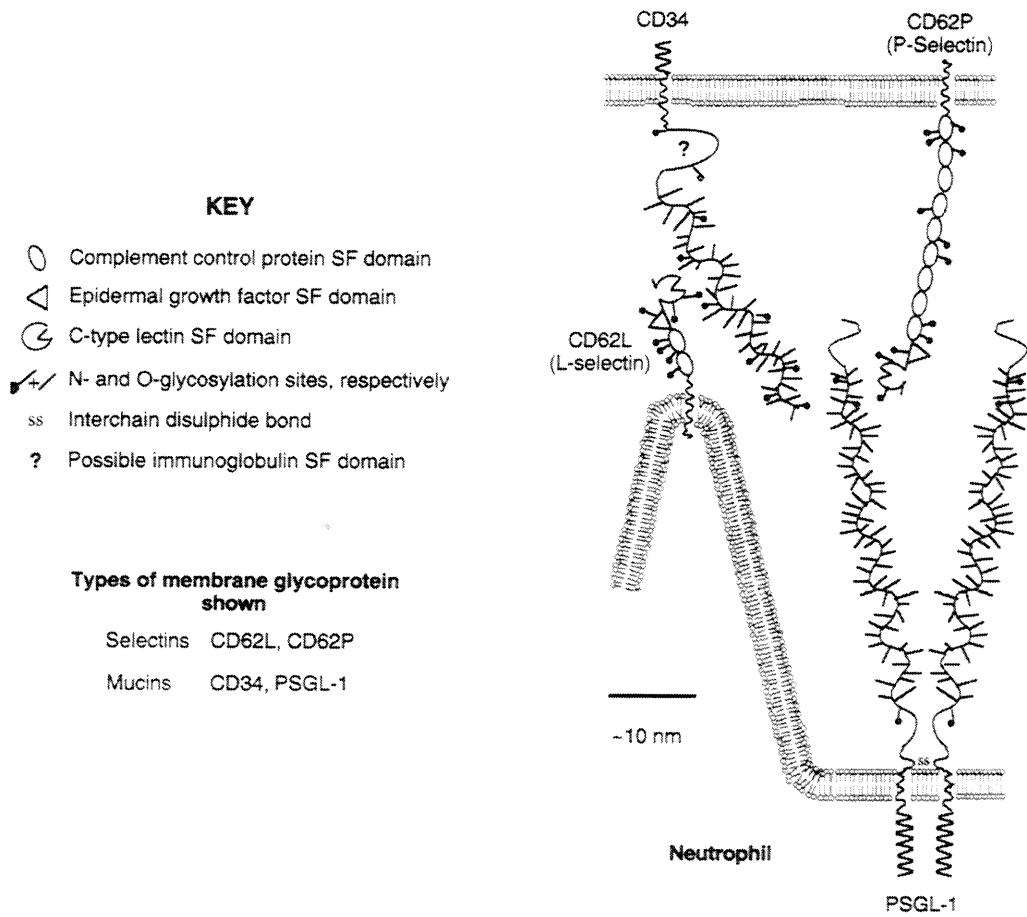


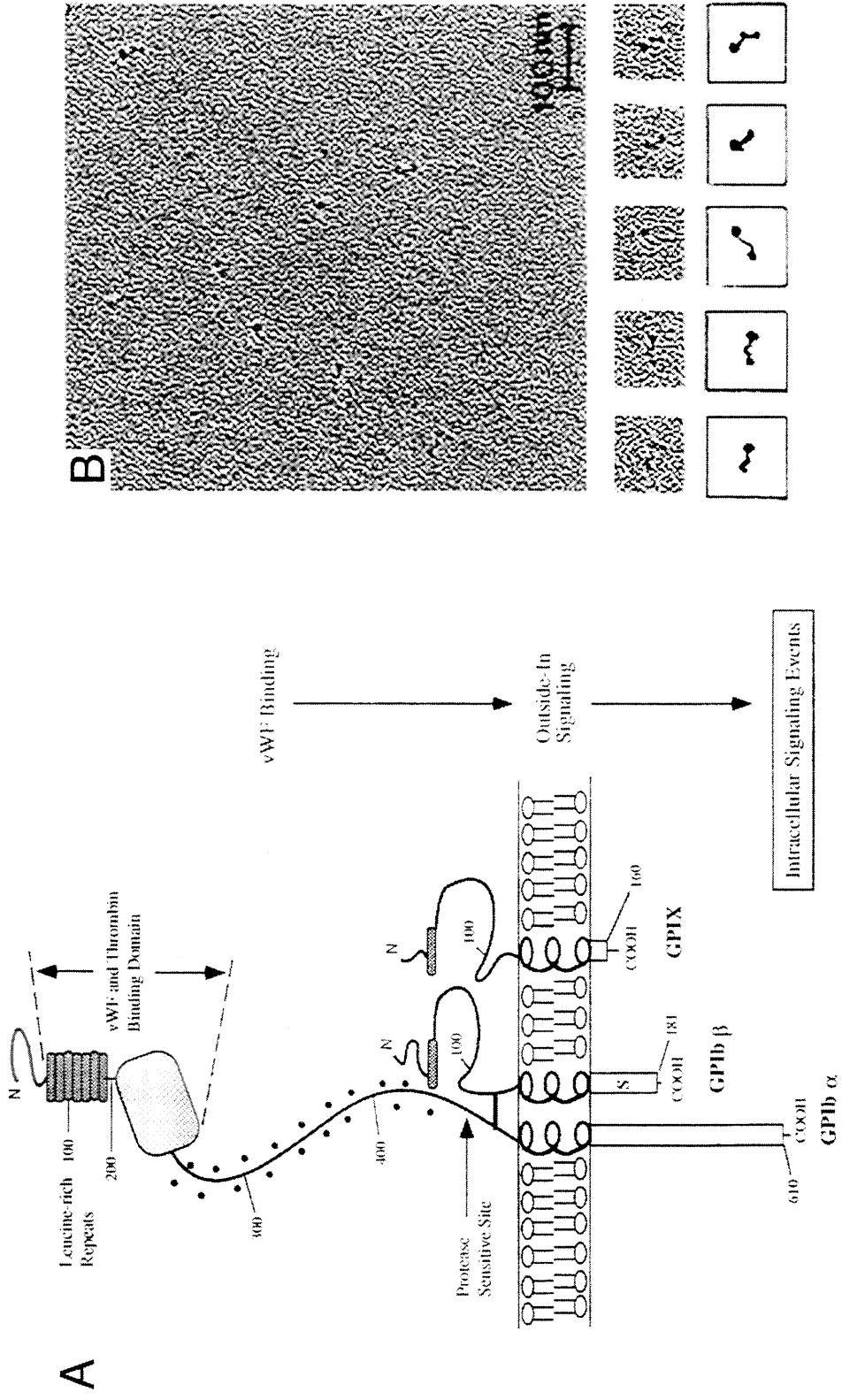


A



B





## CHAPTER 2

### **The major tyrosine-phosphorylated protein in the postsynaptic density fraction is *N*-methyl-D-aspartate receptor subunit 2B**

Published as an article in *Proc. Natl. Acad. Sci. USA* Vol. 91, pp. 3954-3958, April 1994.

Classification: Neurobiology/ Biochemistry

**The major tyrosine-phosphorylated protein in the postsynaptic density fraction  
is N-methyl-D-aspartate receptor subunit 2B**

(synapse/ synaptic plasticity/ signal transduction/ glutamate receptor)

Il Soo Moon, Michelle L. Apperson, and Mary B. Kennedy

Division of Biology 216-76, California Institute of Technology, Pasadena, CA 91125

Submitted for review, November 15, 1993

Abbreviations: NMDA, N-methyl-D-aspartate; AMPA,

$\alpha$ -amino-3-hydroxy-5-methyl-4-isoxazole propionic acid; PSD, postsynaptic density;

NR2B, NMDA receptor subunit 2B; NOG, N-octylglucoside

**ABSTRACT**

The postsynaptic density (PSD) is a specialization of the submembranous cytoskeleton that is visible in the electron microscope on the cytoplasmic face of the postsynaptic membrane. A subcellular fraction enriched in structures with the morphology of PSDs contains signal transduction molecules thought to regulate receptor localization and function in the central nervous system. We have purified a prominent tyrosine-phosphorylated glycoprotein of apparent molecular mass 180 kDa, termed PSD-gp180, that is highly enriched in the rat forebrain PSD fraction. The sequences of four tryptic peptides generated from the protein reveal that it is the 2B subunit of the *N*-methyl-D-aspartate (NMDA) type glutamate receptor. We have confirmed the identity of PSD-gp180 by showing that it reacts with antibodies raised against a unique fragment of the 2B subunit of the NMDA receptor. We also show that the 2B subunit is the most prominently tyrosine-phosphorylated protein in the PSD fraction based upon recognition by an anti-phosphotyrosine antibody. Two types of NMDA receptor subunits have been identified by molecular cloning (Nakanishi, S. (1992) *Science* 258, 597-603). The single type 1 subunit is expressed throughout the brain and is necessary for formation of the receptor channel. The four type 2 subunits (2A, 2B, 2C, and 2D) are expressed in discrete brain regions, contain unusually long unique COOH termini, and confer distinct kinetic properties on NMDA receptors that contain them. Our findings suggest that, in the forebrain, NMDA receptor subunit 2B may serve to anchor NMDA receptors at the postsynaptic membrane through its interaction with the PSD. The prominent presence of tyrosine phosphate further suggests that the NMDA receptor may be regulated by tyrosine phosphorylation or that it may participate in signaling

**through tyrosine phosphorylation and through its ion channel.**

Regulation of synaptic transmission by prior neural activity is an important mechanism of information processing in the central nervous system. Such regulation occurs in part through modulation of transmitter receptors in the postsynaptic membrane (1, 2). Excitatory synapses in the central nervous system contain two major classes of postsynaptic glutamate receptors:  $\alpha$ -amino-3-hydroxy-5-methyl-4-isoxazole propionic acid (AMPA)-type receptors generate the basal postsynaptic potential; whereas NMDA-type receptors display unique voltage-dependent activation properties and play a critical role in initiation of long-term potentiation, a form of synaptic plasticity believed to be important for formation of memories (3, 4).

The postsynaptic density (PSD) is a specialization of the submembranous cytoskeleton visible in the electron microscope that appears to represent a tight complex of postsynaptic junctional proteins (for a recent review see (5)). A subcellular fraction from rat forebrain called the PSD fraction is enriched in structures with the morphology of PSDs (6, 7). AMPA receptor subunits are associated with the PSD fraction (8-10) and may be enriched there (8). The fraction also contains high-affinity glutamate binding sites with some of the pharmacological properties of NMDA receptor sites (11), as well as proteins that may participate in receptor regulation and in regulation of other forms of synaptic efficacy. These include the subunits of  $\text{Ca}^{2+}$ /calmodulin-dependent protein kinase II (12-15), a src-like protein tyrosine kinase (16), a cAMP-dependent protein kinase anchoring protein (17), and PSD-95, a close homologue of the *Drosophila* discs-large tumor suppressor protein which participates in formation of septate junctions and growth control in developing flies (18).  $\text{Ca}^{2+}$ /calmodulin-dependent protein kinase II (19) and PSD-95 (18) have been shown to be highly enriched in the PSD fraction and are associated with PSDs in situ as determined by immunocytochemical staining of brain synaptosomes (ref.

15 and C. Hunt, L. Schenker, and M.B.K., unpublished observation) reinforcing the notion that the major proteins of the PSD fraction represent a functional protein complex.

Here we show that a 180 kDa glycoprotein highly enriched in the PSD fraction is subunit 2B of the NMDA receptor (NR2B). We show also that NR2B is the most prominently tyrosine-phosphorylated protein in the PSD fraction.

Two distinct types of NMDA receptor subunits were identified recently by molecular cloning (20-22). Like most ionotropic receptors, NMDA receptors are composed of multiple subunits with homologous sequences (23, 24). NMDA receptor subunit 1 (termed NR1) has a molecular mass (106 kDa) close to that of the subunits of the AMPA class of glutamate receptors. In contrast, the NMDA receptor subunits termed 2A, 2B, 2C, and 2D are considerably larger, having molecular masses from 135 kDa to 166 kDa. Their larger sizes result from long COOH-termini that are only distantly related to each other in sequence. Phosphorylation sites for protein kinase C have been localized to the extreme carboxyl terminus of the NR1 subunit (25), suggesting that the long COOH domains of the homologous type 2 subunits also extend into the cytosol where they could mediate additional regulation by phosphorylation (25, 26). NR1 is expressed throughout the brain and is essential for formation of a receptor channel; whereas, the NR2 subunits are not essential for channel formation, have more restricted expression patterns, and appear to modulate receptor channel kinetics in different ways (22-24). The findings reported here suggest that NR2B associates tightly with the PSD structure and thus may mediate specific interactions with PSD proteins and other cytosolic proteins perhaps through tyrosine phosphorylated domains.

## MATERIALS AND METHODS

**Purification of PSD-gp180.** The crude PSD fraction (90 mgs; 3-5 mgs/ml) was prepared as previously described (18) by a modification of the method of Carlin et al. (7). The PSD fraction was extracted with 1% N-octylglucoside (NOG) at 4°C for 30 min with stirring. Insoluble material was pelleted by centrifugation at 200,000 g for 30 min at 4°C. The pellet (NOG-P) (2 mg/ml) was treated with Endoglycosidase F/N-glycosidase F (Boehringer Mannheim) in 0.2% SDS according to the supplier's instructions. To purify individual proteins, the deglycosylated proteins (63 mgs) were fractionated on 60 preparative 6% SDS polyacrylamide gels. Each gel was stained with 0.2% (w/v) Coomassie blue R-250 in 10 mM Tris-Cl (pH 8.0), 0.01% SDS for 30 min. Bands containing two proteins, PSD-gp180 and a second protein termed PSD-up180, were cut from the gels, pooled, and chopped into 3-5 mm pieces. Protein (approx. 400 µg each) was electroeluted from the pieces in an Elutrap device (Schleicher & Schuell) at 250 V in 25 mM N-ethylmorpholine (pH 8.5), 0.01% SDS overnight at room temperature into approximately 6 ml of 0.5% SDS, 25 mM N-ethylmorpholine. Because the purified proteins still contained a small amount of bound Coomassie dye that interfered with determination of protein by the method of Peterson, protein was estimated after SDS-gel electrophoresis by comparison to a set of Coomassie stained BSA standards.

**Preparation of antibodies against the C-terminus of NR2B.** Bacteriophage clones containing cDNA inserts encoding NR2B were selected from a  $\lambda$ gt11 library (Clontech) by screening with an oligonucleotide sequence deduced from peptide sequence 2 (Table I). A restriction fragment (PmlI to EcoRI) encoding 334 amino acids of the C-terminus of NR2B (from 1149 to the carboxyl terminus) was ligated into the pGEX-3X expression vector (Pharmacia). A GST fusion protein containing the NR2B fragment was

expressed in *E. coli*, and purified from inclusion bodies by electrophoresis through a 6% SDS-polyacrylamide gel. The protein was visualized after soaking the gel in 0.25 M KCl. Bands containing the fusion protein were cut from the gel and used to immunize mice from which polyclonal ascites fluid was prepared as described by Ou et al. (27). Antibodies from the ascites fluid recognize a single band of approximately 180 kDa at 1:5,000 dilution on immunoblots of proteins from a rat brain homogenate (data not shown). Control ascites fluid generated without immunization with NR2B does not react with any proteins in the PSD fraction.

**Immunoblots with anti-NR2B and anti-phosphotyrosine.** For the experiments described in Figs. 2 and 3, the crude PSD fraction was prepared as previously described (18), except that 0.1 mM orthovanadate was included to inhibit dephosphorylation of tyrosine residues. Transfer to nitrocellulose and incubation with antibodies was carried out as described by Cudmore and Gurd (28). Antibody 4g10 against phosphotyrosine was purchased from Upstate Biotechnology Inc. (NY). Primary antibodies were visualized after incubation with alkaline-phosphatase-conjugated rabbit IgG according to the supplier's instructions (Boehringer Mannheim).

**Immunoprecipitation.** Crude PSD fraction (500  $\mu$ g) prepared in the presence of 0.1 mM orthovanadate was brought to 0.7% SDS and boiled for 3 min. The solution was adjusted to a final concentration of 10 mM Tris-Cl (pH 7.4), 1 mM EDTA, 150 mM NaCl, 1% Triton X-100, 1% Sodium deoxycholate, 0.1% SDS (RIPA buffer) in a final volume of 1 ml. Ascites fluid ( $\alpha$ -NR2B or control) was added at 1:50 dilution, and the mixture was incubated for 4 hr at 4°C with mixing. The solution was cleared by centrifugation for 20 min at 12,000 rpm in an Eppendorf centrifuge at 4°C. Protein A-agarose beads (250  $\mu$ l, Pierce Chemical Co.) washed in RIPA buffer were added to the

supernatant and incubation was continued for an additional 4 hr. The beads were collected by centrifugation and washed 5 times with RIPA buffer. Sample solution for SDS-polyacrylamide gel electrophoresis was added and the mixture was boiled for 3 min. Beads were pelleted by centrifugation and a volume of the supernatant corresponding to 100  $\mu$ g of the original PSD fraction was applied to each lane of a 6% SDS gel.

**Analytical Methods.** Except where noted, protein was measured by the method of Lowry (29) as modified by Peterson (30). SDS polyacrylamide gel electrophoresis was performed by the method of Laemmli (31).

## Results

**Purification of PSD-gp180.** A crude PSD fraction was isolated from rat forebrains as described under Materials and Methods. We investigated the proteins contained in a broad band at 180 kDa (Fig. 1) because they have previously been shown to contain tyrosine phosphate (32), to be phosphorylated by a calmodulin-dependent protein kinase (33), and to remain associated with the PSD fraction following extraction with the harsh detergent sarcosyl (18, 34). Three proteins associated with this broad band were resolved from one another. The first was selectively removed by extraction of the PSD fraction with 1% N-octyl glucoside (NOG; Fig. 1A). Enzymatic deglycosylation shifted the electrophoretic mobility of a second protein band (PSD-gp180) to an apparent molecular mass of 160 kDa and did not alter the mobility of a third protein band (PSD-up180) (Fig. 1A). We electroeluted several hundred  $\mu$ g of each individual protein from preparative SDS gels for sequencing as described under Materials and Methods. Each electroeluted protein appeared as a single band upon SDS-gel electrophoresis (Fig. 1B).

**Sequencing and identification of NR2B.** Purified PSD-gp180 (approx. 300  $\mu$ g) was trypsinized as previously described (18, 35) and four tryptic peptides were purified and sequenced (Table I). A search of the GenBank data base performed with the BLAST network service through the National Center for Biotechnology Information revealed that all four sequences are present in the 2B subunit of the rat brain NMDA receptor (NR2B) (21, 22, 36, 37). Sequences 2 through 4 are unique to NR2B; sequence 1 is found in all four type 2 NMDA receptor subunits.

**Identification of NR2B by antibody binding.** We raised antibodies against a portion of the carboxyl terminal domain that is unique to NR2B to verify that PSD-gp180

is NR2B. Immunoblots of the NOG-treated PSD fraction were probed with these antibodies and revealed that NR2B was present at an apparent molecular mass of 180 kDa before deglycosylation. Its mobility shifted completely to an apparent molecular mass of 160 kDa after deglycosylation (Fig. 2). The  $\alpha$ -NR2B antibodies also recognized purified, electroeluted PSD-gp180 protein.

**Reaction of NR2B with anti-phosphotyrosine antibodies.** It was previously reported that a 180 kDa glycoprotein from the PSD fraction is a tyrosine-phosphorylated protein (30). To test whether NR2B contains tyrosine phosphate, blots of the PSD fraction were probed with monoclonal antibody 4g10 against phosphotyrosine (Fig. 2). The major tyrosine-phosphorylated protein band in the PSD fraction comigrated at 180 kDa with NR2B and shifted to an apparent molecular mass of 160 kDa after deglycosylation (lanes 4 and 5), in parallel with NR2B (lanes 1 and 2). In addition, purified, electroeluted PSD-gp180 reacted with the anti-phosphotyrosine antibody (lane 6). Preabsorption of the anti-phosphotyrosine antibody with 2 mM phosphotyrosine eliminated staining of the 180 and 160 kDa bands as expected; whereas preabsorption with phosphoserine or phosphothreonine did not reduce the staining (data not shown). To eliminate the possibility that a distinct protein comigrating with PSD-gp180 might contain the tyrosine phosphate, we immunoprecipitated NR2B from the PSD fraction after solubilization and found that the immunoprecipitated protein contains phosphotyrosine (Fig. 3). Indeed, immunoprecipitation from the solubilized PSD fraction of nearly all the protein reacting with anti-NR2B antibodies removed over two-thirds of the anti-phosphotyrosine immunoreactivity at 180 kDa (data not shown). Taken together, the data in Figs. 2 and 3 demonstrate that NR2B is the most highly tyrosine-phosphorylated protein in the PSD fraction based upon recognition by the anti-phosphotyrosine antibody.

**Enrichment of NR2B in the PSD fraction.** If NR2B is specifically associated with the PSD, it should be highly enriched in the PSD fraction, as are two other proteins previously identified as significant components of the PSD, the  $\alpha$  subunit of  $\text{Ca}^{2+}$ /calmodulin-dependent protein kinase II and PSD-95 (15, 18). To assess the level of enrichment of NR2B in the PSD fraction, we prepared immunoblots of rat forebrain homogenates, synaptosomes, and three different PSD fractions extracted with successively harsher detergent washes, probing with anti-NR2B antibodies (Fig. 4). NR2B was highly enriched in the PSD fractions, appearing approximately ten-fold more concentrated than in synaptosomes (compare lanes 2, 4, and 5), and 30 to 50-fold more concentrated than in the homogenate (compare lanes 1, 4, and 5).

## DISCUSSION

We have shown that NR2B is significantly enriched in the PSD fraction and is the most highly tyrosine-phosphorylated protein present there. The latter conclusion is based upon the assumption that antibody 4g10, which was raised against a phosphotyramine conjugate, reacts uniformly with tyrosine-phosphorylated proteins. This assumption is supported by studies demonstrating that 4g10 binds to a broad range of tyrosine-phosphorylated proteins on immunoblots, although differences in the affinities of 4g10 for tyrosine-phosphorylated proteins have not been strictly ruled out (38). NR2B may be identical to the tyrosine-phosphorylated protein termed gp180 described by Gurd (32); however, we have not compared it directly with the protein purified by his protocol.

The concentration of NR2B in the PSD fraction is higher than that of NR2A which is also expressed in the forebrain (22). NR2A would be expected to comigrate on SDS gels with NR2B because they have nearly identical molecular masses. However, our peptide sequences (Table I) did not match any unique to NR2A, indicating that it is absent or present in considerably lower quantity than NR2B. In addition, more than 2/3 of the protein migrating at 180 kDa was immunoprecipitated by a specific anti-NR2B antibody. Nevertheless, the small amount of tyrosine-phosphorylated protein remaining at the 180 kDa position of SDS gels after immunoprecipitation of NR2B may be NR2A. The relatively high concentration of NR2B in the PSD fraction indicates either that it is expressed at higher levels than NR2A, or that it binds more avidly to PSD proteins and therefore remains in the PSD fraction during the detergent extraction that removes other synaptic membrane proteins. If the latter is true, we suggest that NR2B may anchor NMDA receptors in the postsynaptic membrane through its association with PSD proteins.

Two potential regulatory roles for tyrosine phosphorylation of NR2B, which are

not mutually exclusive, are suggested by studies of other membrane receptors. Agrin, a protein released from motor neuron terminals, induces clustering of acetylcholine receptor subunits at postsynaptic sites (39). Agrin also induces tyrosine phosphorylation of the  $\beta$ -subunit of the chick acetylcholine receptor (40). The tyrosine phosphorylation precedes receptor clustering; furthermore, agents that block the tyrosine phosphorylation also block agrin-induced receptor clustering, indicating that tyrosine phosphorylation is a critical part of the clustering mechanism in chick muscle. Thus, by analogy, it is possible that tyrosine phosphorylation of NR2B may catalyse clustering of NMDA receptors.

An intriguing possibility is that the tyrosine phosphorylation may permit interaction of the NMDA receptor with proteins that contain src-homology-2 domains (termed SH2 domains; 41), creating an assembly point for cytosolic signal transduction complexes (42). For example, it was recently demonstrated that binding of growth factors to receptor tyrosine kinases results in the formation of a complex between autophosphorylated tyrosine residues in the cytoplasmic tails of the receptors and SH2 domains contained in a protein termed Grb2 (43). Formation of this complex leads to activation of the Ras GTP-binding protein. Activated Ras then catalyzes, through a protein kinase cascade, activation of MAP kinase. Formation of such complexes might permit the NMDA receptor to participate in similar signal transduction pathways, and could underlie the recent observation that activation of NMDA receptors results in phosphorylation and activation of MAP kinase in hippocampal neurons (44).

It will be important to localize in the NR2B sequence the sites of tyrosine phosphorylation and the domains of interaction with PSD proteins. These studies may help to clarify the functional significance of the unusually long carboxyl terminal domains of the type 2 NMDA receptor subunits.

Acknowledgements: Supported by grants from the NIH (National Institute of Neurological Disorders and Stroke 28710 and 17660) and NSF (FAW, GER-9023446) to M.B.K., and fellowships from NIH (General Medical Sciences 07616) to M.L.A. and from the Del Webb Foundation to I.S.M.. We thank Aram Isaiants for excellent technical assistance and Dirk Krapf of the Caltech Applied Microsequencing Facility for peptide sequences.

**References**

1. Kauer, J. A., Malenka, R. C., & Nicoll, R. A. (1988) *Neuron* **1**, 911-917.
2. Manabe, T., Renner, P., & Nicoll, R. A. (1992) *Nature* **355**, 50-55.
3. Collingridge, G. L., Kehi, S. J., & McLennan, H. (1983) *J. Physiol.* **334**, 33-46.
4. Bliss, T. V. P., & Collingridge, G. L. (1993) *Nature* **361**, 31-39.
5. Kennedy, M. B. (1993) *Curr. Opin. in Neurobiol.* **3**, 732-737.
6. Cotman, C. W., Banker, B., Churchill, L., & Taylor, D. (1974) *J. Cell Biol.* **63**, 441-455.
7. Carlin, R. K., Grab, D. J., Cohen, R. S., & Siekevitz, P. (1980) *J. Cell Biol.* **86**, 831-843.
8. Rogers, S. W., Hughes, T. E., Hollmann, M., Gasic, G. P., Deneris, E. S., & Heinemann, S. (1991) *J. Neurosci.* **11**, 2713-2724.
9. Blackstone, C. D., Moss, S. J., Martin, L. J., Levey, A. I., Price, D. L., & Huganir, R. L. (1992) *J. Neurochem.* **58**, 1118-1126.
10. McGlade-McCulloh, E., Yamamoto, H., Tan, S.-E., Brickey, D. A., & Soderling, T. R. (1993) *Nature* **362**, 640-642.
11. Fagg, G. E., & Matus, A. (1984) *Proc. Natl. Acad. Sci. USA* **81**, 6876-6880.
12. Kennedy, M. B., Bennett, M. K., & Erondy, N. E. (1983) *Proc. Natl. Acad. Sci. USA* **80**, 7357-7361.
13. Kelly, P. T., McGuinness, T. L., & Greengard, P. (1984) *Proc. Natl. Acad. Sci. USA* **81**, 945-949.
14. Goldenring, J. R., McGuire, J. S., & DeLorenzo, R. J. (1984) *J. Neurochem.* **42**, 1077-1084.

15. Kennedy, M. B., Bennett, M. K., Bulleit, R. F., Erondy, N. E., Jennings, V. R., Miller, S. M., Molloy, S. M., Patton, B. L., & Schenker, L. J. (1990) *C. S. H. S. Q. B.* **55**, 101-110.
16. Ellis, P. D., Bissoon, N., & Gurd, J. W. (1988) *J. Neurochem.* **51**, 611-620.
17. Carr, D. W., Stofdo-Hahn, R. E., Fraser, I. D. C., Cone, R. D., & Scott, J. D. (1992) *J. Biol. Chem.* **267**, 16816-16823.
18. Cho, K.-O., Hunt, C. A., & Kennedy, M. B. (1992) *Neuron* **9**, 929-942.
19. Miller, S. G., & Kennedy, M. B. (1985) *J. Biol. Chem.* **260**, 9039-9046.
20. Moriyoshi, K., Masu, M., Ishii, T., Shigemoto, R., Mizuno, N., & Nakanishi, S. (1991) *Nature* **354**, 31-37.
21. Kutsuwada, T., Kashiwabuchi, N., Mori, H., Sakimura, K., Kushiya, E., Kazuaki, A., Meguro, H., Masaki, H., Kumanishi, T., Arakawa, M., & Mishina, M. (1992) *Nature* **358**, 36-41.
22. Monyer, H., Sprengel, R., Schoepfer, R., Herb, A., Higuchi, M., Lomeli, H., Burnashev, N., Sakmann, B., & Seeburg, P. H. (1992) *Science* **256**, 1217-1221.
23. Nakanishi, S. (1992) *Science* **258**, 597-603.
24. Seeburg, P. H. (1993) *Trends Neurosci.* **16**, 359-365.
25. Tingley, W. G., Roche, K. W., Thompson, A. K., & Huganir, R. L. (1993) *Nature* **364**, 70-73.
26. Raymond, L. A., Blackstone, C. D., & Huganir, R. L. (1993) *Trends Neurosci.* **16**, 147- 153.
27. Ou, S. K., Hwang, J. M., & Patterson, P. H. (1993) *J. Immunol. Meth.* **165**, 75-80.
28. Cudmore, S. B., & Gurd, J. W. (1991) *J. Neurochem.* **57**, 1240-1248.
29. Lowry, O. H., Rosebrough, N. J., Farr, A. L., & Randall, R. J. (1951) *J. Biol. Chem.*

193, 265-275.

30. Peterson, G. L. (1983) *Methods in Enzymol.* **91**, 95-119.
31. Laemmli, U. K. (1970) *Nature* **227**, 680-685.
32. Gurd, J. W. (1985) *Brain Res.* **333**, 385-388.
33. Gurd, J. W. (1985) *J. Neurochem.* **45**, 1128-1135.
34. Kelly, P. T., & Montgomery, P. R. (1982) *Brain Res.* **233**, 265-286.
35. Aebersold, R. H., Leavitt, J., Saavedra, R. A., Hood, L. E., & Kent, S. B. H. (1987) *Proc. Natl. Acad. Sci. USA* **84**, 6970-6974.
36. Meguro, H., Mori, H., Araki, K., Kushiya, E., Kutsuwaea, T., Yamazaki, M., Kumanishi, T., Arakawa, M., Sakimura, K., & Mishina, M. (1992) *Nature* **357**, 70-74.
37. Ishii, T., Moriyoshi, K., Sugihara, H., Sakurada, K., Kadotani, H., Yokoi, M., Akazawa, C., Shigemoto, R., Mizuno, N., Masu, M., & Nakanishi, S. (1993) *J. Biol. Chem.* **268**, 2836-2843.
38. Wang, J.Y.J. (1988) *Analyt. Biochem.* **172**, 1-7.
39. Nitkin, R. M., Smith, M. A., Magill, C., Fallon, J. R., Yao, Y.-M. M., Wallace, B. G., & McMahan, U. J. (1987) *J. Cell Biol.* **105**, 2471-2478.
40. Wallace, B. G., Qu, Z., & Huganir, R. L. (1991) *Neuron* **6**, 869-878.
41. Pawson, T., & Gish, G. D. (1992) *Cell* **71**, 359-362.
42. Cantley, L. C., Auger, K. R., Carpenter, C., Duckworth, B., Graziani, A., Kapeller, R., & Soltoff, S. (1991) *Cell* **64**, 281-302.
43. Egan, S. E., & Weinberg, R. A. (1993) *Nature* **365**, 781-783.
44. Bading, H., & Greenberg, M. E. (1991) *Science* **253**, 912-914.

**FIGURE LEGENDS**

**Table 1.** Peptides were sequenced by the Caltech Applied Microsequencing Facility on an Applied Biosystems automatic sequencer. Initial yields were 41, 3, 28, and 23 pmoles for sequences 1 through 4, respectively. The sequence numbering for NR2B is based upon the numbering of the protein product of the cDNA described under accession number M91562 in the GenBank database. At the position marked X in sequence 1, we obtained no identifiable amino acid derivative; this residue is asparagine (N) in NR2B. In sequence 2, the last residue was identified as aspartate (D), whereas it is asparagine (N) in NR2B. Deamidation of the tryptic peptide may have caused this discrepancy.

**Figure 1.** Purification of PSD-gp180. A, Separation of three protein bands with apparent molecular masses of 180 kDa. A crude PSD fraction (PSD) was extracted with N-octylglucoside (NOG) as described under Material and Methods. One of the 180 kDa proteins (\*) was solubilized during the extraction (NOG-S); two others (<, PSD-up180; <, PSD-gp180) remained associated with the NOG-insoluble pellet (NOG-P). Treatment of the pellet with a mixture of endoglycosidases shifted the mobility of PSD-gp180; the two proteins were then separable by SDS polyacrylamide gel electrophoresis (NOG-P Endogly). Proteins in each fraction were separated by electrophoresis on a 6% SDS gel and stained with Coomassie Blue. B, Electroeluted PSD-gp180 and PSD-up180. After deglycosylation of the NOG-insoluble pellet, PSD-up180 and PSD-gp180 were purified to near homogeneity by electroelution from preparative SDS gels as described under Materials and Methods. A 2 µg aliquot of each protein was electrophoresed in a 6% SDS gel and stained with Coomassie Blue. Molecular size standards (in kilodaltons) are at left.

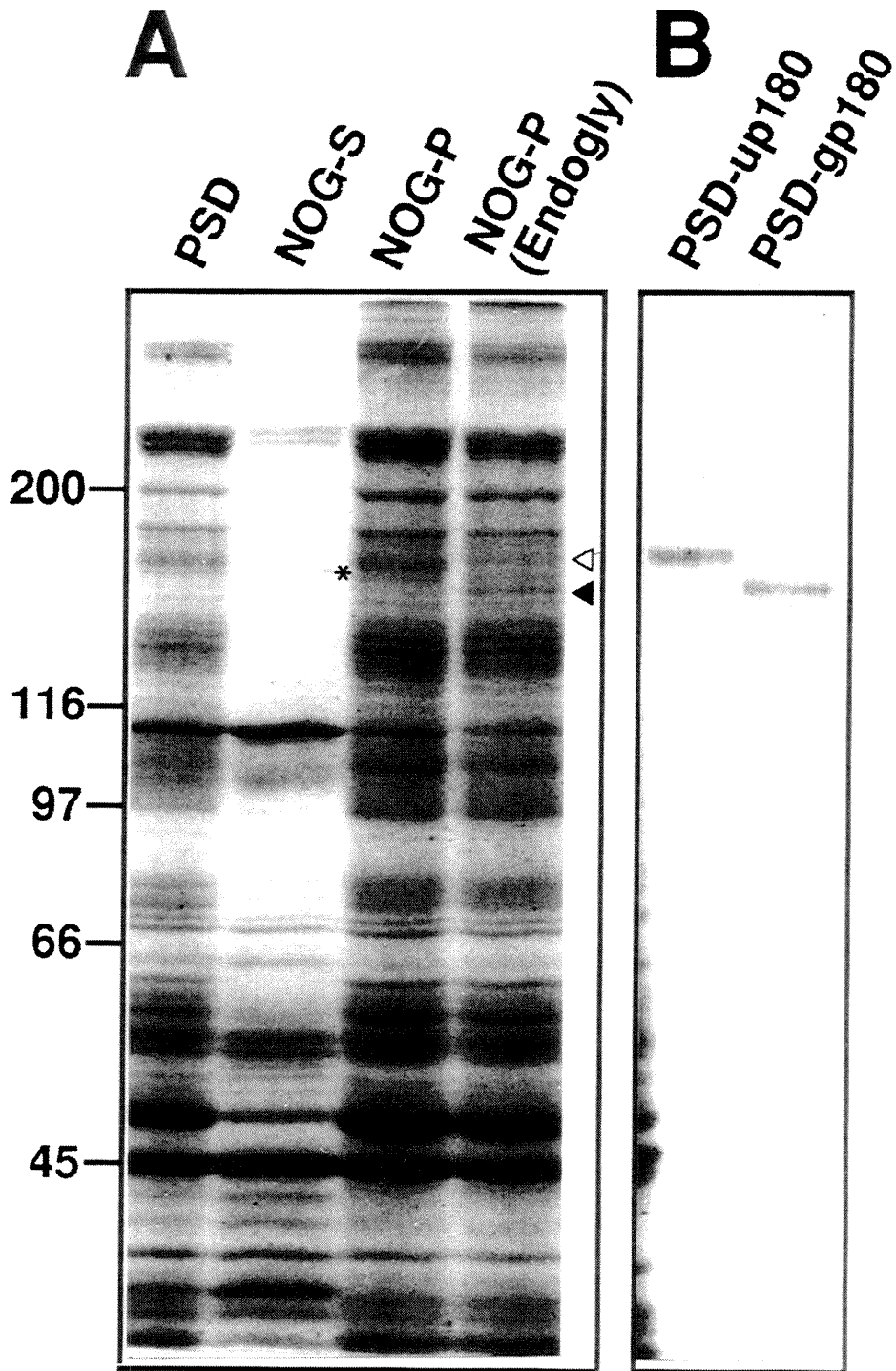
**Figure 2.** Reaction of proteins in the PSD fraction with  $\alpha$ -NR2B and  $\alpha$ -phosphotyrosine antibodies. The PSD fraction before (Endogly -) and after (Endogly +) deglycosylation (20  $\mu$ g), and purified electroeluted PSD-gp180 (0.2  $\mu$ g) were probed with antibodies raised against NR2B ( $\alpha$ -NR2B, 1:5,000), with antibodies against phosphotyrosine ( $\alpha$ -P-Tyr; 4g10, 1:2,000), and with control ascites fluid ( $\alpha$ -NR2B control; 1:5,000) as described under Materials and Methods. Lanes 1, 2, 4, 5, 7, and 8 contained NOG-treated PSD fractions; lanes 3, 6, and 9 contained electroeluted PSD-gp180 (purified in the absence of orthovanadate). Molecular size standards (in kilodaltons) are at left.

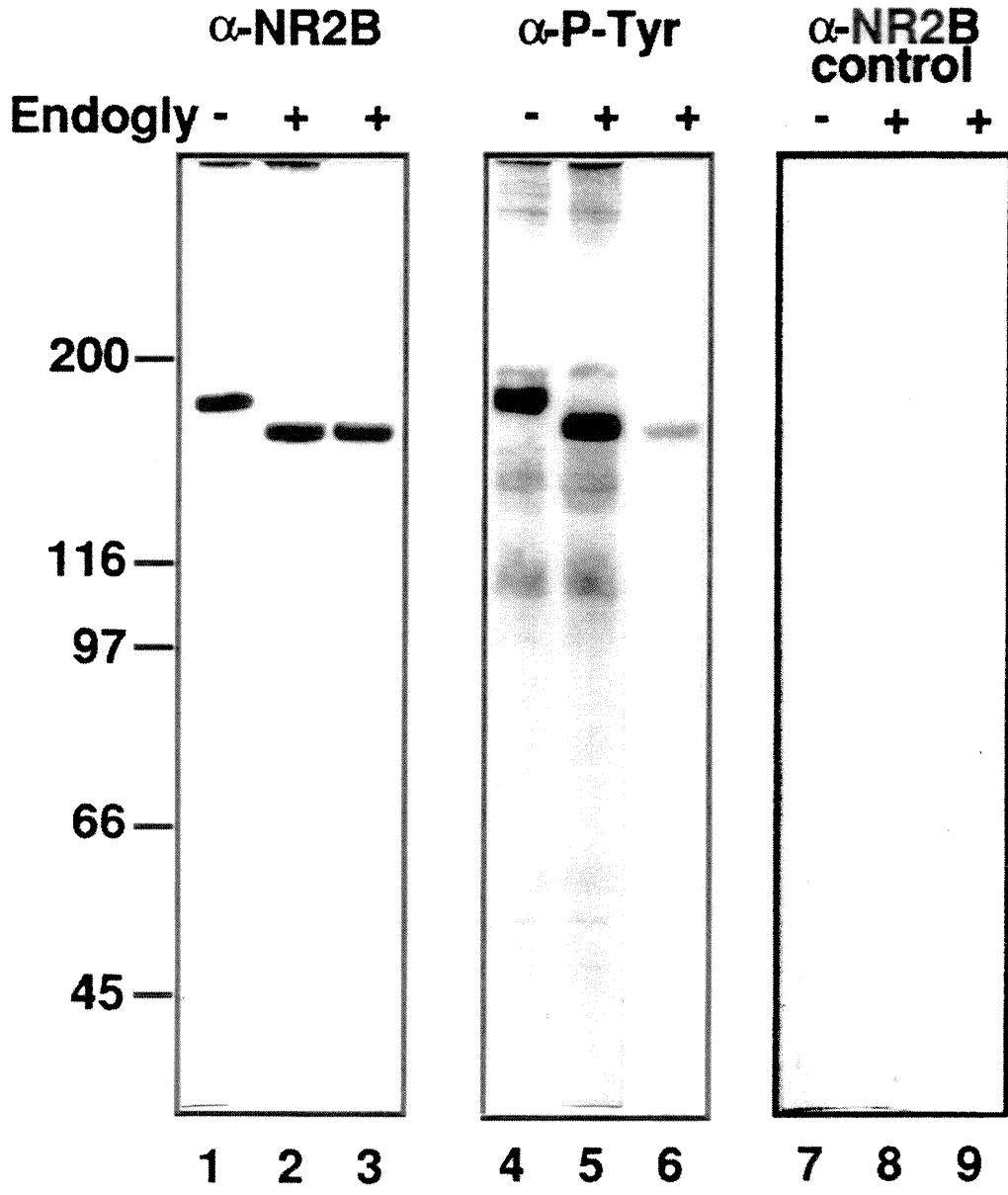
**Figure 3.** Reaction of immunoprecipitated PSD-gp180 with anti-phosphotyrosine antibody. PSD-gp180 protein was immunoprecipitated from the crude PSD pellet (prepared in the presence of orthovanadate) with anti-NR2B antibodies as described under Materials and Methods. Proteins immunoprecipitated by anti-NR2B (lanes marked  $\alpha$ -NR2B and  $\alpha$ -P-Tyr), and proteins immunoprecipitated by the control ascites fluid (lanes marked Control) were probed with anti-NR2B antibodies (lanes marked  $\alpha$ -NR2B and  $\alpha$ -NR2B Control) or anti-phosphotyrosine antibody (lanes marked  $\alpha$ -P-Tyr and  $\alpha$ -P-Tyr Control) as described in Fig. 2. Molecular size standards (in kilodaltons) are at right.

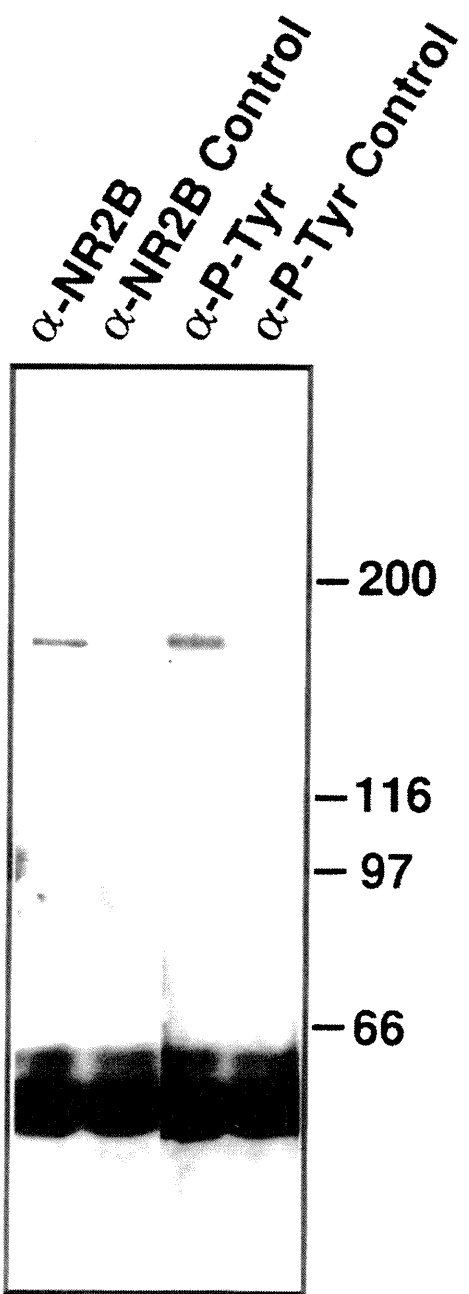
**Figure 4.** Enrichment of PSD-gp180 in the PSD fraction. Fifty  $\mu$ g each of rat forebrain homogenate (Hom) and synaptosomes (Syn) (lanes 1 and 2); and 5  $\mu$ g each of crude PSD fraction (1T), PSD fraction extracted twice with 0.5% Triton X-100 (2T), and PSD fraction extracted once with Triton X-100 followed by 3% sarcosyl (1T + S) (lanes 3-6) were electrophoresed in a 6% SDS gel and transferred to nitrocellulose. The blots were probed

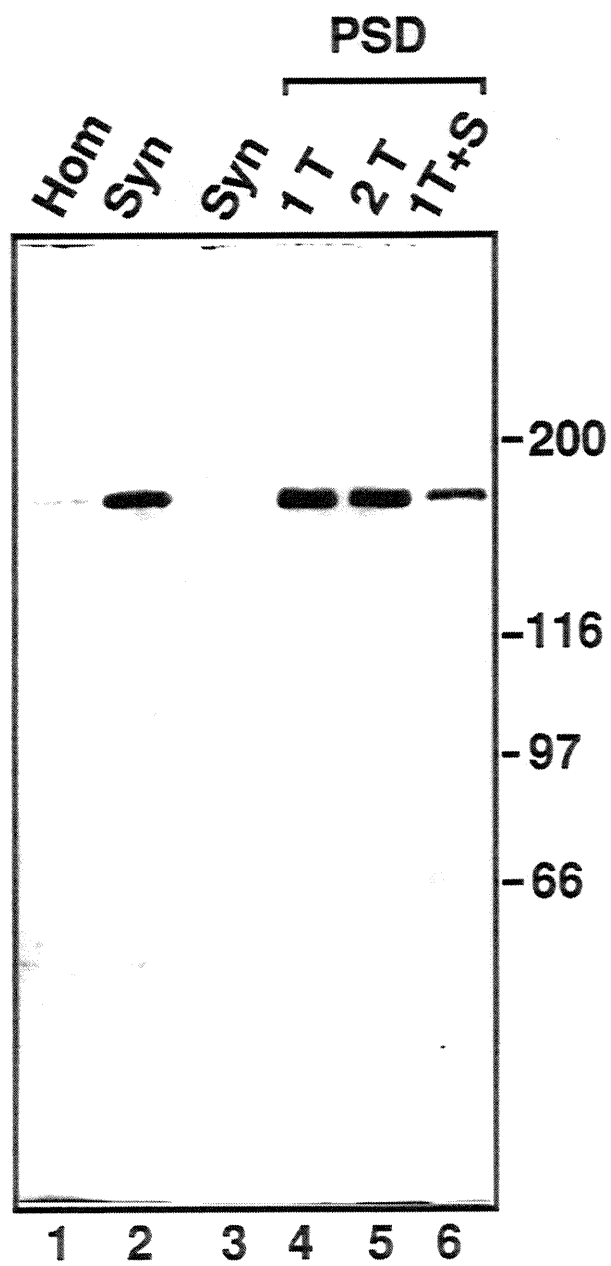
with mouse polyclonal anti-NR2B antibody as described in Fig. 2. Forebrain homogenate, synaptosomes, and detergent extracted PSD fractions were prepared as previously described (18). Molecular size standards (in kilodaltons) are at right.

TABLE I		
Peptides	Amino Acid Sequence	Sequence in NR2B
1	FGTVPXGSTE	683-692
2	SDVSDISTHTVTYGD	1058-1072
3	FYLDQFR	1132-1138
4	NLTNVDWEDR	1200-1208









## **CHAPTER 3**

### **Characterization of densin-180, a new brain-specific synaptic protein of the O-sialoglycoprotein family**

In preparation for submission to the Journal of Neuroscience (1996).

**Characterization of densin-180, a new brain-specific  
synaptic protein of the O-sialoglycoprotein family**

Michelle L. Apperson, Il Soo Moon\*, and Mary B. Kennedy

Division of Biology 216-76, California Institute of Technology, Pasadena, CA 91125

\*Present Address: Department of Anatomy, DongKuk University, School of Medicine,  
Kyongju, Kyungpook, South Korea

Running title: Molecular cloning of densin-180

Corresponding Author: Mary B. Kennedy

Division of Biology 216-76

California Institute of Technology

Pasadena, CA 91125

Phone: 818-395-3923

FAX: 818-449-0679

email: <kennedym@starbase1.caltech.edu>

Acknowledgements: We thank Kai Zinn for suggesting the cloning strategy, Tetsuichiro Saito for help with designing PCR primers, Randy Paterno for help with initial experiments, Dirk Krapf of the Caltech Applied Microsequencing Facility for peptide sequences, and Frank Asuncion and Leslie Schenker for excellent technical assistance. This work was supported by NIH grants NS28710 and NS17660, and NSF grant GER-9023446 to M.B.K., and by fellowships from NIH-GMS07616 and Merck to M.L.A. and from the Del Webb foundation to I.S.M.

**ABSTRACT**

We purified an abundant protein of apparent molecular mass 180 kDal from the postsynaptic density fraction of rat brain and obtained the amino acid sequences of three tryptic peptides generated from the protein. The sequences were used to design a strategy for cloning the cDNA encoding the protein by the polymerase chain reaction. The open reading frame of the cDNA encodes a novel protein of predicted molecular mass 167 kDal. We have named the protein densin-180. Antibodies raised against the predicted amino and carboxyl sequences of densin-180 recognize a 180 kDal band on immunoblots that is enriched in the postsynaptic density fraction. Immunocytochemical localization of densin-180 in dissociated hippocampal neuronal cultures shows that the protein is highly concentrated at synapses along dendrites. The message encoding densin-180 is brain-specific and is more abundant in forebrain than in cerebellum. The sequence of densin-180 contains 17 leucine-rich repeats, a sialomucin domain, an apparent transmembrane domain, and a PDZ domain. This arrangement of domains is similar to that of several adhesion molecules, in particular GPIIb $\alpha$  which mediates binding of platelets to vonWillebrand factor. We propose that densin-180 participates in specific adhesion between presynaptic and postsynaptic membranes at glutamatergic synapses.

## INTRODUCTION

Glutamatergic synapses are likely to be important for information storage in the brain, yet until recently, little was known about the protein machinery at the postsynaptic membrane that is likely to function in adhesion, neurotransmitter receptor clustering and signal transduction at the synapse. Molecules important for these functions are likely to be found in the postsynaptic density (PSD), an electron-dense thickening just beneath the postsynaptic membrane. Our lab and others have focused on the characterization of proteins found in the PSD fraction. The PSD fraction is prepared after detergent extraction of synaptosomes (Cotman et al., 1974, Cohen et al., 1977, and Carlin et al., 1980). A common criticism of characterizing proteins of this fraction is that non-PSD proteins may adhere to the PSD during homogenization. To avoid this possibility, we have concentrated on studying proteins that remain associated with the PSD fraction after extraction with the relatively harsh detergent N-lauroyl sarcosinate (sarcosyl). We refer to the proteins that remain in the insoluble pellet after sarcosyl extraction as “core” PSD proteins.

Our lab previously identified three “core” PSD proteins that have potentially important functions at the synapse. First, the  $\alpha$  subunit of the type II calcium/calmodulin dependent protein kinase (CaMKII) is enriched in the “core” fraction and has also been localized to the PSD by immuno-electron microscopy (Kennedy et al., 1983). This enzyme is likely to mediate signal transduction in response to calcium influx at the synapse and is important in synaptic plasticity. A second PSD protein is PSD-95 (Cho et al., 1992), a novel brain-specific protein with significant homology to the *Drosophila* discs-large protein (dlg), (Woods and Bryant, 1991). Cho et al. identified three repeats in PSD-95 and dlg that are now called PDZ domains. Like the  $\alpha$  subunit of CaMKII,

PSD-95 has been localized to the PSD by immuno-electron microscopy of synaptosomes (Hunt et al., 1996). The third core PSD protein that we identified is the 2B subunit of the NMDA receptor (NR2B), which we showed is the major tyrosine phosphorylated protein in the PSD fraction (Moon et al., 1994). Recently, PSD95 has been shown to bind directly to NR2B *in vitro*, and NR2B and PSD-95 colocalize at synapses in dissociated hippocampal neuronal cultures (Kornau et al., 1995). This may reflect a mechanism for clustering NMDA receptors in the postsynaptic membrane.

The PSD has been proposed to mediate adhesion between the pre and postsynaptic membranes. A dense material fills the synaptic cleft and has been proposed to contain adhesion and extracellular matrix molecules. There is a very tight correlation between sites of vesicle docking at the presynaptic membrane and sites of thick postsynaptic densities beneath the postsynaptic membrane that is likely to be mediated by adhesion molecules. Here, we describe the cloning of densin-180, a “core” PSD protein which has characteristics of a synaptic adhesion molecule.

## **MATERIALS AND METHODS**

### **Purification of densin-180 and sequencing of tryptic peptides**

The crude PSD fraction was prepared as described previously (Cho et al., 1992), by a modification of the method developed in Carlin et al., 1980. The densin-180 protein was purified as described in Moon et al., 1994 (previously termed PSD-up180). Briefly, 63 mg of detergent-extracted, deglycosylated PSD proteins were fractionated by electrophoresis on 60 preparative 6% SDS-PAGE gels. The densin-180 protein band was cut from each gel. Gel pieces were pooled, chopped into 5 mm pieces, and electroeluted into 25 mM N-ethyl morpholine, pH8.5 / 0.1% SDS at 250V in an Elutrap device (Schleicher & Schuell). The electroeluted protein (1.2 mg) was fractionated on a second set of 8 preparative 6% SDS-PAGE gels, transferred to nitrocellulose, and trypsinized as previously described (Aebersold et al., 1987). The trypsinized densin-180 protein was concentrated to 0.4 ml and fractionated on a C4 high performance liquid chromatography (HPLC) column with a gradient of 3.5% to 73.5% acetonitrile in 0.1% trifluoroacetic acid. We hand-collected fractions of 0.1 to 1.0 ml corresponding to the elution of major peaks of absorbance at 280nm. Most of the major peaks were not single peptides and were further fractionated on a second C18 HPLC column. Peak fractions were again collected by hand, flash frozen in liquid nitrogen, concentrated to 50-100  $\mu$ l, and submitted to the Caltech Biopolymer Analysis Facility for peptide sequencing on an ABI automated gas phase sequencer. Amino acid sequences were obtained from seven of these samples with initial yields of 1-25 pmoles.

### **Molecular cloning of densin-180**

Degenerate oligonucleotide primers were designed based on the three unique peptide sequences, synthesized on an ABI automated oligonucleotide synthesizer, and used as primers to amplify 5 week old rat forebrain cDNA by the polymerase-chain reaction (PCR) (Saiki et al., 1988). The cDNA was prepared from mRNA with the "First Strand cDNA" kit purchased from Clontech. The PCR reactions contained 0.2  $\mu$ M each of sense and antisense primer, 2.5 mM each of dATP, dCTP, dGTP and dTTP (Boehringer Mannheim), 3.75 ng/ $\mu$ l cDNA, 125 mU/ $\mu$ l Taq polymerase (Boehringer Mannheim), 1X Taq polymerase buffer (supplied with enzyme) and 0.5 mM extra  $MgCl_2$ . PCR products from large-scale reactions (100  $\mu$ l) were purified by agarose gel electrophoresis, inserted into the TA plasmid supplied with the TA cloning kit (InVitrogen), and the plasmid was amplified by growth in *E. coli*. We sequenced the ends of each cloned PCR product by priming with oligonucleotides complementary to the M13 and T7 promoter sites in the TA plasmid. This permitted us to check which PCR products encoded the entire sequence of the original pair of peptides, including those amino acids that were not encoded in the original PCR primers. The sequence of the ends of one 1.2 kb product encoded the complete sequences of peptides 1 and 3. This product was purified by agarose gel electrophoresis, labeled with  $^{32}P$  according to the "Random Primed DNA Labeling Kit" (USB), and used to screen a  $\lambda$ ZapII cDNA library prepared from 13 to 16 day old rat brains (Snutch et al., 1990, PNAS 87:3391-3395, generously provided by T.Snutch). Positive cDNA clones were plaque purified, then excised from  $\lambda$ ZapII with the ExAssist<sup>TM</sup>/SOLR<sup>TM</sup> system (Stratagene). The cDNA inserts were aligned and classified by restriction mapping. The cDNAs were ligated into the BlueScript plasmid (Stratagene) and sequenced by the method of Sanger (Sanger et al., 1977) according to the instructions

supplied with the “Sequenase” kit (USB). Initial sequencing from primers complementary to the Bluescript vector and to the PCR product revealed that clone 1.1 (5.2 kb) contained a 5' ribosome binding site and initiation codon as well as a long open-reading frame including sequences encoding peptides 1 and 3. We sequenced exonuclease digests of clone 1.1 generated with the Erase-a-Base System™ (Promega) in both directions. Gaps in the sequence were filled in using oligonucleotide sequence primers. These primers were also used for the partial sequencing of other clones. Programs of the Wisconsin Package (Genetics Computer Group) and local programs at the Caltech Sequence Analysis Facility were used for sequence assembly, motif searches, and hydrophobicity analysis.

### **Preparation of antibodies against densin-180**

We amplified two regions of the densin-180 cDNA encoding amino acids 466-958 and 1374-1495 by PCR, then cloned the products into the pGEX2T vector (Pharmacia Biotech, Inc.). The PCR products were sequenced to ensure that no mutations were introduced during the PCR reaction. The recombinant pGEX2T plasmids were grown in protease-deficient (lon-) E.Coli cultures at 30° C to an optical density of 0.5 at 600nm wavelength. A one liter culture was induced with 0.1 mM IPTG for 5 hours at 30° C and cells were pelleted by centrifugation at 5,000 g for 10 min. Pellets were resuspended in 40 mls of lysis buffer (20 mM sodium phosphate, pH 7.4 / 0.15 M NaCl / 1X protease inhibitor cocktail [Boehringer Mannheim] / 0.5 mM DTT / 10 U/ml DNase [Boehringer Mannheim]). The cells were lysed by sonication (2 minutes, level 6, 50% pulse with Branson Sonifier 450), Triton X-100 was added to 1%, and the solution was mixed well. Lysates were cleared by centrifugation for 10 minutes at 10,000g. The supernatant fractions were applied to a washed column containing 100 mg glutathione-agarose beads

(Sigma Chemicals). The column was washed twice with 40 mls PBS (20 mM sodium phosphate, pH 7.4 / 0.15 M NaCl) and the GST fusion proteins were eluted with 10 mM reduced glutathione (Sigma Chemicals) / 50 mM Tris-Cl pH 8 / 1% TritonX-100. The purity and concentration of the proteins in each eluted fraction was estimated by SDS-PAGE and by subsequent staining with Coomassie blue.

The fusion protein containing amino acids 466-958 of densin-180 was further purified by electrophoresis on 6% SDS-PAGE gels. The full-length fusion protein was visualized by soaking in 0.25 M KCl and cut from the gel for injection into Swiss-Webster mice as an antigen for production of polyclonal ascites fluid (Ou et al., 1993). One mouse (M2) produced antibodies specific for densin-180 when used for immunoblots, immunoprecipitations or immunostaining. This M2 ascites fluid (3 ml) was purified by 50% ammonium sulfate precipitation overnight at 4°C followed by centrifugation at 10,000g for 10 minutes. The protein pellet was resuspended in 1 ml of 25 mM Tris-HCl pH 7.5 and dialyzed against two changes of the same buffer overnight. Purified M2 Ascites fluid was used for immunoblots of PSD fraction (at 1:3,000 dilution), immunoprecipitation from PSD fraction (at 1:10 dilution) and immunofluorescent staining (at 1:150 to 1:300 dilution).

The fusion protein containing residues 1374-1495 of densin-180, corresponding to the carboxyl-terminus containing the PDZ domain, eluted from the glutathione column as 95% full-length protein and was dialyzed against PBS, diluted to 1 mg/ml in PBS and used to immunize rabbits (Cocalico Biologicals, Inc). The rabbit polyclonal antibodies (termed CT245) were highly specific for densin-180 on immunoblots and could be used for immunocytochemistry. CT245 serum was used for immunoblots of the PSD fraction (at 1:25,000 to 1:50,000 dilution) and for immunofluorescent staining (at 1:2500 to 1:5,000

dilution).

### **Immunoblots**

Proteins were separated by SDS-PAGE under reducing conditions, electrophoretically transferred to nitrocellulose, and blocked for 2 hours to overnight in 5% normal goat serum (NGS) diluted in TTBS (0.2% Tween-20, 10 mM Tris-Cl pH 7.5, 0.2 M NaCl). After 1 wash in TTBS for 10 minutes, blots were incubated in primary antibodies diluted in TTBS / 1% NGS for 3 hours to overnight. Blots were washed three times in TTBS, then incubated for 1 hour in alkaline-phosphatase-conjugated goat anti-mouse or goat anti-rabbit secondary antibodies (Boehringer Mannheim) diluted in TTBS / 1%NGS. After three 10 minute washes with TTBS, blots were developed according to the suppliers instructions.

### **Subcellular fractions of rat brain**

Forebrain homogenates, synaptosomes and detergent-extracted PSD fractions were prepared from Sprague-Dawley rats exactly as described in (Cho et al., 1992).

For the membrane extraction experiments, we prepared a crude membrane fraction by homogenizing 2 rat forebrains in 20 mls of Buffer A (0.32 M Sucrose / 1 mM sodium bicarbonate / 1 mM  $MgCl_2$  / 0.5 mM  $CaCl_2$  / 0.1 mM PMSF / 1 mg/ml leupeptin) at 4° C with 6 strokes of a teflon/glass homogenizer rotating at 900 rpm. The homogenate was cleared by centrifugation at 2500g for 10 minutes, and the supernatant was divided into 10 separate tubes containing 2 mls each. Membranes were pelleted by centrifugation at 170,000g for 45 minutes and the crude membrane pellets were resuspended in 2 mls of each test extraction buffer by 5 up and down strokes in a teflon glass homogenizer. The

extractions were incubated at 4<sup>0</sup>C for 30 minutes and the membrane residue was pelleted by centrifugation at 170,000g for 45 minutes. Supernatants were collected and the pellets were resuspended in HKA buffer (10 mM HEPES-KOH pH7.5/140 mM Potassium Acetate/1 mM MgCl<sub>2</sub>/0.1 mM EGTA/0.1 mM PMSF/5 mg/ml leupeptin). The pellet and supernatant fractions were frozen in aliquots at -80° C for use in immunoblots. We used the following extraction buffers: 1 M NaCl, 2% CHAPS, 2% Triton X-100, 1 M NaCl/2% CHAPS or 1 M NaCl/2% Triton X-100, all in HKA buffer, or 0.2 M Sodium bicarbonate buffer, pH11. The presence of densin-180 in each fraction was assessed by immunoblotting. Immunoblots with antibody specific for synapsin I were used for comparison. Approximately 90% of synapsin was solubilized in 2% CHAPS, 1 M NaCl/2% CHAPS, 2% Triton X-100, 1 M NaCl/2% Triton X-100, and pH 11 buffers, but only 30% was solubilized in 1 M NaCl.

### **Deglycosylation with neuraminidase**

Aliquots of PSD protein (40 µg) were denatured by boiling for 3 minutes in 0.8% SDS. N-octyl glucoside was added to a final concentration of 3%. Deglycosylation reactions were prepared containing denatured PSD protein (0.8 mg/ml), 0.2 M sodium phosphate buffer, pH 7.2, and Complete<sup>TM</sup> Protease inhibitor cocktail (Boehringer Mannheim). Forty mU of neuraminidase from *Arthrobacter ureafasciens* (Boehringer Mannheim) was added in two aliquots and the reaction proceeded for a total of 24 hours at 37° C. Control reactions contained no added neuraminidase or included the neuraminidase inhibitor N-Bromo-succinimide at 10 mM, added in two aliquots with the neuraminidase. Fresh protease inhibitors were added twice during the reaction to all tubes. Reactions were terminated by boiling in SDS/PAGE sample buffer for 3 minutes. Proteins were

fractionated by SDS/gel electrophoresis, and densin-180 was detected by immunoblotting.

### **Digestion of densin-180 with O-sialoglycoprotease**

Twenty four  $\mu\text{g}$  of non-denatured PSD protein was incubated with 36  $\mu\text{g}$  O-sialoglycoprotease from *Pasteurella hemolytica* (ACCURATE Chemical & Scientific Corporation) in 20 mM sodium phosphate pH 7.4/0.15 M NaCl/ 0.2 mM PMSF in a final volume of 60  $\mu\text{l}$ . Protease reactions were incubated at 37° C for 15 minutes, 1 hour, or 3 hours. Control reactions without added protease were incubated for 3 hours. Reactions were terminated by boiling in SDS-PAGE sample buffer for 3 minutes, and proteolytic products were fractionated by SDS-PAGE. Fragments of densin-180 were detected on immunoblots probed with either M2 or CT245 anti-densin-180 antibodies. Control immunoblots were probed with anti-PSD-95 (1:10,000; Cho et al., 1992) or anti-NMDA receptor 2B antibodies (1:80,000; Kornau et al., 1995).

### **Phosphorylation and immunoprecipitation of densin-180**

Phosphorylation reactions contained 24  $\mu\text{g}$  of PSD protein, 50 mM Tris-Cl pH8, 10 mM  $\text{MgCl}_2$ , 0.4 mM EGTA, 10 mM DTT and 10  $\mu\text{g/ml}$  added calmodulin in a final volume of 50  $\mu\text{l}$ . Some reactions also contained 0.6 mM calcium and/or a mixture of 4A11 (0.3  $\mu\text{g}/\mu\text{l}$ ) and 6E9 (0.4  $\mu\text{g}/\mu\text{l}$ ) anti-CaMKII inhibiting monoclonal antibodies (Molloy and Kennedy, 1991). After a 3 min pre-incubation at 30° C,  $^{32}\text{P}$ -ATP (10,000 cpm/pmol) was added to a final concentration of 25 $\mu\text{M}$  and the reaction was incubated for 2 min at 30° C. Phosphorylation was terminated by addition of SDS (0.2% final), followed by boiling for 3 min. For immunoprecipitation, the phosphorylated protein was brought to a

final concentration of 0.28 mg/ml phosphorylated PSD protein in 1X RIPA buffer [10 mM Tris-Cl pH 7.4 / 1 mM EDTA / 150 mM NaCl / 1% Triton X-100 / 1% sodium deoxycholate / 0.1% SDS] in a final volume of 85  $\mu$ l. The solutions were pre-cleared by incubation with 50 $\mu$ g washed protein A-Sepharose beads (Pierce) at 4° C for 2 hours. Precleared supernatant was collected and incubated with M2 antibody (10  $\mu$ l) overnight at 4° C. This solution was added to 100 $\mu$ g washed Protein A-beads and incubated at 4° C for two hours. After 3 washes in 1X RIPA buffer, the beads were boiled for 5 minutes in 50 $\mu$ l 1.5 X SDS-gel buffer and applied to a 7.5% SDS-PAGE minigel. After electrophoresis, the gel was stained with Coomassie R-250, dried, and subjected to autoradiography. The amount of densin-180 protein was estimated by comparing the Coomassie-stained densin-180 band with stained bovine serum albumin standards. Bands corresponding to densin-180 were cut from the gel and their radioactivity was determined in a Beckman liquid scintillation counter. The stoichiometry of densin phosphorylation was estimated at 1 mol/mol by calculating a calcium-induced incorporation of 0.21 pmol <sup>32</sup>P- phosphate into 40 ng (.22 pmoles) of densin-180 protein.

### **Isolation of mRNA and Northern blotting**

Total RNA was isolated from rat tissues (frozen in liquid nitrogen and purchased from Pel Freeze Biologicals or Harlan Bioproducts) with the acid guanidinium thiocyanate-phenol-chloroform-extraction method (Chomczynski and Sacchi, 1987) and purified on CsCl gradients. PolyA+ RNA was isolated with the PolyATtract mRNA Isolation System (Promega). RNA from different tissues was fractionated on 1% agarose gels and transferred to Zeta-Probe membranes (BIO-RAD) overnight in 20X SSC (3 M NaCl/0.3 M Trisodium citrate). RNA transfer was confirmed by staining with methylene

blue. A cDNA probe corresponding to nucleotides 1950-2400 of the densin-180 cDNA was amplified by PCR. The PCR product and human  $\beta$ -actin cDNA (Clontech) were radiolabeled by random priming (Random Primed DNA Labeling Kit from USB) to specific activities of  $10^9$  and  $10^7$  cpm/ $\mu$ g, respectively. The RNA blots were probed with the labeled cDNAs according to the protocol suggested for use with the Zeta-Probe membrane. Labeled bands were detected by autoradiography.

### **Immunocytochemical labeling of dissociated hippocampal neurons**

Hippocampi from E18 rats were dissociated by trypsinization and cells were plated on laminin-coated coverslips (15 mm in diameter) at a density of approximately 200 per  $\text{mm}^2$ . Cultures were plated and maintained in the B27 media described by (Brewer et al., 1993). After 2 to 4 weeks *in vitro*, the coverslips were removed from the culture wells and placed cell-side up into wells containing ice-cold PBS. After washing briefly in ice-cold methanol, cultures were fixed with  $-20^\circ\text{C}$  methanol for 20 minutes, washed once with PBS for 15 minutes, then pre-blocked in 5% normal goat serum/0.05% TritonX-100/450 mM NaCl/20 mM phosphate buffer, pH 7.4 for one hour at  $4^\circ\text{C}$ . Next, primary antibodies were added in the preblock buffer at appropriate dilutions and incubated overnight at  $4^\circ\text{C}$ . In addition to the M2 and CT245 anti-densin-180 antibodies, the following antibodies were also used for immunofluorescent staining: anti-synapsin I rabbit antiserum at a 1:1000 dilution, affinity-purified anti-PSD-95 rabbit antiserum at 60  $\mu\text{g}/\text{ml}$  final concentration (both described in Cho et al., 1992), and 6G9 anti- $\alpha\text{CaMKII}$  at 20  $\mu\text{g}/\text{ml}$  (Erondy and Kennedy, 1985). After 3 washes in the preblock solution, the coverslips were incubated in goat anti-mouse or goat anti-rabbit secondary antibodies conjugated to FITC or Cy3 fluorophores (diluted 1:100 in preblock) at RT. Coverslips

were washed once in the preblock buffer for 15 min, twice with PBS for 15 min, post-fixed 5 min with 2% paraformaldehyde, washed twice with PBS for 10 min, and twice with 0.1 M sodium bicarbonate pH 9.2 for 5 min. Coverslips were then mounted on slides in 80% glycerol / 4 mg/ml p-phenylenediamine / 0.1 M sodium bicarbonate buffer, pH9.2, left at RT for 2 hours, then either viewed immediately, or stored at -20° C for no longer than one week. Cultures were viewed in a fluorescence laser-scanning confocal microscope (Zeiss LSM310). A 63X oil immersion objective was used at electronic zoom factors of 1 or 2. Images were scanned at 64 sec. Fluorescein was excited at 488nm and Cy3 at 543nm. Images were collected through filters appropriate for the two fluorophores. The contrast and brightness setting were optimized to spread the data over the 8-bit range. Contrast settings were 360-410 and brightness settings were 6000-6800. Double images were colorized and aligned in Adobe Photoshop without adjusting the original data. Final images were printed at 300 dpi resolution on a Kodak XLS 8300 Printer.

The concentrations of the antibodies were estimated by comparison to IgG standards on SDS-PAGE gels after staining with Coomassie Blue R-250. The M2 mouse IgG was ~0.3 mg/ml and the CT245 rabbit IgG was ~5 mg/ml. Preabsorption of anti-densin-180 antibodies with antigen at a 1:3 molar ratio entirely blocked staining at the contrast and brightness settings above.

## RESULTS

### PCR cloning based on tryptic peptide sequences

The purification of densin-180 (previously termed PSDup-180) was described previously Moon et al., 1994. Briefly, the crude PSD fraction was isolated from rat forebrain, extracted with 1% NOG, deglycosylated and applied to 6% preparative SDS polyacrylamide gels. Densin-180 was then electroeluted and trypsinized as described under Materials and Methods. Seven tryptic peptides were purified sufficiently for automated sequencing. A search of the GenBank data base performed with the BLAST network service revealed that three of these peptide sequences are not homologous to any known protein.

Initial attempts to select cDNA clones by screening several libraries with radiolabeled “guessmer” oligonucleotides based on the sequence of peptide 1 proved unsuccessful. Therefore, we used a PCR-based approach similar to that of (Saiki et al., 1988). Several sets of degenerate 29 base sense and antisense oligonucleotide primers were designed based on the sequences of the three peptides (Figure 1A). The neutral base inosine was included at 8 or fewer positions to reduce primer degeneracy to no more than 32-fold. All possible combinations of sense and antisense primers were used for PCR amplification of rat brain cDNA. Out of all possible primer combinations, only the (1Sense + 3Antisense) reaction produced a 1.2 kb PCR product that was absent in control reactions containing only the primers (Figure 1C). This product was cloned and sequenced. The strategy for obtaining and analyzing this clone is diagrammed in Figure 1B. The sequence immediately 3' downstream of the 1Sense primer encoded the amino acids Val-Arg, matching the corresponding amino acid sequence of peptide 1. In addition, the complementary sequence immediately 3' downstream of the 3Antisense primer

encoded the amino acids Ser-Gln-Ser, corresponding to the amino acid sequence of peptide 3. We found that the 1.2 kb fragment could be amplified from rat brain cDNA, but not from cDNA made from other tissues (data not shown), suggesting that the encoded protein is brain specific. Partial sequences of the PCR product were compared to the database and found to encode a novel protein.

### **Cloning and sequencing of full length densin-180 cDNAs**

The PCR product was labeled by random priming and used to screen a Lambda Zap II rat brain cDNA library (kindly provided by Dr. Terry Snutch). Five independent positive cDNA clones spanning 6.8 kb were aligned by restriction mapping and partial sequencing (Figure 1D). The entire 5.2 kb cDNA clone 1.1 was sequenced; we found that it contains the complete densin-180 open reading frame. It includes an initiation codon at position 186 preceded by a stop codon at 177, which fits the consensus for translation initiation sites (Kozak, 1989). There is also a purine-rich Shine-Dalgarno ribosome binding consensus motif beginning about 10 nucleotides upstream of the initiation codon (Shine and Dalgarno, 1974). This initiation codon is followed by a single 4485 bp open reading frame encoding a 1495 residue protein with a molecular weight of 167,499. The complete nucleotide sequence and the amino acid sequence that it encodes is shown in Figure 2. All three of the original tryptic peptide sequences (Figure 1) are present in the amino acid sequence. Sequences 1 and 3 match exactly and sequence 2 has one mismatch (Arg at position 8 corresponds to a Trp in densin-180). This mismatch most likely results from an ambiguous call during the peptide sequencing and explains the absence of specific PCR products from the 1Sense/2Antisense and 2Sense/3Antisense primer combinations.

The message encoding densin-180 may be alternatively spliced. Partial sequencing

of two more of the cDNAs (2.1 and 3.1; Fig. 1D) revealed possible splice variants. A 76 nucleotide sequence is missing at the 5' end of clone 2.1 when compared to clone 1.1 (underlined in Figure 2). This sequence spans nucleotides 111 to 186 of the densin-180 sequence and includes the ribosome binding site and the adenosine of the ATG initiation codon. Clone 3.1 contains a 249 bp deletion between nucleotides 1631 and 1881 of clone 1.1 that does not shift the reading frame (underlined in Figure 2).

### **Domain structure of densin-180**

A search of the GenBank data base performed with the BLAST network service through the National Center for Biotechnology Information revealed significant homology in the N-terminus of densin-180 with the superfamily of leucine-rich repeat (LRR) containing proteins. Alignment of the 15 contiguous LRRs in densin-180 reveals a repeating 23-residue consensus sequence (Figure 3A) that fits the general consensus defined for LRRs from a variety of transmembrane and secreted proteins, including adhesion molecules (for review of LRR-containing proteins, see (Kobe and Deisenhofer, 1994 and Kobe and Deisenhofer, 1995b). LRRs vary from 20 to 29 residues in length, with 24 residues most common. Clusters of cysteine residues are found immediately flanking the LRRs. At the amino terminus, three cysteine residues are found between amino acids 19 and 37, and on the carboxyl side six cysteine residues are found between residues 486 and 546. Cysteine-rich domains typically flank the LRRs of adhesion molecules, but the densin-180 cysteine clusters seem to be of a different type since they do not match the consensus described in (Kobe and Deisenhofer, 1993).

Amino acids 825-915 define a region rich in serine, threonine and proline residues similar to repeats found in mucin. Mucin-like repeats are thought to serve as sites of

attachment of O-linked sugars in mucin and many other proteins, including GPIb $\alpha$  (for review, see Strous and Dekker, 1992 and Van Klinken et al., 1995).

The BLAST search identified a clear PDZ domain at the carboxyl-terminus, spanning residues 1405 to 1492. (Figure 3B). The PDZ motif was first defined in PSD-95, another PSD protein identified in our laboratory. The motif is present in a variety of other proteins associated with intracellular junctions including the *Drosophila* discs-large (dlg) protein (Woods and Bryant, 1991) and the human tight junction protein, ZO-1 (Itoh et al., 1993).

Initial analysis of the densin-180 sequence failed to reveal a hydrophobic signal sequence expected in a transmembrane protein. However, the SIGCLEAVE program identified an embedded signal sequence spanning amino acids 28-40 with cleavage at residue 41 and a score of 3.6. The SIGCLEAVE program uses the von Heijne method to locate signal sequences and is 95% accurate with a score of 3.5 or higher. Using the method of Kyte and Doolittle to predict regions of high hydrophobicity in the sequence, we have assigned a transmembrane domain from residues 1223 to 1246, placing the PDZ domain on the cytosolic side. The 24-residue putative transmembrane domain is atypical because it contains nine charged and polar amino acids. Helical wheel projections of this region using the HELICALWHEEL program reveal an amphipathic helix-like structure with one face of the alpha-helical surface containing exclusively hydrophobic residues and the rest of the surface containing a mixture of hydrophobic, charged and polar residues (data not shown).

Analysis of the sequence with the MOTIFS program identified an Arg-Gly-Asp (RGD) tripeptide sequence between the LRR domain and the cysteine rich repeats (amino

acids 437-439 in Figure 2). The RGD tripeptide was originally identified as a sequence in fibronectin that mediates cell attachment. RGD sequences from fibronectin and a number of other proteins have been found mediate adhesion via binding to integrins (for review, see D'Souza et al., 1991). Finally, we identified two consensus sequences that are potential sites of phosphorylation by CaM Kinase II (Figure 2; see below).

The arrangement of domains in densin-180 is similar to that of the family of LRR-containing glycoproteins, although there is little significant sequence homology with any of them. One of the most well-characterized of the LRR-containing glycoproteins is the platelet adhesion molecule GPIb $\alpha$  (Lopez et al., 1987). Both densin-180 and GPIb $\alpha$  contain leucine-rich repeats flanked by cysteine rich domains and mucin homology domains in the putative extracellular portion of the proteins (Figure 3C). The PDZ domain of densin-180, which likely represents a protein binding site (Kornau et al., 1995 and Kim et al., 1995), is in a position analogous to the cytosolic actin binding protein (ABP)-binding domain of GPIb $\alpha$ . GPIb $\alpha$  is part of a protein complex that mediates binding of von Willebrand factor via its LRR domain and flanking cysteine-rich domain. The binding induces adhesion of platelets to blood vessels (for review, see Williams et al., 1995). The C-terminus of GPIb $\alpha$  has been shown to interact with actin binding protein (ABP) to mediate association with the cytoskeleton (Andrews and Fox, 1992).

### **Densin-180 associates with the particulate fraction**

The domain structure of densin-180 places it in the family of LRR-containing glycoproteins which span the membrane, yet the putative transmembrane domain contains several charged and polar amino acids. To test whether densin-180 associates with

membrane fractions, we extracted crude membranes from rat forebrain with detergent and/or salt. Immunoblots of the soluble and particulate fractions were prepared and probed with specific mouse polyclonal antibodies raised against recombinant densin-180 protein. These antibodies react strongly with a 180 kDa band that migrates at the position of the densin-180 protein on an SDS gel (Fig. 4). Densin-180 is not solubilized by extraction with 2% Triton X-100, or 2% CHAPS, conditions that solubilize many membrane proteins, but do not solubilize proteins tightly bound to the PSD fraction. When the membranes were extracted with 1 M NaCl to disrupt protein interactions densin-180 also remained in the pellet fraction. However, when the membranes were extracted with a combination of 1 M NaCl and 2% Triton X-100 or of 1 M NaCl and 2% CHAPS, approximately half of the densin-180 was solubilized. Taken together, the solubility profile is consistent with anchoring of densin-180 in the membrane fraction by a combination of lipid and protein interactions.

Extraction with sodium bicarbonate buffer, pH 11, also solubilized about half of the densin-180. It is generally assumed that high pH buffers extract mainly peripheral membrane proteins, yet its sequence and biochemical characteristics (see below) suggest that densin-180 is a transmembrane protein. This unusual extraction profile could reflect the atypical sequence of densin-180's putative transmembrane domain. The ability of the two positive (R, K) and two negative (D, E) residues in this domain to form salt bridges with other transmembrane proteins may explain the sensitivity of densin-180 to extraction in pH11 buffers.

### **Densin-180 is a sialoglycoprotein**

The predicted amino acid sequence of densin-180 implies a molecular weight of

167 kDa, but the densin-180 protein migrates at an apparent molecular weight of 188 kDa on a 7.5% SDS polyacrylamide gel. One explanation for this discrepancy could be that it is glycosylated, as would be expected for a transmembrane protein. We tested whether densin-180 is glycosylated by treating the PSD fraction with various glycosidases. Only very slight shifts in the mobility of densin-180 were observed after treatment with N-glycosidase F or O-glycosidase. However, a shift in its apparent molecular weight from approximately 188 kDa to 148 kDa was evident after treatment with neuraminidase from *Arthrobacter ureafasciens* (Figure 5A). The shift in molecular weight was due to the neuraminidase activity and not to contaminating protease activity because addition of a specific inhibitor of the *Arthrobacter ureafasciens* neuraminidase, 10 mM *N*-bromosuccinimide, inhibited the shift in molecular weight. Thus, the densin-180 protein is heavily glycosylated with sialic acid residues.

An O-sialoglycoprotein endoprotease has recently been identified from *Pasteurella haemolytica* that specifically cleaves proteins containing mucin-like O-linked glycans (Abdullah et al., 1992 and reviewed in Mellors and Sutherland, 1994). Substrates that have been identified contain 15 or more closely spaced O-linked glycosylation sites along the protein backbone (Norgard et al., 1993). These substrates include GPIb $\alpha$  (Yeo and Sutherland, 1993), cranin (Smalheiser and Kim, 1995), glycophorin A (Abdullah et al., 1992), CD34 and CD43 (Sutherland et al., 1992), and epiglycanin (Kemperman et al., 1994). To test the sensitivity of densin-180 to this protease, an aliquot of the non-denatured PSD fraction was incubated with protease for varying times (Fig. 5B and 5C). PMSF was included in all incubations to inhibit serine proteases. The digested PSD proteins were fractionated by SDS-PAGE, transferred to nitrocellulose, and incubated with

antibodies M2 and CT245, which are specific for the extracellular and intracellular portions of densin-180, respectively. After 3 hours of incubation with protease, complete loss of the 185 kDa densin-180 band was evident in both immunoblots. The pattern of proteolysis detected with each antibody was consistent with initial proteolysis at a site near the mucin homology domain of densin-180, producing extracellular fragments with approximate molecular weights of 140 and 120 kDa detected by the M2 antibody. The largest major breakdown product detected with the CT245 antibody had a molecular weight of approximately 65 kDa, corresponding to a site of initial proteolysis in the mucin homology domain of densin-180. The CT245 antibody also detects a 21 kDa protease-resistant fragment even after 3 hour incubations (Figure 5B), suggesting that the C-terminal region of densin-180 may be inaccessible to the protease because of tight interactions with other PSD proteins. Epitopes of other sialoglycoproteins have been shown to resist proteolysis (see Mellors and Sutherland, 1994). Control blots of PSD digests detected no O-sialoglycoprotein sensitivity for either NR2B or PSD-95, even after 3 hours incubations (data not shown).

### **Densin-180 is phosphorylated by CaM Kinase II**

CaM Kinase II (CaMKII) is highly concentrated in the PSD as determined by both biochemical and immunocytochemical experiments (Kennedy et al., 1983 and Kennedy et al., 1990) and can be activated *in vitro* in the PSD fraction. We labeled substrates of CaMKII in the PSD fraction by carrying out a phosphorylation reaction for two minutes at 30° C in the presence of calcium, calmodulin, and <sup>32</sup>P-ATP. After phosphorylation, densin-180 was immunoprecipitated from the PSD fraction. Figure 6 shows an autoradiogram of the immunoprecipitates. Phosphorylation was stimulated by calcium and

reached a stoichiometry of approximately one picomole phosphate per picomole protein, estimated as described under Materials and Methods. The reaction was inhibited approximately 90% by addition of two antibodies against CaMKII that have been shown to inhibit kinase activity (Fig. 6, lane 3; Molloy and Kennedy, 1991). Thus, densin-180 is specifically phosphorylated by endogenous CaMKII in the PSD fraction. This phosphorylation and the extensive glycosylation of densin-180 are consistent with the transmembrane orientation proposed in Fig. 3C.

### **Densin-180 mRNA is detected only in brain**

Northern blots prepared with PolyA+ RNA from several tissues of 10 week old rats and from forebrain of 5 week old rats were probed for messages encoding densin-180. A single 7.4 kb message was detected in forebrain, and faintly in cerebellum (Figure 7A). There was no detectable densin-180 mRNA in any of the other tissues. Densin-180 mRNA was expressed at a higher level in the forebrain of 5 week old than of 10 week old rats (leftmost lane of Fig. 7A), suggesting age-dependent regulation of mRNA expression.

### **Densin-180 is highly enriched in PSD fractions**

One criterion for specificity of the association of a protein with the PSD fraction is its enrichment in the PSD fraction, compared to other subcellular fractions. This enrichment has been shown for CaMKII (Kennedy et al., 1983), PSD-95 (Cho et al., 1992), and the 2B subunit of the NMDA receptor (Moon et al., 1994). We prepared immunoblots of rat brain homogenates, synaptosomes, and three different PSD fractions extracted with successively harsher detergent (Figure 7B). The 180 kDa densin-180 band

is highly enriched in synaptosomes as compared to crude homogenate and is also enriched in all of the detergent-extracted PSD fractions compared to synaptosomes. Densin-180 remained associated with the PSD fraction even after extraction with N-lauroyl sarcosinate and therefore can be considered a “core” PSD protein.

### **Densin-180 is located at synapses in dissociated hippocampal neurons**

Antibodies to densin-180 were used for immunocytochemical staining of dissociated rat brain hippocampal cell cultures. Hippocampal neurons plated at E18 were grown in culture for two to four weeks (Brewer et al., 1993). Cells were stained as described under Materials and Methods with antibodies against densin-180, synapsin I, PSD-95 and the  $\alpha$  subunit of CaMKII. Confocal imaging revealed that the staining for densin-180 was membrane-associated and punctate along dendrites with little cytoplasmic staining above background (Figure 8). Staining of the axon initial segment was also frequently observed (Figure 8B). The pattern of staining was identical for the M2 and CT245 antibodies (Appendix I). Staining with both antibodies was completely blocked by overnight preabsorption with their antigens (Appendix I).

We used mouse and rabbit anti-densin-180 antibodies to double-label with antibodies against other synaptic markers. Staining for synapsin I overlaps significantly with densin-180 staining (Figure 8A) and thus confirms that densin-180 is a synaptic protein. Synapsin I associates with synaptic vesicles in the presynaptic terminals of neurons. At higher magnification, it is evident that the synapsin I is present in a larger area than densin-180, extending away from the dendrite. This structure likely corresponds to the presynaptic terminal (Figure 8A, inset).

Double-labeling with antibodies to densin-180 and PSD-95 revealed a more strict

correlation of the extent of staining (Figure 8B, inset). Finally, double-labeling with densin-180 and the  $\alpha$  subunit of CaMKII resulted in correlated punctate staining along dendrites. However, densin-180 is not found in as large quantities in the cytoplasm of dendritic shafts or cell bodies as is CaMKII (Fig. 8C). Images of this staining at high magnification, reveal that densin-180 is located along dendrites at what appear to be spines (inset, Figure 8C). The high degree of colocalization of densin-180 with the postsynaptic density markers PSD-95 and CaMKII provides additional evidence for localization of densin-180 at the synaptic junction. We have not yet determined whether densin-180 is presynaptic, postsynaptic, or both.

## DISCUSSION

We have employed direct sequencing of protein bands from the PSD fraction, followed by molecular cloning, to characterize proteins associated with the PSD because the highly insoluble nature of the PSD renders traditional biochemical purification schemes inadequate. In the study reported here, the strategy was complicated by the existence of more than one comigrating protein in the region of the densin-180 band (Moon et al., 1994). To circumvent this potential problem, we used a PCR strategy that allowed us to confirm the presence of DNA encoding at least two of our peptide sequences in PCR clones before screening cDNA libraries, reducing the risk of cloning a minor contaminant of the PSD fraction. This strategy enabled us to clone densin-180, a novel LRR-containing molecule expressed only in the brain. The domain structure of densin-180 places it in the leucine-rich repeat containing family of proteins and suggests it is an adhesion molecule. Two cDNA variants were characterized by restriction mapping and partial sequence analysis, in addition to the one described in detail here. One of these lacks the ribosome-binding domain of the 5'-untranslated region, suggesting that alternative splicing might regulate the expression of densin-180. The second variant lacks the carboxy-flanking cysteine rich domain that might be important in ligand binding and is found in a most LRR glycoproteins.

The LRR-containing family of proteins has a wide range of functions including cell adhesion and signal transduction. The crystal structure of one member of the family, porcine ribonuclease inhibitor protein (RI) has been reported. The structure was determined for the protein alone and bound to ribonucleaseA (Kobe and Deisenhofer, 1993 and Kobe and Deisenhofer, 1995a). The structures reveal the molecular basis for the tight

association of RI with the ribonuclease and serve as a model for the high affinity protein-binding by LRRs from other proteins.

The largest group of LRR-containing proteins serve as adhesion molecules. Proteins in this group often contain cysteine rich domains flanking the LRR on the amino- and carboxyl-terminal sides. Many proteins involved in *Drosophila* development are LRR-containing proteins (see Hortsch and Goodman, 1991, for review). *Drosophila* LRRs that mediate homotypic adhesion include chaoptin, important for eye development (Krantz and Zipursky, 1990), connectin, involved in axon pathfinding and formation of neuromuscular connections (Nose et al., 1992, and Meadows et al., 1994), and toll, which is required for formation of dorsal/ventral polarity in the embryo (Hashimoto et al., 1988) and (Keith and Gay, 1990). In mammalian platelets, all four members of the GPIIb complex contain LRRs, but only GPIIb $\alpha$  binds directly to von Willebrand factor inducing adhesion of platelets to blood vessels. In the mammalian brain, densin-180 is a new member of a growing family of LRR glycoproteins that include trk (Martin-Zanca et al., 1989), trkB (Klein et al., 1989); (Schneider and Schweiger, 1991), oligodendrocyte myelin glycoprotein (Mikol et al., 1990) and NLRR-3 (Taniguchi et al., 1996).

Densin-180 contains an RGD cell attachment motif between the last LRR and the C-terminal cysteine rich domain (Fig. 2). NLRR-3 cloned from mouse brain is an LRR-glycoprotein that contains an RGD sequence in the predicted  $\alpha$ -helical region of the eighth LRR. RGD motifs in extracellular matrix molecules have been shown to mediate intracellular responses by binding to integrins (D'Souza et al., 1991). There is evidence for integrins at the synapse since RGD peptides block long-term potentiation (Xiao et al., 1991) and a 55 kDa RGD-binding protein purified from synaptic membranes cross-reacts

with anti- $\alpha_5\beta_1$  integrin antibodies (Bahr and Lynch, 1992). Thus, densin-180 and NLRR-3 may interact with integrins.

We have identified densin-180 as a sialomucin by two criteria; the large shift in its apparent molecular weight on SDS-gels after neuraminidase treatment (Fig. 5A), and its sensitivity to proteolysis by O-sialoglycoprotein endopeptidase (Fig. 5B and 5C). The O-sialoglycoprotein endopeptidase is highly specific for sialomucins and is used as a diagnostic tool (Mellors and Sutherland, 1994). GPIb $\alpha$  (Yeo and Sutherland, 1993) and cranin (Smalheiser and Kim, 1995) are also sensitive to this protease. Cranin has recently been identified (Smalheiser and Kim, 1995) as the brain form of alpha-dystroglycan, a putative agrin receptor that mediates acetylcholine receptor clustering at the neuromuscular junction (Fallon and Hall, 1994).

The O-glycosylated domain in sialomucins forms an extended filamentous conformation, 2.5 Angstroms per residue in length (see Strous and Dekker, 1992). The extended structure is surrounded by a cloud of negative charges associated with the sialic acid residues (Jentoft, 1990). In some cases, the negative charges play a protective role by repelling adhesion molecules on other cells. In other cases, O-linked sialic acids are required for specific binding to lectin domains of selectins (Cummings and Smith, 1992). Finally, the filamentous domain can act as a stiff rod to extend a ligand binding domain for interaction with other cells or with the extracellular matrix (reviewed in van der Merwe and Barclay, 1994).

The solubility properties of densin-180 are unusual and are reminiscent of those of  $\alpha$ -dystroglycan, which has been reported as a transmembrane protein, a peripheral protein, and a membrane-associated extracellular protein (Ervasti and Campbell, 1993 and Ma et

al., 1993). Densin-180 is most effectively solubilized either by a combination of non-ionic detergent and high salt or by pH11 buffers. A portion of densin-180 is extracellular as evidenced by its glycosylation. We have identified a possible membrane spanning domain near the carboxyl terminus followed by a PDZ protein-interaction domain (Fig. 3B). It seems most likely that the PDZ domain is located in the cytosol where it would associate with intracellular proteins. However, a definitive model of densin-180's membrane orientation remains to be established.

The cytoplasmic domains of transmembrane proteins often have important functions in signal transduction across the membrane. Examples in the LRR family are toll protein, which contains an interleukin-1-like cytoplasmic domain (Hashimoto et al., 1988) and gp150, which contains a receptor protein tyrosine phosphatase (PTPase)-binding domain that is phosphorylated on a tyrosine residue *in vitro* (Tian and Zinn, 1994). In addition, the ABP binding domain at the C-terminus of GPIIb $\alpha$  is likely to mediate cytoskeletal rearrangement in response to ligand binding (Andrews and Fox, 1992). Densin-180 contains a PDZ domain at its carboxyl terminus that may participate in binding to cytoplasmic elements. PDZ domains have been identified as protein-binding motifs. For example, the second PDZ domain (PDZ2) of PSD-95 interacts with a short sequence SDV\*, termed tSXV, at the extreme C-terminus of the 2B subunit of the NMDA-type glutamate receptor and this interaction has been proposed to anchor NR2B in the PSD (Kornau et al., 1995). Additionally, the PDZ2 domain from PSD-95 binds to tSXV motifs in a subset of potassium channels (Kim et al., 1995), and the PDZ domains of syntrophin and nNOS (Brenman et al., 1996). PDZ domains thus appear to play a role

in the association of proteins in signal transduction complexes, in particular at cellular junctions. The identification of a 21 kDa protease-resistant C-terminal fragment of densin-180 after a 3 hour digestion of densin in the PSD, suggests that this putative cytoplasmic domain may be tightly embedded in the PSD via the PDZ domain. Similar protease-resistant epitopes have been observed in O-sialoglycoprotease digestions of CD34 (Sutherland et al., 1992). It is notable that there is a consensus CaMKII phosphorylation site only two amino acids from the densin-180 C-terminus, immediately following the PDZ domain (Fig. 2). It is possible that the phosphorylation of densin-180 by CaMKII (Fig. 6) regulates the association of densin-180 with binding partners in the PSD.

Immunocytochemical studies suggest a localization of densin-180 at the synaptic membrane (Fig. 8). Double-immunofluorescence labeling with densin-180 and synapsin I, a synaptic vesicle marker, reveals clear co-localization of the two molecules. However, at higher magnification a slight shift of some of the synapsin I staining away from the dendrite relative to the densin-180 staining is apparent (Fig. 8A), suggesting that Densin-180 immunoreactivity is closely associated with the junctional membrane. We have not yet determined whether densin-180 is concentrated on the postsynaptic side of the junction. Double-immunofluorescence labeling of densin-180 and PSD-95, a PSD-marker, reveals that the two molecules precisely colocalize in mature cultured neurons, within the limit of resolution of the laser-scanning confocal microscopy. Interestingly, an exception to the co-localization of densin-180 with PSD-95 is at the axon initial segment. Anti-PSD-95 does not label the initial segment, while densin-180 labels this structure strongly (Fig. 8B). Densin-180 partially colocalizes with CaMKII at what appear to be spines, but does not colocalize with CaMKII in the cytoplasm of dendrites and cell bodies.

Densin-180 and the platelet surface protein GPIb $\alpha$  contain an assembly of similar domains in their structure that suggests they may function in similar way. GPIb $\alpha$  mediates adhesion of platelets to von Willebrand factor (vWF) that is exposed in the extracellular matrix of injured blood vessels. This adhesion has a very rapid rate of bond formation and a high resistance to tensile stress, functioning to immobilize platelets on vWF in the presence of high shear forces. However, this adhesion is also highly reversible and is not sufficient to permanently immobilize platelets to the blood vessel wall. Rather, the GPIb $\alpha$  association with vWF facilitates binding of  $\alpha_{\text{IIb}}\beta_3$  integrins on the platelet surface to the RGD domain of vWF. We hypothesize that a similar type of adhesion may be mediated by densin-180 at the synapse. Possibly, the RGD sequence in densin-180 binds directly to integrins on the surface of apposing synaptic terminals, eliminating the requirement for large extracellular matrix molecules in the synaptic cleft.

In conclusion, the location of densin-180 at the synapse and the similarity of its domain structure to those of adhesion molecules imply a role for densin-180 in the adhesion of pre and postsynaptic membranes. Its domain structure suggests several hypotheses. First, the sialomucin region of densin-180 may form an extended conformation across the synaptic cleft to present the LRR-containing ligand binding domain to the apposing synaptic membrane. Second, the presence of an RGD sequence in this domain suggests that a synaptic membrane ligand may be an integrin-like protein. Third, the O-linked sugars could also mediate selective adhesion through selectin-like molecules. Together, these extracellular motifs have the potential for the tight yet flexible adhesion that may be important in synapse formation, maintenance and plasticity. Fourth, on the cytoplasmic face, densin-180 may participate in assembly and maintenance of the PSD structure through its PDZ domain. Finally, densin-180 function may be regulated by

CaMKII-mediated signal transduction. We are presently testing these hypotheses.

**REFERENCES**

- Abdullah, K. M., Udoh, E. A., Shewen, P. E., and Mellors, A. (1992). A neutral glycoprotease of *Pasteurella haemolytica* A1 specifically cleaves o-sialoglycoproteins. *Infect. Immun.* *60*, 56-62.
- Aebersold, R. H., Leavitt, J., Saavedra, R. A., Hood, L. E., and Kent, S. B. H. (1987). Internal amino acid sequence analysis of proteins separated by one- or two-dimensional gel electrophoresis after in situ protease digestion on nitrocellulose. *Proc. Natl. Acad. Sci. USA* *84*, 6970-6974.
- Andrews, R. K., and Fox, J. E. B. (1992). Identification of a region in the cytoplasmic domain of the platelet membrane glycoprotein-Ib-IX complex that binds to purified actin-binding protein. *J. Biol. Chem.* *267*, 18605-18611.
- Bahr, B. A., and Lynch, G. (1992). Purification of an Arg-Gly-Asp selective matrix receptor from brain synaptic plasma membranes. *Biochem. J.* *281*, 137-142.
- Brenman, J. E., Chao, D. S., Gee, S. H., McGee, A. W., and Craven, S. E. (1996). Interaction of nitric-oxide synthase with the postsynaptic density protein PSD-95 and  $\alpha$ -1-syntrophin mediated by PDZ domains. *Cell* *84*, 757-767.
- Brewer, G. J., Torricelli, J. R., Evege, E. K., and Price, P. J. (1993). Optimized survival of hippocampal neurons in B27-supplemented Neurobasal <sup>TM</sup>, a new serum-free medium

combination. *J. Neurosci. Res.* *35*, 567-576.

Carlin, R. K., Grab, D. J., Cohen, R. S., and Siekevitz, P. (1980). Isolation and characterization of postsynaptic densities from various brain regions: enrichment of different types of postsynaptic densities. *J. Cell Biol.* *86*, 831-843.

Cho, K.-O., Hunt, C. A., and Kennedy, M. B. (1992). The rat brain postsynaptic density fraction contains a homolog of the *Drosophila* discs-large tumor suppressor protein. *Neuron* *9*, 929-942.

Chomczynski, P., and Sacchi, N. (1987). Single-step method of RNA isolation by acid guanidinium thiocyanate phenol chloroform extraction. *Analyt. Biochem.* *162*, 156-159.

Cohen, R. S., Blomberg, F., Berzins, K., and Siekevitz, P. (1977). The structure of postsynaptic densities isolated from dog cerebral cortex I. overall morphology and protein composition. *J. Cell Biol.* *74*, 181-203.

Cotman, C. W., Banker, B., Churchill, L., and Taylor, D. (1974). Isolation of postsynaptic densities from rat brain. *J. Cell Biol.* *63*, 441-455.

Cummings, R. D., and Smith, D. F. (1992). The selectin family of carbohydrate-binding proteins: structure and importance of carbohydrate ligands for cell adhesion. *BioEssays* *14*, 849-856.

D'Souza, S. E., Ginsberg, M. H., and Plow, E. F. (1991). Arginyl-glycyl-aspartic acid (RGD) - a cell adhesion motif article. *TIBS* 16, 246-250.

Erondu, N. E., and Kennedy, M. B. (1985). Regional distribution of type II  $Ca^{2+}$ /calmodulin-dependent protein kinase in rat brain. *J. Neurosci.* 5, 3270-3277.

Ervasti, J. M., and Campbell, K. P. (1993). A role for the dystrophin-glycoprotein complex as a transmembrane linker between laminin and actin. *J. Cell Biol.* 122, 809-823.

Fallon, J. R., and Hall, Z. W. (1994). Building synapses: agrin and dystroglycan stick together. *TINS* 17, 469-473.

Hashimoto, C., Hudson, K. L., and Anderson, K. V. (1988). The *Toll* gene of drosophila, required for dorsal-ventral embryonic polarity, appears to encode a transmembrane protein. *Cell* 52, 269-279.

Hortsch, M., and Goodman, C. S. (1991). Cell and substrate adhesion molecules in *drosophila*. *Annu. Rev. Cell Biol.* 7, 505-557.

Hunt, C. A., Schenker, L. J., and Kennedy, M. B. (1996). PSD-95 is associated with the postsynaptic density and not with the presynaptic membrane at forebrain synapses. *J. Neurosci* 16, 1380-1388.

Itoh, M., Nagafuchi, A., Yonemura, S., Kitani-Yasuda, T., Tsukita, S., and Tsukita, S.

(1993). The 220-kD protein colocalizing with cadherins in non-epithelial cells is identical to ZO-1, a tight junction-associated protein in epithelial cells: cDNA cloning and immunoelectron microscopy. *J. Cell Biol.* *121*, 491-502.

Jentoft, N. (1990). Why are proteins O-glycosylated? *TIBS* *15*, 291-294.

Keith, F. J., and Gay, N. J. (1990). The drosophila membrane-receptor toll can function to promote cellular adhesion. *EMBO J.* *9*, 4299-4306.

Kemperman, H., Wijnands, Y., Wesseling, J., Niessen, C. M., Sonnenberg, A., and Roos, E. (1994). The mucin epiglycanin on TA3/Ha carcinoma cells prevents  $\alpha_6\beta_4$ -mediated adhesion to laminin and kalinin and E-cadherin-mediated cell-cell interaction. *J Cell Biol* *127*, 2071-2080.

Kennedy, M. B., Bennett, M. K., and Erondy, N. E. (1983). Biochemical and immunochemical evidence that the "major postsynaptic density protein" is a subunit of a calmodulin-dependent protein kinase. *Proc. Natl. Acad. Sci. USA* *80*, 7357-7361.

Kennedy, M. B., Bennett, M. K., Bulleit, R. F., Erondy, N. E., Jennings, V. R., Miller, S. M., Molloy, S. S., Patton, B. L., and Schenker, L. J. (1990). Structure and regulation of type II calcium/calmodulin-dependent protein kinase in central nervous system neurons. *C. S. H. S. Q. B.* *55*, 101-110.

Kim, E., Niethammer, M., Rothschild, A., Jan, Y. N., and Sheng, M. (1995). Clustering

of shaker-type K<sup>+</sup> channels by interaction with a family of membrane-associated guanylate kinases. *Nature* 378, 85-88.

Klein, R., Parada, L. F., Coulier, F., and Barbacid, M. (1989). TrkB, a novel tyrosine protein-kinase receptor expressed during mouse neural development. *EMBO J.* 8, 3701-3709.

Kobe, B., and Deisenhofer, J. (1993). Crystal structure of porcine ribonuclease inhibitor, a protein with leucine-rich repeats. *Nature* 366, 751-756.

Kobe, B., and Deisenhofer, J. (1994). The leucine-rich repeat: a versatile binding motif. *TIBS* 19, 415-421.

Kobe, B., and Deisenhofer, J. (1995a). A structural basis of the interactions between leucine-rich repeats and protein ligands. *Nature* 374, 183-186.

Kobe, B., and Deisenhofer, J. (1995b). Proteins with leucine-rich repeats. *Curr. Opin. Struct. Biol.* 5, 409-416.

Kornau, H.-C., Schenker, L. T., Kennedy, M. B., and Seeburg, P. H. (1995). Domain interaction between NMDA receptor subunits and the postsynaptic density protein PSD-95. *Science* 269, 1737-1740.

Kozak, M. (1989). The scanning model for translation: an update. *J. Cell. Biol.* 108,

229-241.

Krantz, D. E., and Zipursky, S. L. (1990). *Drosophila* chaoptin, a member of the leucine-rich repeat family, is a photoreceptor cell-specific adhesion molecule. *EMBO J.* 9, 1969-1977.

Lopez, J. A., Chung, D. W., Fujikawa, K., Hagen, F. S., Papayannopoulou, T., and Roth, G. J. (1987). Cloning of the  $\alpha$ -chain of human platelet glycoprotein-IB - a transmembrane protein with homology to leucine-rich  $\alpha$ -2-glycoprotein. *Proc. Natl. Acad. Sci. USA* 84, 5615-5619.

Ma, J., Nastuk, M. A., McKechnie, B. A., and Fallon, J. R. (1993). The agrin receptor. *J. Biol. Chem.* 268, 25108-25117.

Martin-Zanca, D., Oskam, R., Mitra, G., Copeland, T., and Barbacid, M. (1989). Molecular and biochemical-characterization of the human trk proto-oncogene article. *Molec. Cell. Biol.* 9, 24-33.

Meadows, L. A., Gell, D., Broadie, K., Gould, A. P., and White, R. A. H. (1994). The cell adhesion molecule, connectin, and the development of the *drosophila* neuromuscular system. *J. Cell Sci.* 107, 321-328.

Mellors, A., and Sutherland, D. R. (1994). Tools to cleave glycoproteins. *TIBTECH* 12, 15-18.

Mikol, D. D., Gulcher, J. R., and Stefansson, K. (1990). The oligodendrocyte myelin glycoprotein belongs to a distinct family of proteins and contains the HNK-1 carbohydrate. *J. Cell Biol.* *110*, 471-479.

Molloy, S. S., and Kennedy, M. B. (1991). Autophosphorylation of type II  $Ca^{2+}$ /calmodulin-dependent protein kinase in cultures of postnatal rat hippocampal slices. *Proc. Natl. Acad. Sci. USA* *88*, 4756-4760.

Moon, I. S., Apperson, M. L., and Kennedy, M. B. (1994). The major tyrosine-phosphorylated protein in the postsynaptic density fraction is *N*-methyl-D-aspartate receptor subunit 2B. *Proc. Natl. Acad. Sci. USA* *91*, 3954-3958.

Norgard, K. E., Moore, K. L., Diaz, S., Stults, N. L., Ushiyama, S., McEver, R. P., Cummings, R. D., and Varki, A. (1993). Characterization of a specific ligand for P-selectin on myeloid cells. *J. Biol. Chem.* *268*, 12764-12774.

Nose, A., Mahajan, V. B., and Goodman, C. S. (1992). Connectin - a homophilic cell-adhesion molecule expressed on a subset of muscles and the motoneurons that innervate them in *Drosophila* article. *Cell* *70*, 553-567.

Ou, S. K., Hwang, J. M., and Patterson, P. H. (1993). A modified method for obtaining large amounts of high-titer polyclonal ascites-fluid. *J. Immunol. Meth.* *165*, 75-80.

Saiki, R. K., Gelfand, D. H., Stoffel, S., Scharf, S. J., Higuchi, R., Horn, G. T., Mullis, K. B., and Erlich, H. A. (1988). Primer-directed enzymatic amplification of DNA with a thermostable DNA-polymerase. *Science* 239, 487-491.

Sanger, F., Nicklen, S., and Coulson, A. R. (1977). DNA sequencing with chain-terminating inhibitors. *Proc. Natl. Acad. Sci. USA* 74, 5463-5467.

Schneider, R., and Schweiger, M. (1991). A novel modular mosaic of cell adhesion motifs in the extracellular domains of the neurogenic *trk* and *trkB* tyrosine kinase receptors. *Oncogene* 6, 1807-1811.

Shine, J., and Dalgarno, L. (1974). The 3'-terminal sequence of Escherichia coli 16S ribosomal RNA: complementarity to nonsense triplets and ribosome binding sites. *Proc. Natl. Acad. Sci. USA* 71, 1342-1346.

Smalheiser, N. R., and Kim, E. (1995). Purification of cranin, a laminin binding membrane protein. *J. Biol. Chem.* 270, 15425-15433.

Strous, G. J., and Dekker, J. (1992). Mucin-type glycoproteins. *Crit. Rev. Biochem.* 27, 57-92.

Sutherland, D. R., Abdullah, K. M., Cyopick, P., and Mellors, A. (1992). Cleavage of the cell-surface O-sialglycoproteins CD34, CD43, CD44, and CD45 by a novel glycoprotease from *Pasteurella haemolytica*. *J Immunol* 148, 1458-1464.

Sutherland, D. R., Marsh, J. C. W., Davidson, J., Baker, M. A., Keating, A., and Mellors, A. (1992). Differential sensitivity of CD34 epitopes to cleavage by *pasteurella-haemolytica* glycoprotease - implications for purification of CD34-positive progenitor cells.

*Experimental Hematology* 20, 590-599.

Taniguchi, H., Tohyama, M., and Takagi, T. (1996). Cloning and expression of a novel gene for a protein with leucine-rich repeats in the developing mouse nervous system.

*Molec. Brain. Res.* 36, 45-52.

Tian, S.-S., and Zinn, K. (1994). An adhesion molecule-like protein that interacts with and is a substrate for a *drosophila* receptor-linked protein tyrosine phosphatase. *J. Biol. Chem.* 269, 28478-28486.

van der Merwe, P. A., and Barclay, A. N. (1994). Transient intercellular adhesion: the importance of weak protein-protein interactions. *TIBS* 19, 354-358.

Van Klinken, B. J. W., Dekker, J., Büller, H. A., and Einerhand, A. W. C. (1995). Mucin gene structure and expression - protection vs adhesion. *Am. J. Physiol.* 269, G613-G627.

Williams, M. J., Du, X., Loftus, J. C., and Ginsberg, M. H. (1995). Platelet adhesion receptors. *Sem. Cell Biol.* 6, 305-314.

Woods, D. F., and Bryant, P. J. (1991). The discs-large tumor suppressor gene of

*drosophila* encodes a guanylate kinase homolog localized at septate junctions. *Cell* 66, 451-464.

Xiao, P., Bahr, B. A., Staubli, U., Vanderklish, P. W., and Lynch, G. (1991). Evidence that matrix recognition contributes to stabilization but not induction of LTP. *NeuroReport* 2, 461-464.

Yeo, E., and Sutherland, D. R. (1993). Platelet GPIb is selectively cleaved by the *pasteurella* glycoprotease: Functional and biochemical studies. *Blood* 82, 612.

**FIGURE LEGENDS**

Figure 1. Tryptic peptide sequences and PCR cloning of densin-180.

A. Amino acid sequences of three densin-180 tryptic peptides were used to design sense (S) and antisense (A) degenerate 29mer oligonucleotide primers [A, adenosine; C, cytosine; G, guanosine; I, inosine; T, thymidine; degenerate nucleotide positions are enclosed in parentheses]. The ten amino acids used to design the sense (right pointing arrows) and antisense (left pointing arrows) are indicated above and below the peptide sequences respectively. B. Densin-180 PCR cloning strategy. Combinations of sense and antisense primers (arrows) were used for PCR amplification from rat forebrain cDNA. PCR products (represented by a gray box) were cloned into a vector and sequences of the insert determined by sequencing from the vector's M13 and T7 primer sites (bold arrows). C. PCR reactions were fractionated on a 1.2% agarose gel and the DNA visualized by ethidium bromide staining. PCR product size was estimated by comparing with DNA molecular weight markers. The 1S + 3A primer combination produced a 1.2 kb PCR product (bold arrow) that is absent in the control 1S or 3A reactions. D. Restriction map and sequencing strategy for cDNA clones encoding densin-180. Clone 1.1 was sequenced in its entirety and the coding region (*open box*), the region of hybridization with the PCR product (*gray box*) and the 5' and 3' noncoding regions (*horizontal lines*.) are indicated on the restriction map (map units are in base pairs). The locations of cDNA clones determined by restriction mapping and sequencing are shown below. The extent and directionality of overlapping cDNA sequences are depicted as arrows for each cDNA clone. Densin-180 cDNA clone 2.1 lacks nucleotides 111 to 186 of the densin180 sequence (*broken line*) containing the ribosome binding site and part of the initiation codon. Clone 3.1 lacks a 249 base pair sequence spanning nucleotides 1632 to 1880 of the

densin-180 sequence (*broken line*).

Figure 2. Densin-180 cDNA sequence and protein translation. The DNA sequence of clone 1.1 determined by sequencing both strands is shown with the protein translation below. This sequence will be submitted to GenBank. DNA sequences that are missing from clones 2.1 and 3.1 are *underlined*. The protein sequences of tryptic peptides 1, 2, and 3 are also *underlined*. Potential N-linked glycosylation sites, CaMKII phosphorylation sites (**bold**) and RGD cell attachment motif are shown as *boxed* residues. The potential transmembrane domain is underlined (*gray bar*) and the sixteen leucine-rich repeats are contained in amino acids 53-420. The amino- and carboxy-flanking cysteine rich domains span amino acids 19-37 and 486-546, respectively. The mucin homology domain (amino acids 825-915) and the PDZ domain (amino acids 1405-1492) are found in the sequence.

Figure 3. Domain structure of densin-180. A. Alignment of the fifteen densin-180 leucine-rich repeats reveal a 23 residue consensus shown below. Corresponding amino acid numbers of densin-180 are indicated to the left of the first repeat and to the right of the sixteenth repeat. B. Identification of a PDZ domain in densin-180. Alignment of amino acids 1400 to 1493 of densin-180 with PDZ domains from four other proteins (three PDZ domains from PSD95, (Cho et al., 1992); three from *Drosophila* discs-large, dlg (Woods and Bryant, 1991); three from the human zona occludens protein, ZO-1, (Itoh et al., 1993); and one from neuronal nitric oxide synthase, nNOS (Bredt et al., 1991). C. The domain structure of densin-180 compared to the LRR-containing glycoprotein, GPIIb $\alpha$ . The leucine-rich repeats (fifteen in densin-180 and seven in GPIIb $\alpha$ , *wavy boxes*), with N-terminal and C-terminal cysteine rich flanking regions (*stippled boxes*), and mucin-like

domains (*boxes with diagonal lines*) are indicated for both proteins. Potential transmembrane domains are depicted as *black boxes*. The ABP binding protein domain of GPIIb $\alpha$  and the PDZ domain of densin-180 at the C-terminal regions of the proteins are represented by *gray boxes*. The position of the RGD sequence is also shown. Scale bar represents 150 amino acids.

Figure 4. Solubility of densin-180 in brain membrane fractions. Crude membrane fractions were isolated from rat brain and extracted with indicated buffers. Immunoblots were prepared with the pellet (P) and supernatant (S) fractions from a 170,000g centrifugation after extraction with 1 M NaCl, 2% CHAPS, 1 M NaCl + 2% CHAPS, 2% Triton, 1 M NaCl + 2% Triton, or 0.2 M Sodium Bicarbonate pH 11, for 1 hour at 4<sup>0</sup>C.

Figure 5. Densin-180 is a mucin-like sialoglycoprotein. A. Densin-180 is heavily glycosylated with sialic acid. Twenty micrograms of denatured PSD fraction were used for anti-densin-180 immunoblots after overnight incubation 37<sup>0</sup>C under the following conditions: control reaction with no added neuraminidase (Lane 1), with added neuraminidase (Lane 2), and with added neuraminidase plus 10 mM N-Bromo-succinimide (Lane 3). The 188 kDa undigested (upper arrow) and 148 kDa digested (lower arrow) densin-180 protein bands are shown. The 205, 118 and 87 kDa molecular weight markers are shown at left. B and C. Proteolysis of densin-180. Twenty-four micrograms of non-denatured PSD fraction was incubated with 0.4 mg/ml final volume of O-sialoglycoprotein endoprotease (Accurate Chemical and Scientific Corporation). All incubations were carried out in the presence of 0.2 mM PMSF to inhibit endogenous proteases in the PSD fraction. Control reactions with no protease added were

incubated for 3 hours at 37<sup>0</sup>C. All reactions were incubated at 37<sup>0</sup>C for 15 minutes (*15m*), 1 hour (*1h*) and 3 hours (*3h*). Reactions were terminated by adding gel sample buffer and boiling for 3 minutes. Immunoblots were prepared with these samples. B. Immunoblot was probed with the CT245 antibody, a rabbit polyclonal serum that reacts with epitopes in part of the potential cytoplasmic domain spanning residues 1374-1495 of densin-180. The CT245 antibody detects the undigested 188 kDa densin-180 protein band (*large black arrow*) and a complex pattern of proteolytic fragments (*gray arrows*) of densin-180. These proteolytic fragments include major bands at approximately 70 kDa, 45 kDa (doublet), 40 kDa (doublet), 30 kDa and 20 kDa. The 20 kDa band (*large gray arrow*) is resistant to proteolysis after 3 hours at 37<sup>0</sup>C. C. Immunoblots were prepared with M2 anti-densin-180, a mouse polyclonal ascites that reacts with epitopes contained in amino acids 466-958 of densin-180's putative extracellular domain. The undigested 188 kDa densin-180 protein band (*large black arrow*) and the 140 and 120 kDa proteolytic fragments (*gray arrows*) of densin-180 detected by the M2 antibody are identified. For both B and C, size standards appear at the side with *open arrowheads* indicating the gel origin (top) and dye front (bottom).

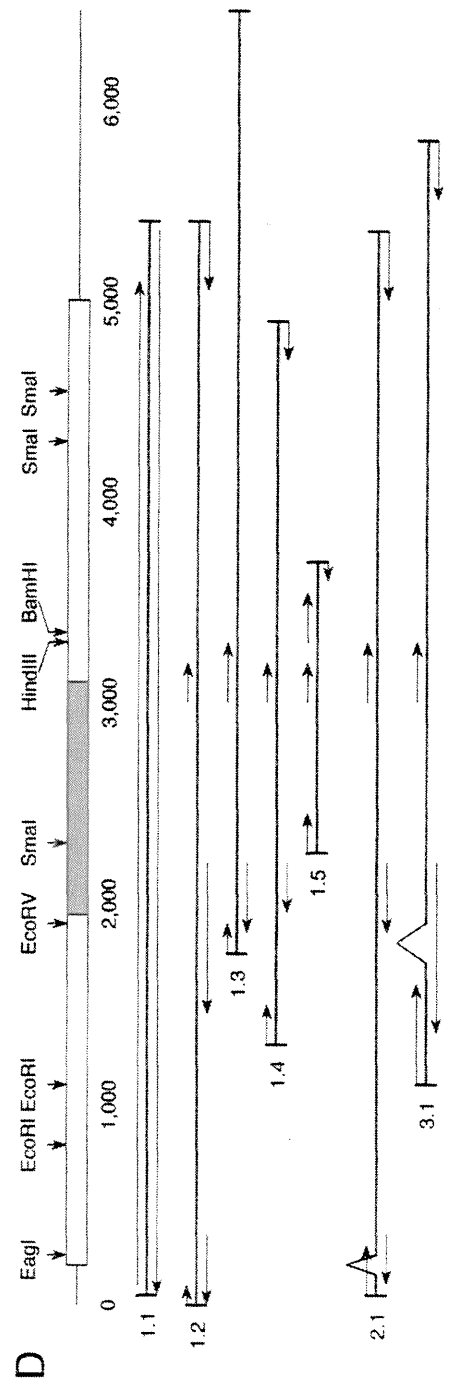
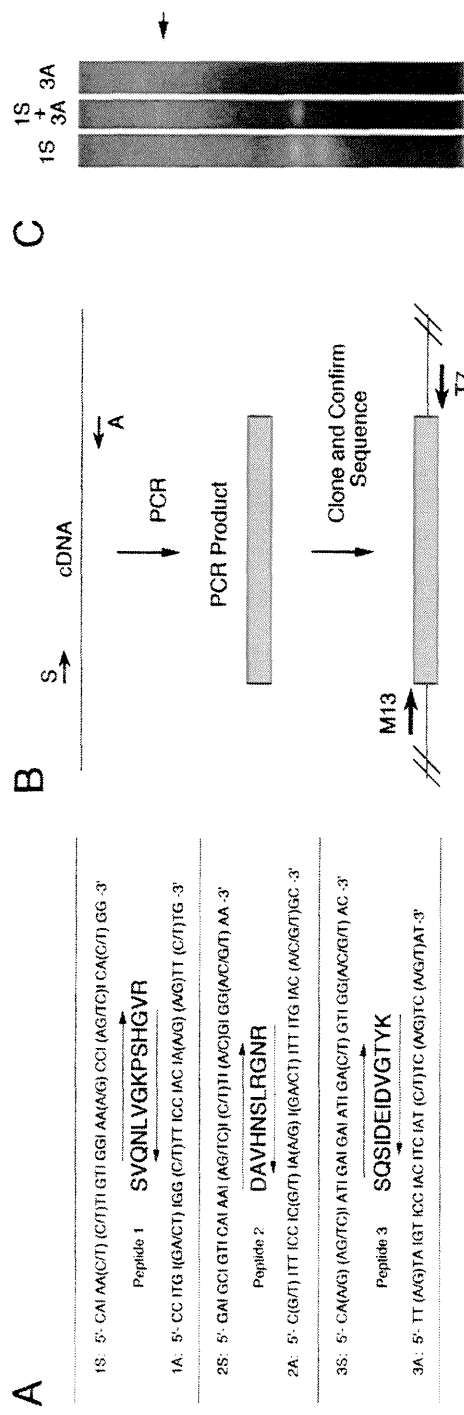
Figure 6. Densin-180 is phosphorylated by endogenous  $\alpha$ CaMKII in the PSD fraction. Control reactions were set up containing 24 $\mu$ g of PSD fraction and 50 mM Tris8, 10 mM MgCl<sub>2</sub>, 0.4 mM EGTA, 10 mM DTT and 10 $\mu$ g/ml added calmodulin (Lane 1). Additional components added to reactions were as follows: 0.6 mM calcium (Lane 2 and 3) and 4A11 (0.3  $\mu$ g/ $\mu$ l) and 6E9 (0.4  $\mu$ g/ $\mu$ l) anti-CaMKII inhibitors (Lane 3). After a 3 minute pre-incubation with these components at 30<sup>0</sup>C, <sup>32</sup>P-ATP (10000 cpm/pmol) was added to 25 $\mu$ M final concentration and incubated for two minutes at 30<sup>0</sup>C. Reactions were

terminated by adding 10% SDS to a final concentration of 1% and boiling for 5 minutes. Densin-180 was immunoprecipitated from the denatured phosphorylation reactions with M2 anti-densin-180 antibody and applied to SDS/6% polyacrylamide gels. The autoradiograph of a 16-hour exposure of the dried gel is shown. Densin-180 protein bands are indicated with an arrow.

Figure 7. Densin-180 mRNA expression is brain-specific and densin-180 protein is enriched in detergent-extracted PSD fractions. A. Densin-180 northern blot. Five micrograms of PolyA+ RNA from 13 different different tissue samples was electrophoresed on a 1% agarose gel. The mRNA was transferred to Zeta-Probe blotting membrane (Bio-Rad) and all lanes were determined to have equal amounts of RNA by methylene blue staining. Blots were probed with a random-prime labelled PCR amplified DNA fragment of densin-180 spanning nucleotides 1100-2170 (Specific activity:  $10^9$  cpm/ $\mu$ g). A single broad band at 7.4 kb was detected (arrow) on autoradiographs exposed for 14 days with intensification screen. The blot was then stripped and re-probed with the 2kb random-prime labelled human  $\beta$ -actin cDNA (from CLONTECH), (Specific activity:  $10^7$  cpm/ $\mu$ g). The autoradiograph of an eight-hour exposure with intensification screen is shown in the lower panel. The two forms of beta-actin are indicated (*arrows*). B. Enrichment of densin-180 protein in detergent-extracted PSD fractions. Immunoblots were prepared with 50 $\mu$ g (lanes 1 and 2) of rat brain homogenate (Hom) and synaptosome fractions (Syn) and 7.5 $\mu$ g (lanes 3-6) each of synaptosome (syn), once triton extracted PSD (1T), twice triton extracted PSD (2T), and once triton then sarcosyl extracted PSD. Densin-180 protein band (arrow) is visualized with M2 anti-densin-180. Molecular weight markers and position of the dye front (*open arrowhead*) are shown at left.

Figure 8. Immunocytochemical localization of densin-180 at synapses in dissociated hippocampal neurons. (A-C) Dissociated E18 hippocampal neurons were grown in culture on coverslips for 14 to 21 days, and fixed with ice-cold methanol. After incubating coverslips 1 hour in pre-block and overnight with primary antibodies, cultures were washed three times with pre-block and incubated with Cy3-conjugated goat anti-mouse and FITC-conjugated goat anti-rabbit secondary antibodies. The coverslips were then washed and mounted in solution containing 80% glycerol, 4 mg/ml p-phenylenediamine and 0.1 M sodium bicarbonate buffer, pH9.2. Confocal images were generated using a Zeiss confocal microscope and double images generated in Adobe Photoshop. Red pseudocolor is used for the Cy3 staining and green for the FITC staining. Regions of overlap are yellow. A. Double staining for synapsin I and densin-180. Anti-synapsin I (Collette 1:1,000) and anti-densin-180 (M2, 1:150) were used for double labelling dissociated cultures after 21 days *in vitro*. A 63X objective image with densin-180 (red) and synapsin I (green) staining is shown. The inset at left is a 3X zoom of the area included in the white box. At right are the unprocessed images of densin-180 (top) and synapsinI (bottom). B. Densin-180 and PSD-95 double staining. Anti-PSD-95 (Frances, affinity pure, 1:100) and anti-densin-180 (M2, 1:150) double staining of cultures grown for 17 days *in vitro* is shown. A 63X objective double-label image with a zoom factor of 1.5 is shown. Axon initial segment densin-180 staining is indicated with an arrow. The upper left inset is a 2X zoom showing examples of colocalized PSD-95 staining (small arrows) and densin-180 staining (large arrows). Also indicated is a region of PSD-95 staining that does not have as much densin-180 staining (small arrowhead). C. Anti- $\alpha$ CaMKII (6G9, 1:500) and anti-densin-180 (CT245, 1:3000) double staining of cultures grown for 14 days *in vitro* is

shown. A 63X objective image with a zoom factor of 2 is shown. The upper left inset is a 2X zoom showing examples of colocalized  $\alpha$ CaMKII staining (small arrows) and densin-180 staining (large arrows). Also indicated is a region of cytoplasmic  $\alpha$ CaMKII staining within the dendrite that does not have densin-180 staining (small arrowhead).





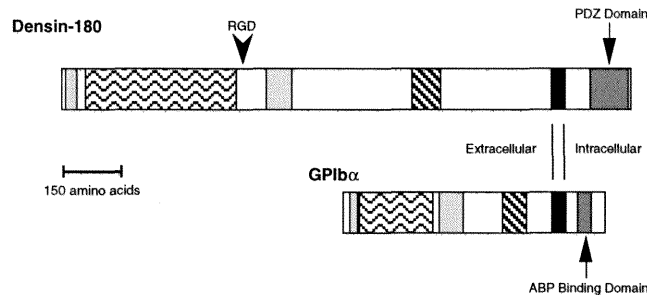
A

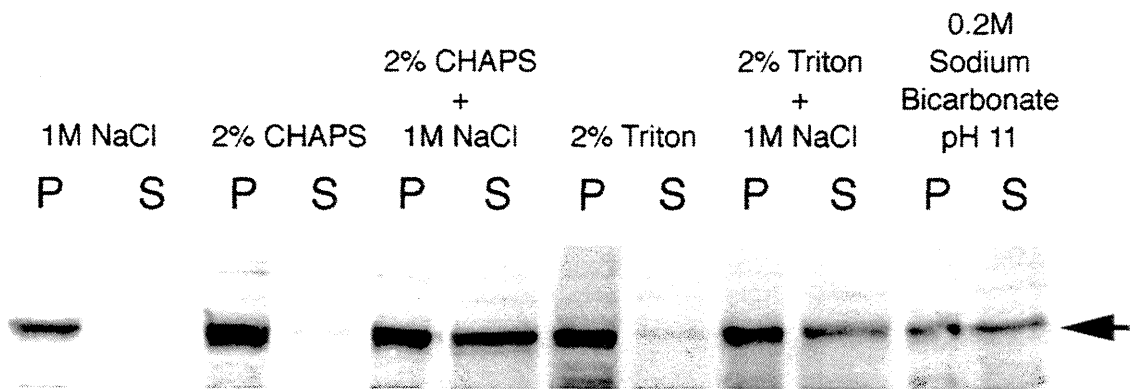
		1		23
LRR1	53-	LEELYLDAN	QIEELPKQLF	NCQA
LRR2		LRKLSIPDN	DLSLPTSIA	SLVN
LRR3		LKELDLSKN	GMQEPFENIK	CCKC
LRR4		LTIEEASVN	PISKLPDGF	QLLN
LRR5		LTQLYLNDA	FLEFLPANFG	RIVK
LRR6		LRILELREN	HLKTLPKSMH	KLAQ
LRR7		LERLDLGN	EFSLEFVLD	QIQN
LRR8		LRLEWMDNN	ALQVLPDSIG	KLKM
LRR9		LVYLDMSKN	RLETVDMDIS	GGEA
LRR10		LEDLLSSN	MLQQLPDSIG	LKK
LRR11		LTTLKVDN	QLTMLPNTIG	NLSL
LRR12		LEEFDCSN	ELESLEPTIG	YLS
LRR13		LRTLAVDEN	FLPELPREIG	SCKN
LRR14		VTVMSLRSN	KLEFLPEEIG	QMQR
LRR15		LRVLNLSDN	RQKNLPSFT	KLKE
LRR16		LAALWLSDN	QSKALIPLQT	E <sup>AHP</sup> -420
Consensus		L--L-L--N	-L--LP--IG	-L--

B

		1		50			
DENSIN	1400-	GYPEQICVRI	EKNPGLGFSI	SGGISGQNP	FKPSDKGI	FV	TRVQPDGPA
1PSD95		...EITLER	QNS.GLGFSI	AGGTDNP..H	I.GDPSI	FI	TKLIPGGAA
2PSD95		...EIKLIK	QPK.GLGFSI	AGGVGNQ..H	I.PGNSI	YV	TKILEGGAH
3PSD95		...RIVLHR	QST.GLGFNI	VGGEDGE...	...GI	FI	SFILAGGPA
1DLG		...DILQER	QNS.GLGFSI	AGGTDNP..H	I.GDTSI	YI	TKLISGAAA
2DLG		...EIDLVR	QKG.GLGFSI	AGGIGNQ..H	I.PGNSI	YV	TKLTDGGRQ
3DLG		...TITIRK	QPA.GLGFNI	VGGEDGQ...	...GI	YV	SFILAGGPA
1ZO1		...TIVLHR	APGFQGIAT	SGGRDNP..H	FQSGFTS	IIV	SDVLKGGPA
2ZO1		...KVTLVKS	RKNEEYGLRP	ASH.....	...IFV		KEISQDSLAA
3ZO1		...KLVKF	RKGDVGLRL	AG.....	...GNDVGI	FV	AGVLEDSPA
NOS		...VRLRFK	RKVGGLGFLV	K.ERVS....	...KPPV	II	SDLIRGAAE
Consensus		----L-L-K	G--GLGFSI	AGG-DN----	----D-GIYV	T-IL	GGPAA
		51		100			
DENSIN		.SNLQPGDK	ILQANGHS...	FVHMEHEK	AVLLKSFQN	TVDLVIQR	RELTV*
1PSD95		QDGRLRVND	ILFVNEVD...	VREWTHSA	AVEALKKAGS	IVRLYVMRR	
2PSD95		KDGRLRIGD	ILAVNSVG...	LEDMHEE	AVALKNTYD	VVYLKVA	KP.
3PSD95		LSGELRKGQ	ILSVNGVD...	LRNASHQR	AVALKNAQR	TVT	ILAQK.
1DLG		ADGRSINDI	ILSVNDVS...	VVDVPHAS	AVDALKKATN	VVKLHVKKR	
2DLG		VDGRSIGDK	ILAVRTNGSE	KNLENVTHEL	AVATLKSIT	.....	
3DLG		LGSELKRGD	ILSVNNGVN...	LTHATHEE	AAQALKTSQG	VVTL	LAQYR.
1ZO1		.EGQLREND	VAMVNGVS...	MDNVEHAF	AVQLRKSQK	NAKIT	IRRK
2ZO1		RDGDIQEGD	VKINGTVT...	ENMSLTD	AKTLERSKG	KLKVAVQR	
3ZO1		KEG.LEEGQ	ILRVNVD...	FTNIRIE	AVLFLDLPK	GEEVT	LARK
NOS		QSGLRAGDI	ILAVNDRP...	LVDLSYDS	AEVERNGIAS	ETHV	VILR.
Consensus		-DGRL--GD-	IL-VN-V---	--LENV-HE-	AV-ALK--G-	-V-LVV-	RK-

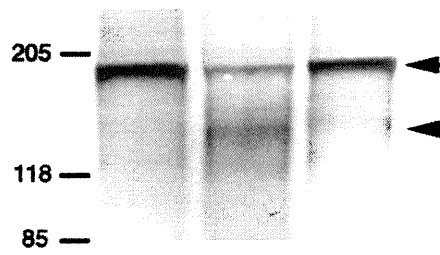
C





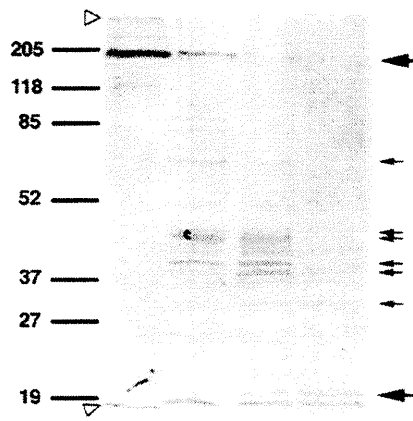
**A**

Neuraminidase	-	+	+
Inhibitor	-	+	+



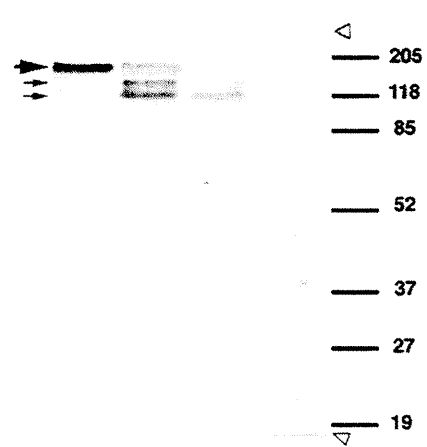
**B**

Protease	-	+	+	+
Incubation Time	3h	15m	1h	3h

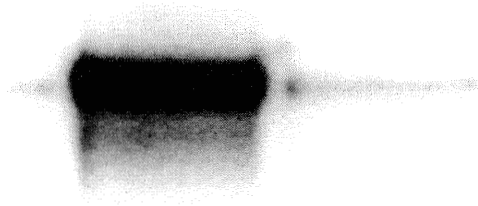


**C**

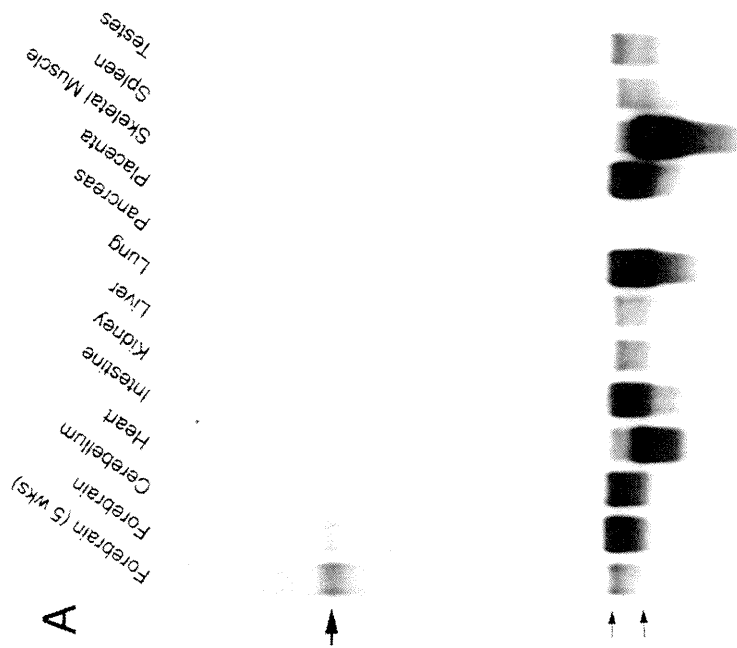
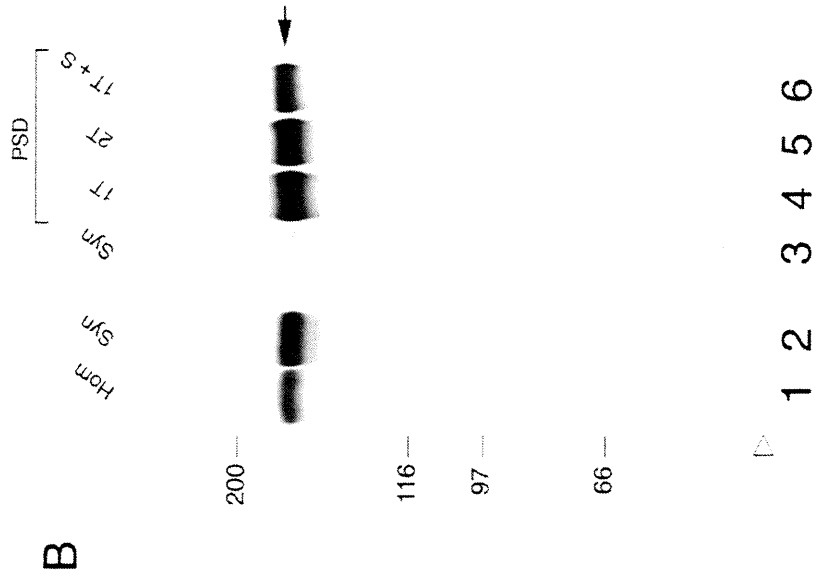
Protease	-	+	+	+
Incubation Time	3h	15m	1h	3h

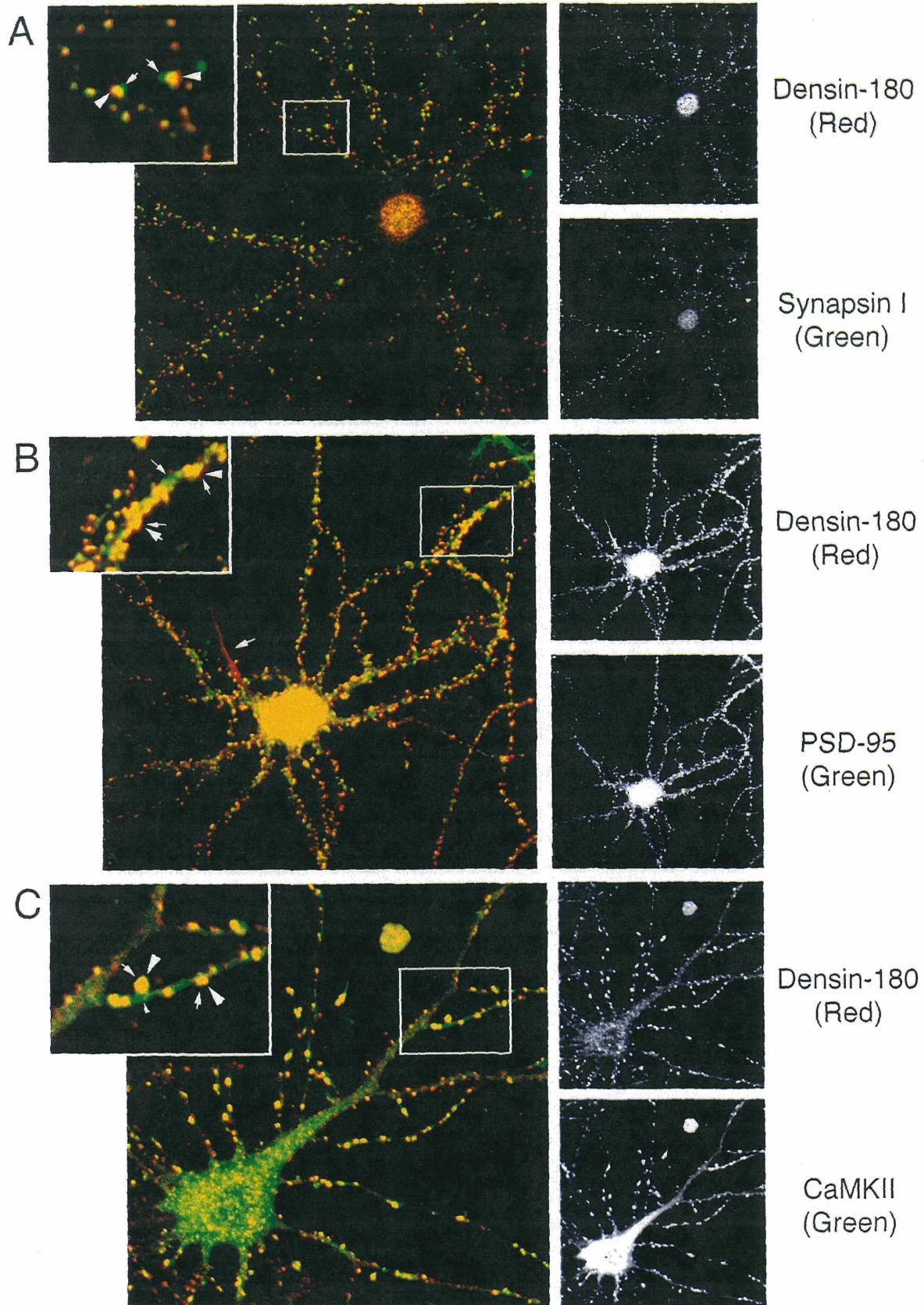


Calcium	-	+	+
Inhibitors	-	-	+



**1**      **2**      **3**





## **CHAPTER 4**

**The expression of densin-180 and other synaptic markers reveals an ordered assembly of postsynaptic density proteins during synapse formation in culture**

## INTRODUCTION

The study of synapse formation at the neuromuscular junction has been an active area of study over the last 15 years, in large part due to the establishment of tissue culture systems. For example, in cultured chick myotubes, researchers are able to visualize axon ingrowth, initial contact with the myotube and synapse maturation *in situ*. They have also been able to purify factors that effect synapse formation in culture. For example, the addition of purified Torpedo agrin to non-innervated myotubes causes clustering of AChRs. Also, ARIA has been identified as a factor released by the presynaptic terminal that induces the expression of the adult form of the AChR. Interestingly, axons find previous synapses if allowed to grow back after axotomy, probably due to the organization of the postsynaptic specialization. The studies of synapse formation at the neuromuscular junction have important biological implications in the treatment of diseases such as myasthenia gravis or muscular dystrophy. These findings are summarized in Haydon and Drapeau, 1995.

Most of what we know about synapse formation in the mammalian brain has been from studies of the formation of specialized brain structures such as barrel fields in rat or ocular dominance columns in the monkey. Groups that study synapse formation in these systems have used pharmacology to determine that the NMDA receptor and calcium are important players in synapse formation in the brain. However, the research of synapse formation in the central nervous system (CNS) has progressed at a much slower rate than than in the neuromuscular junction (NMJ), in part due to the lack of a good system to study the function of individual proteins. Also, the relatively small size of the CNS synapse makes protein localization by conventional light microscopy more difficult (synaptic junctions are on the order of  $1 \mu\text{m}^2$  in the CNS and  $500 \mu\text{m}^2$  for the NMJ

synapse).

Our lab and others have turned to confocal imaging of cultured dissociated hippocampal neurons to visualize individual synapses. This technique has been used to colocalize PSD-95 and NR2B at synapses (Kornau et al., 1995). I have previously reported the colocalization of densin-180 with the synaptic markers PSD-95,  $\alpha$ CaMKII and synapsin I (Chapter 3). Here, I describe the order of assembly of densin-180, synapsin I, PSD-95, and  $\alpha$ CaMKII during the synapse formation in dissociated hippocampal neurons in culture.

## **MATERIALS AND METHODS**

### **Immunoblots of rat brain fractions**

Rat brain homogenates were prepared from rats anesthetized with halothane. Brains were rapidly dissected after decapitation and homogenized in PBS + protease inhibitors (Boehringer Mannheim) + DNase 50U/ml, in a glass teflon homogenizer. Homogenates were flash frozen in aliquots and stored at -80°C until used for preparation of immunoblots probed with anti-densin-180 (M2, 1:3000 dilution [see Chapter 3 for description of antibodies]).

### **Immunofluorescent staining of dissociated hippocampal neuronal cultures**

We cultured dissociated hippocampal neurons exactly as described in Chapter 3. Culture coverslips were fixed at 3, 5, 7, 9, 14 or 21 days after plating (days *in vitro*, DIV). The fixed cells were then double labeled as described in Chapter 3 using the same antibodies. For clarification, the antibodies used were CT245 (rabbit anti-densin-180), M2 (mouse polyclonal anti-densin-180), 6G6 (mouse monoclonal anti-PSD-95), 6G9 (mouse monoclonal anti- $\alpha$ CaMKII), or Collette (rabbit anti-synapsin I). The antibodies were used at the following dilutions: CT245 serum, 1:5000; M2 ascites, 1:150; 6G6 ascites, 1:500; 6G9 ascites, 1:500; Collette, 1:1000.

### **Controls for brightness and contrast settings in younger cultures**

The Zeiss laser scanning microscope has a very high sensitivity, so it is possible to detect nonspecific staining if the contrast values are set very high. This becomes a problem when viewing weak staining in young cultures. Thus, in each experiment we used staining of

older cultures as a positive control for our antibodies. This enabled us to determine the range of contrast and brightness settings we could use and still get specific staining of synapses in older cultures (specificity was determined by preabsorptions, see Chapter 3 and Appendix I). The same range of contrast and brightness values was then used to view the younger cultures. These controls were especially important in determining the relative amount of 6G9 staining in younger cultures (see results). Generally, the brightness values were set at 9650-9700 and the range of contrast values varied between primary antibodies. Contrast values used for each primary were as follows: M2 and CT245 , 400-420; 6G6, 390-410, Collette, 350-375 and 6G9, 360-380.

## RESULTS

### **Expression of the densin-180 protein increases during synaptogenesis in the brain**

Densin-180 is an adhesion molecule-like protein that is enriched in the PSD fraction and localized at the synapse (Chapter 3). I characterized the expression of densin-180 during synapse formation in the brain by preparing immunoblots with homogenates from rat brains at different developmental stages. Immunoblots were visualized with alkaline phosphatase-conjugated secondary antibodies, a method that is not quantitative but can determine relative levels of protein. Densin-180 protein is first detected at P2 and increases gradually through P14 where it reaches a maximum level (Figure 4.1A). This time course is similar to the expression of PSD-95 and  $\alpha$ CaMKII (Figure 4.1B) that are induced between postnatal day 8 and 18, a period of rapid synaptogenesis in the brain (see Cho et al., 1992). However, one notable difference is that densin-180 reaches a maximum level of expression 4 days earlier than PSD-95 or  $\alpha$ CaMKII.

### **Densin-180 is highly expressed before synaptogenesis, then becomes clustered during synaptogenesis in dissociated hippocampal neurons**

To further characterize the expression pattern of densin-180 during neuronal differentiation and synapse formation, dissociated E18 hippocampal neurons were fixed for staining at various developmental stages in culture (Figure 4.2). Densin-180 was expressed in golgi-like staining in the cell body and patchy staining neurites at 1 to 3 days *in vitro* (DIV). The patchy membrane-like surface staining increased through 5 days *in vitro* (DIV) when the first densin-180 clusters began to form. These clusters increased in number and size through 14 DIV. By 14 DIV, the majority of densin-180 staining is found as clusters and the patchy membrane and Golgi-like staining is diminished. The largest

increase in numbers of cells with clusters and the number of clusters per cell occurred between about 7 and 10 DIV, a period of active synapse formation in culture (Bartlett and Banker, 1984).

### **Clusters of densin-180 appear at early synapses in cultured hippocampal neurons double-labeled with synapsin I**

As mentioned in Chapter 3, our lab has developed a method for staining dissociated hippocampal neurons with antibody markers of the synapse. I decided to use double-labeling of densin-180 with synapsin I, PSD-95 and  $\alpha$ CaMKII antibodies to determine the order of assembly of PSD proteins during synaptogenesis.

Dissociated hippocampal neuronal cultures were double labeled with M2 anti-densin-180 and Collette anti-synapsin I. Synapsin I antibodies typically stain the cytoplasm of axons in young cultures through 5 to 7 DIV. At around 7 DIV, synapsin I staining becomes associated with clusters at sites of presynaptic boutons. Figure 4.3A shows the typical synapsin I staining at 7 DIV (green). Interestingly, the clusters of densin-180 staining colocalize with these early synapses detected with synapsin I staining. By 9 DIV, there is an increase in the clustered synapsin I staining and a decrease in the cytoplasmic axon staining (Figure 4.3B). Clusters of densin-180 colocalize with some of these synapsin I clusters. Differences between the two patterns of staining are also indicated in Figure 4.3. Densin-180 has a high cell body staining that does not overlap with synapsin I staining. The axon-associated synapsin I staining and some of the clusters of synapsin I staining do not colocalize with densin-180 staining.

### **Clusters of densin-180 staining colocalize with PSD-95**

Having established that densin-180 staining first appears in clusters at the earliest synapses, I tested whether the other PSD proteins gave similar patterns of staining. At 7 DIV, PSD-95 first appears at sites of densin-180 clusters (Figure 4.4A). The staining of PSD-95 is extremely bright with very low background in the cell body or cytoplasm, consistent with a high degree of localization of PSD-95 protein at synaptic sites. Figure 4.4B shows “coclusters” at 9 DIV in which clusters of densin-180 staining is colocalized with PSD-95 punctate staining (arrows). Some of the “coclusters” have slightly more PSD-95 or densin-180 staining (arrowheads in Figure 4.4B). This variation could be due to slight differences in the focal planes of the two lasers used in the double images. As development progresses between 5 and 14 DIV, there is a decrease in the patchy membrane staining of densin-180 and an increase in the number of PSD-95/densin-180 “coclusters” per cell. By 2-3 weeks *in vitro*, there is almost complete colocalization of the two antibody staining patterns (see Chapter 3, Fig. 8B).

### **Induction of $\alpha$ CaMKII expression is not required for densin-180 cluster formation**

Next, we viewed double-labeled images of  $\alpha$ CaMKII and densin-180 at various stages of neuron development in culture (Figures 4.5 and 4.6). Figure 4.5A shows the typical pattern of very early  $\alpha$ CaMKII staining at 7 DIV. The  $\alpha$ CaMKII staining is associated with the cell body in large clusters that do not seem to colocalize with the densin-180 cell body staining. At 9 DIV, the majority of neurons still have relatively low  $\alpha$ CaMKII expression. However, there are some cells that have the very high cytoplasmic staining and punctate staining along the dendrites that are typical of mature neurons. The cells that have high  $\alpha$ CaMKII staining always have clustered densin-180 staining along the dendrites (Figure 4.5B). On the other hand, there are a number of neurons that have

clusters of densin-180 staining and do not stain for  $\alpha$ CaMKII, even at 14 DIV (one such neuron is shown in Figure 4.6). Other members of our lab have seen similar patterns in 21 to 28 DIV cultured neurons that were double-labeled for  $\alpha$ CaMKII and PSD-95. The staining pattern reveals a small number of cells in the cultures that stain positively for clusters of PSD-95, but do not stain with  $\alpha$ CaMKII. These older  $\alpha$ CaMKII-negative neurons are often bipolar in shape and may represent inhibitory neurons.

## DISCUSSION

Our lab has studied proteins that are concentrated in the postsynaptic density fraction of the brain. Here, I presented data that suggests that densin-180 expression in the brain is induced at about the same time as two other PSD proteins,  $\alpha$ CaMKII and PSD-95. The expression of all three proteins is induced during a period of rapid synaptogenesis in the brain.

To determine the order of expression of these synaptic markers in the individual neuron, I used double labeling of primary hippocampal cultures. First, I characterized the expression of densin-180 during synaptogenesis in these cultures by double labeling with synapsin I, a marker of the presynaptic terminal. At early ages, there is an obvious lack of colocalization of these two markers. The densin-180 protein is expressed in the cell body and along the dendrites, but synapsin I is present in the cytoplasm of axons. I could detect early sites of synapse formation at 5 to 9 days *in vitro* that have clusters of synapsin I staining that are likely to be associated with the development of presynaptic boutons. These presynaptic boutons partially overlapped with clustered densin-180 staining.

Next, I was able to distinguish “coclusters” of densin-180/PSD-95 staining along dendrites in early synapses, but I was not able to resolve whether one clustered before the other. One possibility is that clusters form through interaction of PSD-95 with the PDZ domain of densin-180. A PDZ-PDZ type of interaction has been postulated for the binding of PSD-95 with nNOS and syntrophin (reviewed in Gomperts, 1996). A direct interaction between densin-180 and PSD-95 has not been determined, but could be tested *in vitro*.

There is also recent evidence for a role of PSD-95 in clustering membrane proteins such as NR2B and potassium channels through a PDZ-tSXV domain interaction (see

Gomperts, 1996 for review). Interestingly, others in the lab have shown that PSD-95 and NR2B are “coclustered” at these early synapses. This suggests that PSD-95 may be responsible for clustering NR2B and/or densin-180 at glutamatergic synapses.

There was a notable difference in the staining of  $\alpha$ CaMKII compared to the other PSD markers (densin-180 and PSD-95). The expression of  $\alpha$ CaMKII appears to be tightly regulated in the neurons and is only detected in cells that already have extensive synaptic labeling. A possibility is that  $\alpha$ CaMKII-negative cells correspond to the younger, undifferentiated neurons in these cultures and that  $\alpha$ CaMKII is induced during differentiation into mature glutamatergic neurons.

The idea that  $\alpha$ CaMKII is a marker of mature synapses is consistent with data from several other labs. First, some early experiments were carried out by Kelly and Cotman on isolated synaptic junction fractions (SJs) from rats of different ages (Reviewed in Cotman and Kelly, 1980). They noticed that the association of the “major PSD protein” with SJ fractions was highly regulated during development. They proposed that the major PSD protein is recruited to synapses at later stages of development to stabilize the PSD. This major PSD protein has been identified as the  $\alpha$  subunit of CaMKII, (Kennedy et al., 1983).

Next, studies of the  $\alpha$ CaMKII knockout mice reveal that they are still able to form glutamatergic synapses. However, the mutant mice are deficient in long term potentiation (LTP), a form of synaptic plasticity (Silva et al., 1992). This observation supports the idea that  $\alpha$ CaMKII is not necessary for synapse formation, but might be essential for mature synapse function. Lastly, in a recent seminar at Caltech, Roberto Malinow presented data suggesting that CaMKII activity is necessary for the induction of LTP in cultured E18 hippocampal neurons. He also suggested that the first appearance of LTP in these neurons is correlated with  $\alpha$ CaMKII expression at about 9 DIV.

Based on this information and the data presented here, I propose the following model for the stepwise assembly of PSD proteins the synapse. First, before synapse formation, densin-180 is highly expressed all over the dendritic membrane surface and is available to mediate adhesion when initial contact is made between dendrite and axon. After contact is made, there is a coordinated differentiation of the pre and postsynaptic components. The differentiation of the presynaptic bouton can be detected by clustering of synapsin I staining. The corresponding assembly of the postsynaptic density of glutamatergic synapses can be detected at sites of densin-180/PSD-95/NR2B coclusters. Some time after these initial synapses are formed,  $\alpha$ CaMKII expression is induced and recruited to the postsynaptic density. The punctate  $\alpha$ CaMKII staining along dendrites may be a marker of mature excitatory synapses on glutamatergic neurons capable of exhibiting long term potentiation.

In conclusion, *in vitro* synapse formation can be followed in dissociated hippocampal cultures using antibodies generated against the synaptic markers densin-180, PSD-95 and  $\alpha$ CaMKII. By following the expression of individual proteins during synapse formation, I have developed a model for the step-wise assembly of these proteins at the synapse. We could test this model by altering the levels of each protein using antisense oligonucleotide experiments. This could further clarify our hypotheses about the involvement of densin-180 in adhesion and initial synapse formation, the role of PSD-95 in NMDA receptor clustering and/or densin-180 clustering at synaptic sites, and the role of the  $\alpha$ CaMKII protein in synapse maturity. The identification of the proteins involved in CNS synapse formation has important biological implications. This information could be useful in studies of synapse formation during brain development, synaptic plasticity in adult brain, and the pathology and treatment of brain diseases.

**REFERENCES**

- Bartlett, W. P. And Banker, G. A. (1984). An electron microscopic study of the development of axons and dendrites by hippocampal neurons in culture. *J. Neurosci.* *4*, 1944-1953.
- Cho, K.-O., Hunt, C. A., and Kennedy, M. B. (1992). The rat brain postsynaptic density fraction contains a homolog of the *Drosophila* discs-large tumor suppressor protein. *Neuron* *9*, 929-942.
- Cotman, C. W., and Kelly, P. T. (1980). Macromolecular architecture of CNS synapses. In *The Cell Surface and Neuronal Function*, C. W. Cotman, G. Poste and G. L. Nicholson, eds. (Amsterdam: Elsevier/North-Holland Biomedical Press), pp. 506-528.
- Gomperts, S. N. (1996). Clustering membrane proteins: it's all coming together with the PSD-95/SAP90 protein family. *Cell* *84*, 659-662.
- Haydon, P. G., and Drapeau, P. (1995). From contact to connection: early events during synaptogenesis. *TINS* *18*, 196-201.
- Kennedy, M. B., Bennett, M. K., and Erondy, N. E. (1983). Biochemical and immunochemical evidence that the "major postsynaptic density protein" is a subunit of a calmodulin-dependent protein kinase. *Proc. Natl. Acad. Sci. USA* *80*, 7357-7361.

Kornau, H.-C., Schenker, L. T., Kennedy, M. B., and Seeburg, P. H. (1995). Domain interaction between NMDA receptor subunits and the postsynaptic density protein PSD-95. *Science* 269, 1737-1740.

Silva, A. J., Stevens, C. F., Tonegawa, S., and Wang, Y. (1992). Deficient hippocampal long-term potentiation in  $\alpha$ -calcium-calmodulin kinase II mutant mice. *Science* 257, 201-206.

**FIGURE LEGENDS**

Figure 4.1. Densin-180 expression is induced during synaptogenesis in the brain.

A. Brain homogenates from E18, P2, P7, P10, P14, P18 and P50 were prepared and 25 micrograms of each were loaded on a 7.5% SDS-polyacrylamide minigel for immunoblot analysis. The densin-180 protein band was visualized with the M2 antibody and an alkaline-phosphatase conjugated goat anti-mouse secondary antibody. B. This panel is adapted from Cho et al. to show the expression of PSD-95 and  $\alpha$ CaMKII in the brain during development. Immunoblots were prepared with brain homogenates as described in Cho et al. The PSD-95 protein was detected with Frances antibody and the  $\alpha$ CaMKII protein was detected with 6G9.

Figure 4.2. Clusters of densin-180 staining form during synaptogenesis in cultured hippocampal neurons. Densin-180 staining of hippocampal neuronal cultures at 3, 5, 9, and 14 days *in vitro* (DIV) is shown. Cells were stained with the M2 anti-densin-180 at a 1:150 dilution and a Cy3-conjugated goat anti-mouse secondary antibody. Images were collected using the Zeiss LSM software with contrast values 410-424 and brightness values were 9650-9700.

Figure 4.3. Densin-180 and synapsin I staining during early synapse formation in culture. This figure shows densin-180 staining with the M2 antibody (red) and synapsin I staining with the Collette antibody staining (green). Secondary antibodies were Cy3 goat anti-mouse and FITC goat anti-rabbit. As shown in (A), cells grown 7 days *in vitro* (DIV) show synapsin I staining in the cytoplasm of axons and in clusters at sites of densin-180

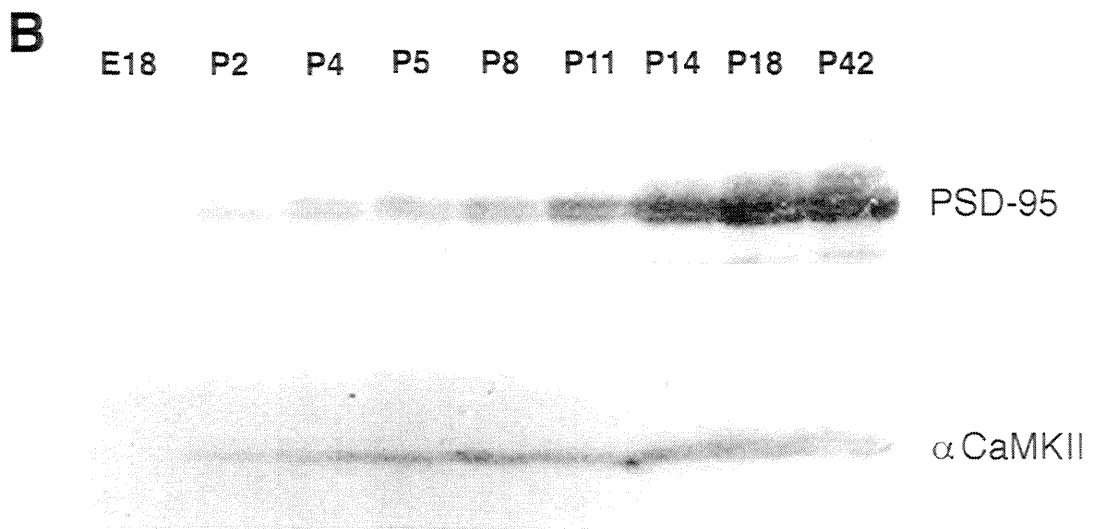
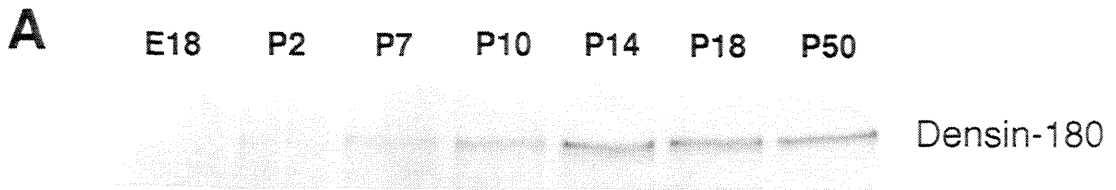
clusters (arrow). Arrowheads denote differences in synapsin axonal staining (top arrowhead) and densin-180 cell body staining (bottom arrowhead). By 9 days *in vitro* (B), more of the synapsin I staining is clustered at sites of densin-180 staining and less synapsin I staining is associated with axons. Arrowheads depict different cell body localizations of synapsin (left arrowhead) and densin-180 (right arrowhead).

Figure 4.4. Densin-180 and PSD-95 staining during early synapse formation in culture. The densin-180 protein is visualized with the CT245 antibody and PSD-95 protein is visualized with 6G6 staining. We used Cy3 goat anti-rabbit and FITC goat anti-mouse secondary antibodies. Densin-180 staining is red and PSD-95 staining is green. Arrows indicate regions of overlapping staining; arrowheads indicate where there is more densin-180 staining relative to PSD-95 (left arrow) or more PSD-95 relative to densin-180 (right arrow). (A) PSD-95 staining is associated with clusters of densin-180 staining at 7 days *in vitro*. These coclusters of double staining increase in number by 9 days after plating (B).

Figure 4.5. Densin-180 and  $\alpha$ CaMKII staining during early synapse formation in culture. The densin-180 protein is visualized with the CT245 antibody (red) and the  $\alpha$ CaMKII staining is visualized with 6G9 staining (green). We used Cy3 goat anti-rabbit and FITC goat anti-mouse secondary antibodies. A double labeled image of cultures fixed at 7 DIV is shown in (A). One cell in this field shows the typical earliest detectable  $\alpha$ CaMKII staining. This staining is present as large aggregates in the cell body (one such aggregate is shown with an arrowhead). All cells in this field stain with anti-densin-180 in the typical pattern for 7 DIV cultures (arrowhead). In (B), there is a single cell with the high cell body

$\alpha$ CaMKII staining usually seen in older neurons (large arrow). However, most cells show the staining pattern of the cell marked with an arrowhead. Small arrows indicate regions of densin clusters that colocalize with  $\alpha$ CaMKII staining.

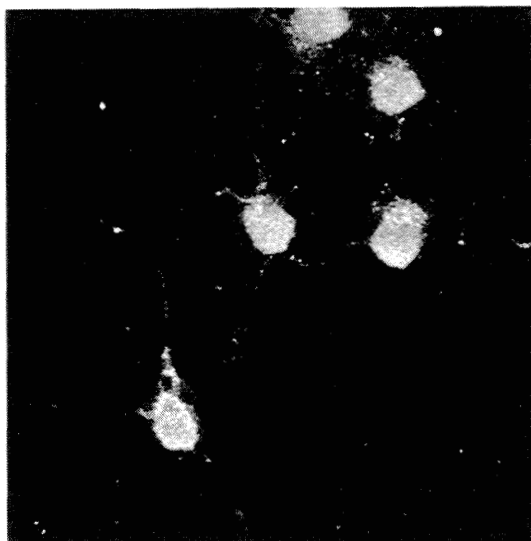
Figure 4.6.  $\alpha$ CaMKII staining is absent from some neurons even after 14 days *in vitro*. Cells were stained with antibodies exactly as described in Figure 4.5. One cell in this image (arrowhead) has the high level of  $\alpha$ CaMKII expression that is typical of most older cultured neurons (4-5 weeks *in vitro*). This staining is highly colocalized with densin-180 clusters along the dendrites of this cell. However, another cell in this image stains with anti-densin-180 but not with anti- $\alpha$ CaMKII (arrow).



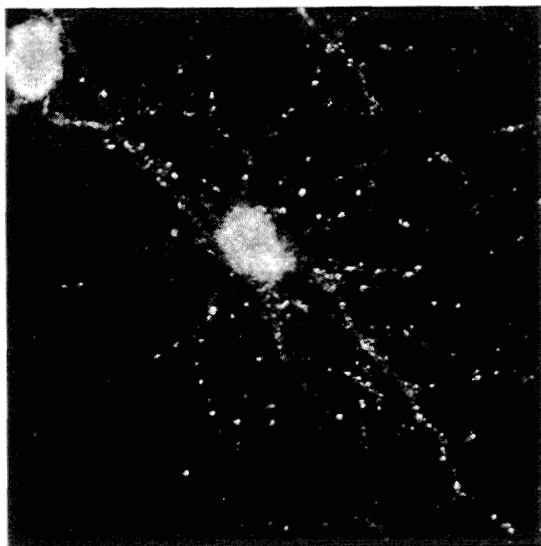
**3 DIV**



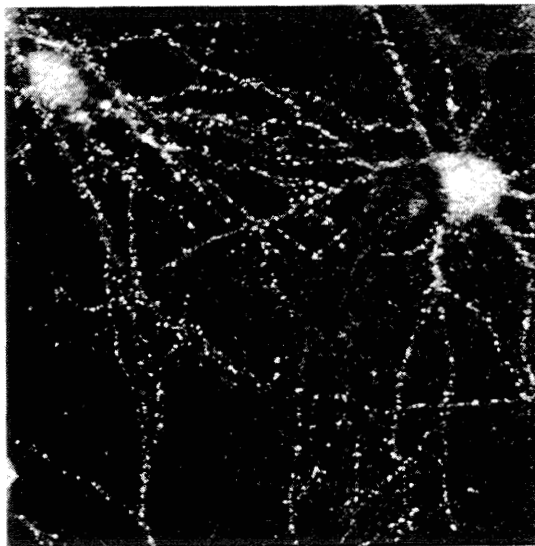
**5 DIV**



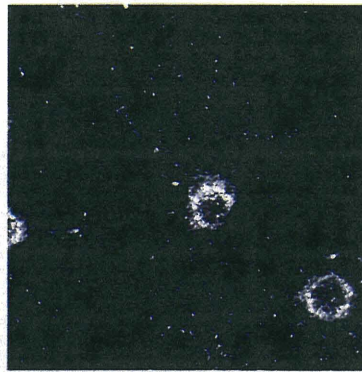
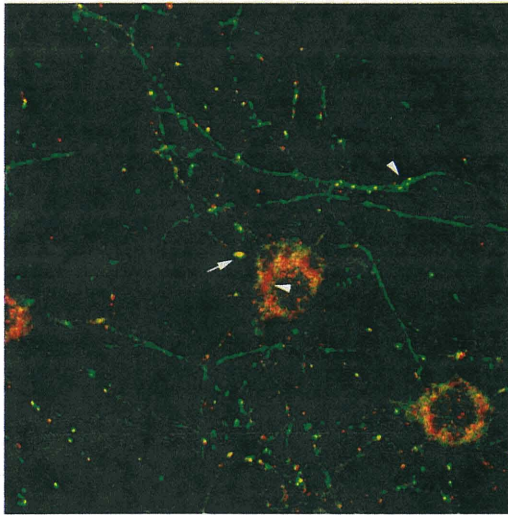
**9 DIV**



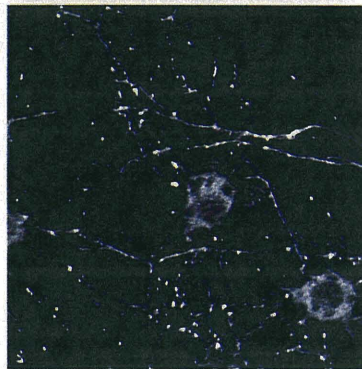
**14 DIV**



**A** 7 DIV



Densin-180  
(red)



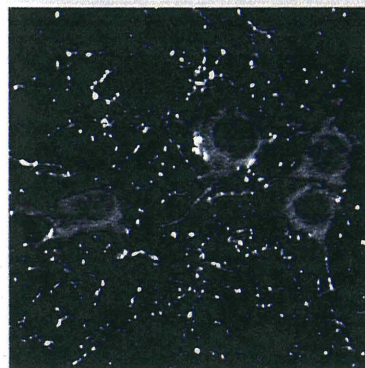
Synapsin I  
(green)

**B**

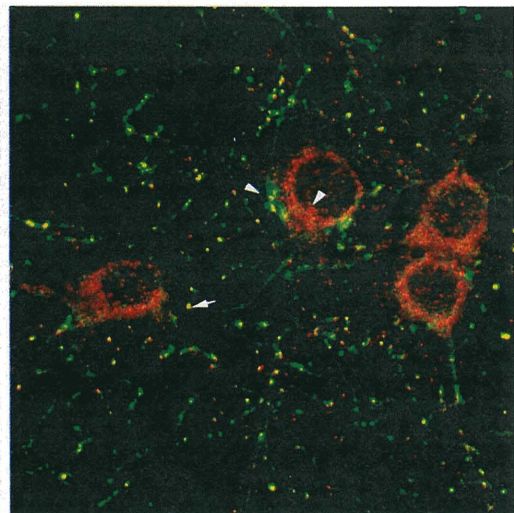
Densin-180  
(red)



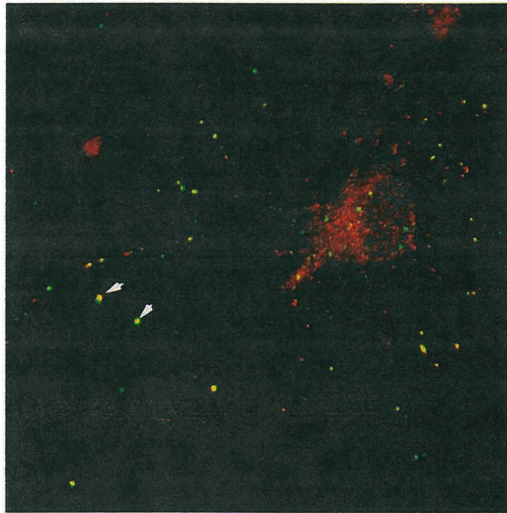
Synapsin I  
(green)



**9 DIV**



**A** 7 DIV



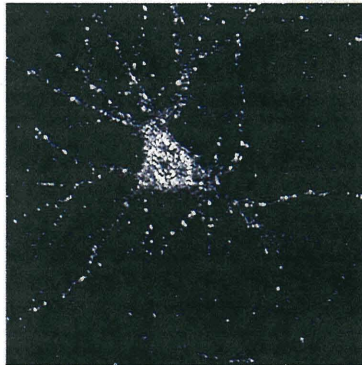
Densin-180  
(red)



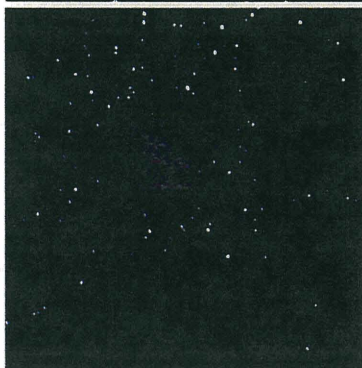
PSD-95  
(green)

**B**

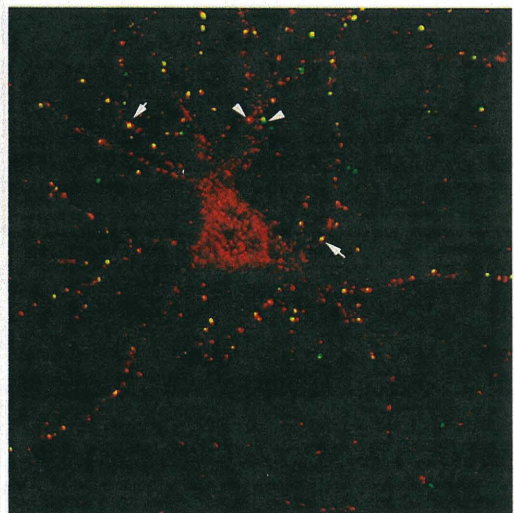
Densin-180  
(red)

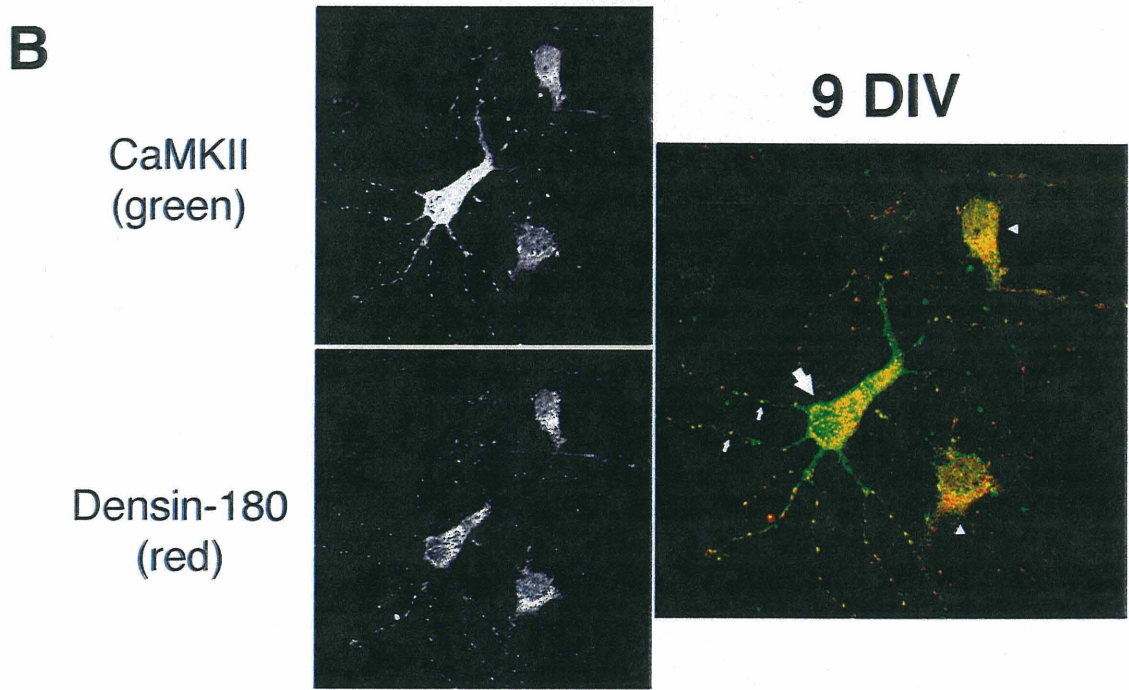
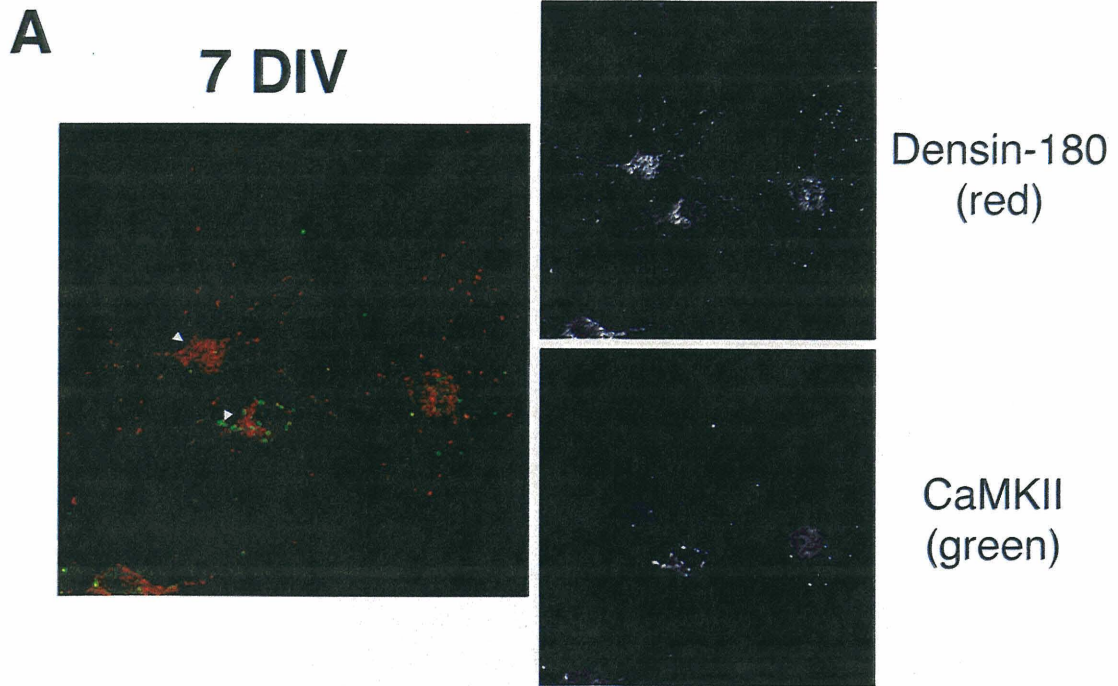


PSD-95  
(green)



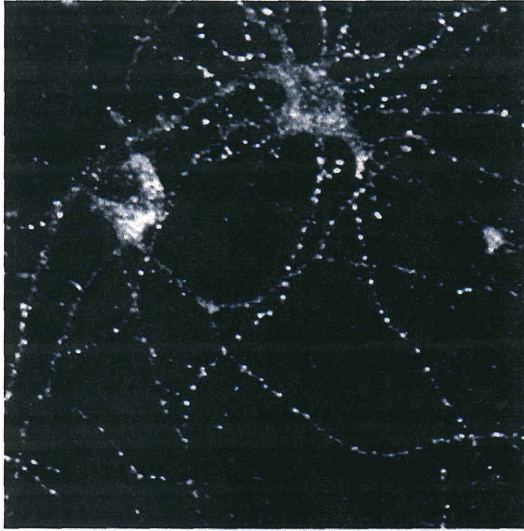
**9 DIV**



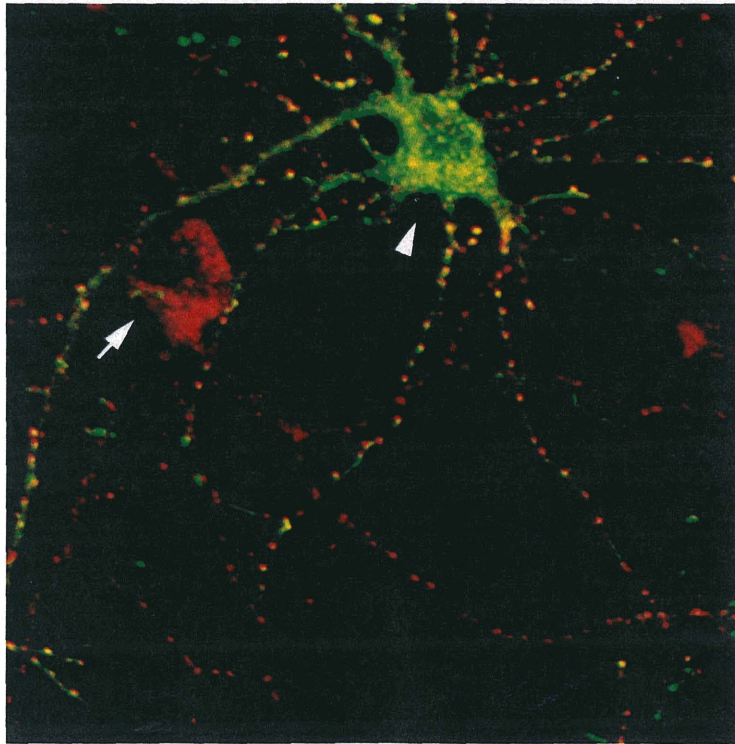


Densin-180  
(red)

CaMKII  
(green)



14 DIV



## **APPENDIX I**

### **Characterization of the specificity of mouse and rabbit anti-densin-180 antibodies**

In this section, I have included some controls that determined the specificity of rabbit (CT245) and mouse (M2) anti-densin-180 antibodies for immunocytochemistry of dissociated hippocampal neuronal cultures.

The materials and methods used for staining with the rabbit and mouse anti-densin-180 antibodies and the conditions used for pre-absorption are described in Chapter 3. Figures I.1 and I.2 show that the punctate clusters, the cell body staining and the patchy membrane staining are all removed by pre-absorption with antigen. Figure I.3 shows that both anti-densin-180 antibodies give identical staining patterns in the same neuron.

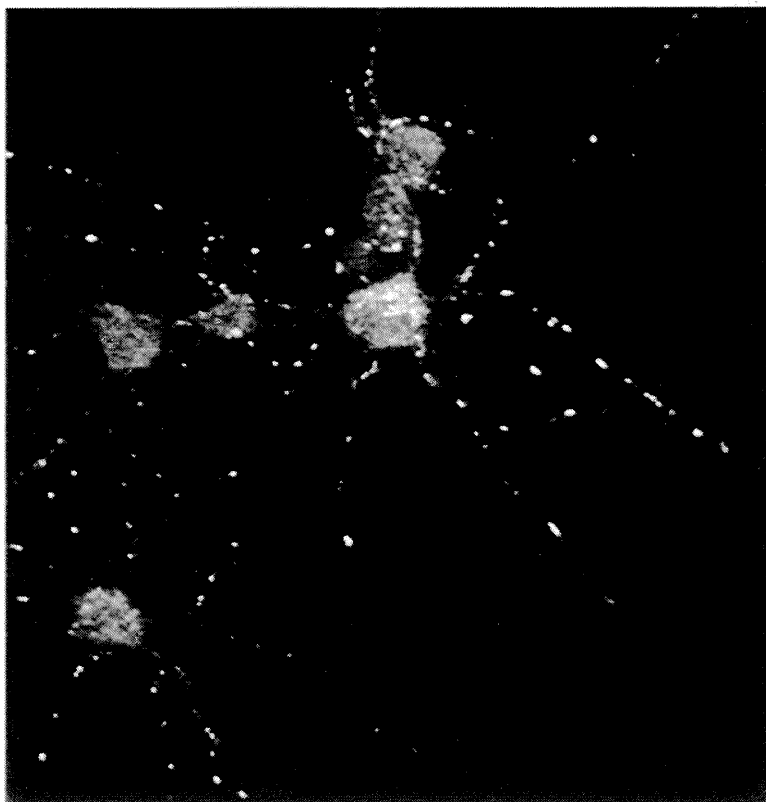
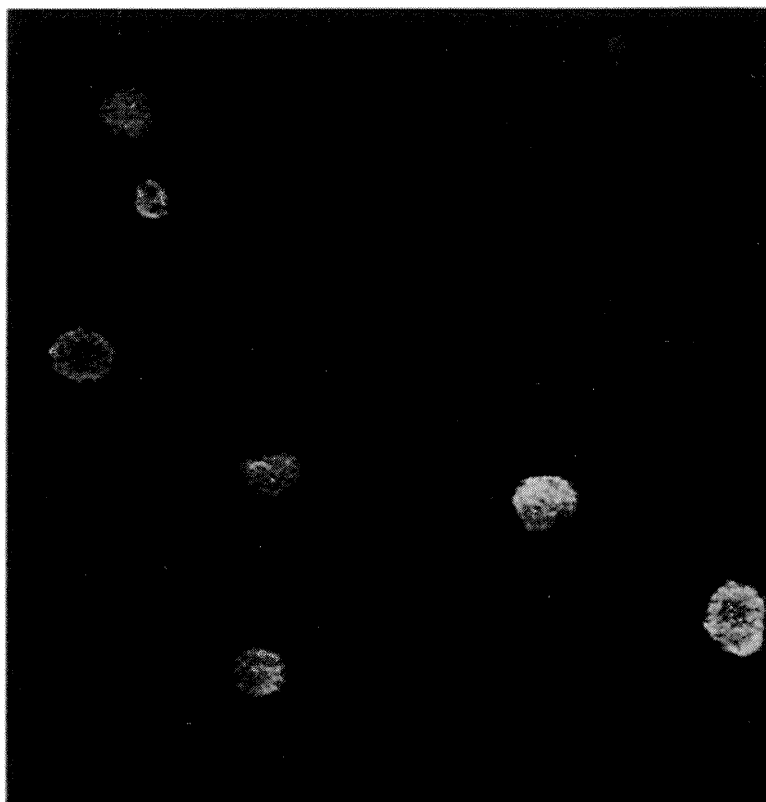
The antibodies raised against the extracellular domain (M2) and the cytoplasmic domain (CT245) of densin-180 could be used for double-labeled immuno-electron microscopy. These antibodies could determine whether the domains of densin-180 are extracellular, presynaptic or postsynaptic. The inset in Figure I.3 shows that we cannot make this determination at the resolution of the light microscope.

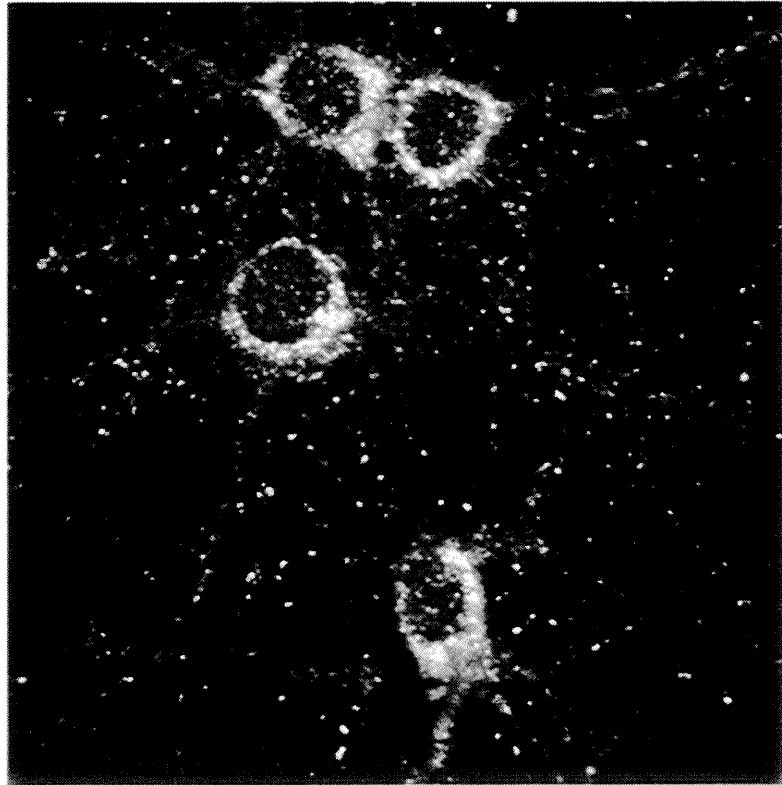
**FIGURE LEGENDS**

Figure I.1. M2 staining (bottom panel, 63X, zoom=1) and pre-absorbed M2 staining (top panel, 63X, zoom=1) of cultured hippocampal neurons at 9 days *in vitro*. Pre-absorption removes all of the membrane and punctate staining but a slight background in the cell body remains.

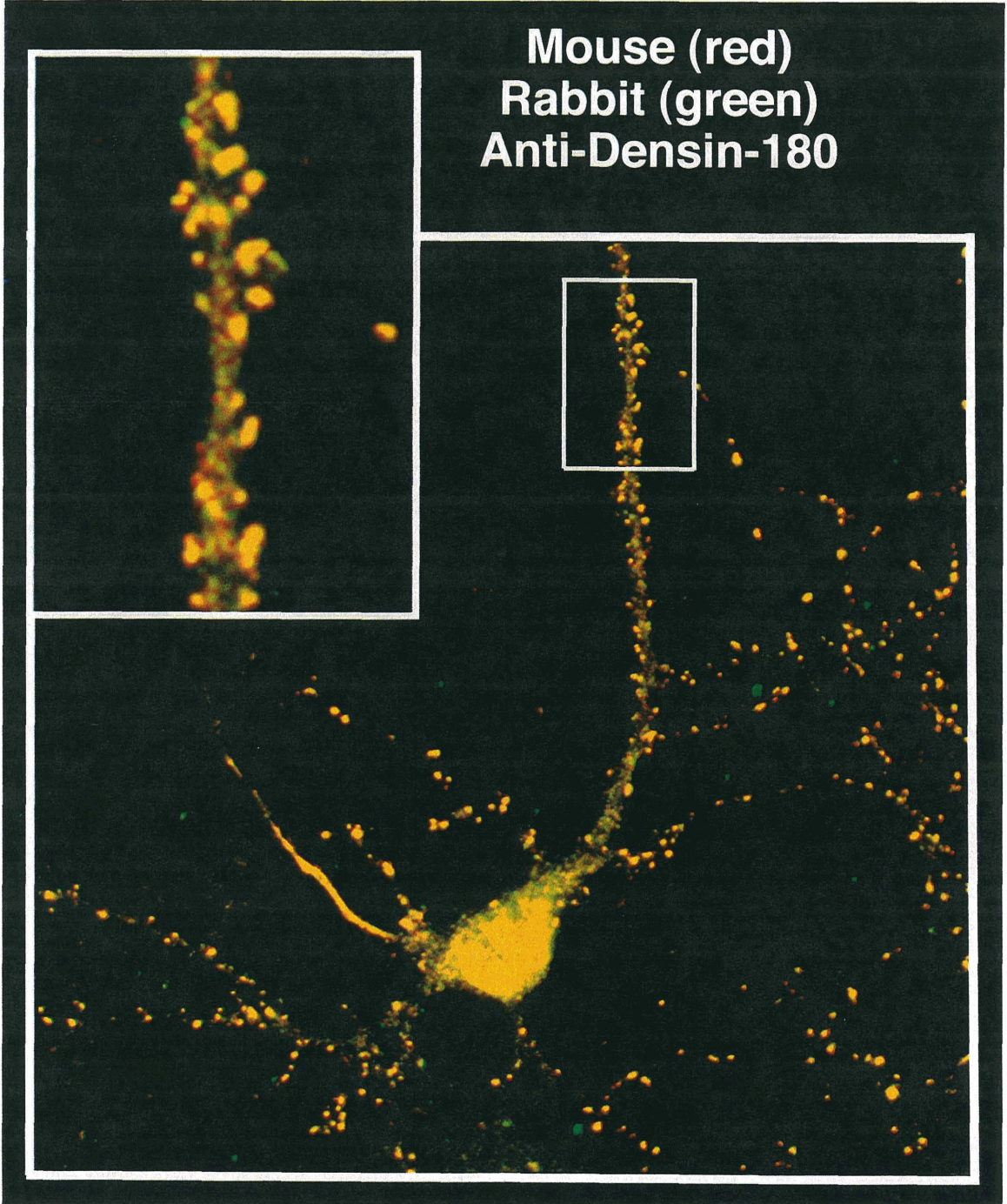
Figure I.2. CT245 staining (bottom panel, 63X, zoom=1.5) and pre-absorbed CT245 staining (top panel, 63X, zoom=1) of cultured neurons at 9 days *in vitro*. The membrane, punctate and variable cell body staining patterns are removed by pre-absorption.

Figure I.3. M2 and CT245 anti-densin-180 double-labeling of cultured hippocampal neurons that were fixed after 14 days *in vitro*.





**Mouse (red)**  
**Rabbit (green)**  
**Anti-Densin-180**



## **APPENDIX II**

### **Brain immunocytochemistry using mouse and rabbit anti-densin-180 antibodies**

I used the M2 and CT245 anti-densin-180 antibodies to stain 50  $\mu\text{m}$  sections from fixed rat brains. For the immunocytochemistry of fixed brain tissue, rats were perfused with fixative (4% paraformaldehyde/0.2% glutaraldehyde/0.1 M NaPO<sub>4</sub> buffer). Next, brains were removed and post-fixed. At 2 hours after the initial perfusion, brains were placed in ice-cold PBS (20 mM NaPO<sub>4</sub>, pH 7.4, 0.9% NaCl). 50 micron sections were made using a vibrotome in an ice-cold chamber filled with PBS. Sections were permeabilized with 0.7% Triton X-100 in PBS for 1 hour at room temperature, rinsed twice with PBS, blocked with 0.1 M glycine in PBS and rinsed twice with water. After a 10 minute incubation, cells were rinsed twice with water and pre-blocked in pre-block buffer (see Chapter 3) for 2 hours. All subsequent antibody incubations and mounting procedures were exactly as described for cultures in Chapter 3, except that wash times were increased to 30 minutes each.

At low magnifications, densin-180 staining with the M2 antibody can be seen throughout the neuropil in the hippocampus, thalamus and cortex regions of the brains of 5 and 10 week old rats (data not shown). At higher power, there is punctate staining in the neuropil of various brain regions that is likely to correspond to synapse staining. In addition, a certain type of neuron stains for densin-180 all over the membrane surface and cell body. A large number of these cells are found throughout the thalamus, brainstem and spinal cord. In addition these “surface-staining” cells represent a small population of neurons scattered throughout the cortex and hippocampus. Lastly, purkinje cells in the cerebellum have a very high cell surface densin-180 staining. All of the staining described disappears after preabsorption of the M2 antibody with antigen (data not shown).

Figure II.1 shows the molecular layer of the hippocampal CA3 region from a 5 week old rat that has been double-labeled with the M2 anti-densin-180 and Frances anti-

PSD-95 antibodies. The primary antibodies were visualized with an FITC-conjugated goat anti-mouse and CY3-conjugated goat anti-rabbit secondary antibodies. The morphology of several “surface-staining” densin-180 positive cells can be seen at higher magnifications (Figure II.1, CA3 region and Figure II.2, CA1 region). Often, these neurons have small cell bodies, thin processes and do not stain with anti-PSD-95 antibodies. The densin-180 staining of these neurons is reminiscent of the staining seen in younger neurons in culture that also do not yet express PSD-95 (see Chapter 4). It is possible that anti-densin-180 stains undifferentiated neurons in the hippocampus that have not formed glutamatergic synapses. This is supported by the observation that the densin-180-positive/PSD-95-negative neurons are rarely found in the cell body layers of the hippocampus that usually contain mature pyramidal neurons.

In many of our double-labeled images, there are thin processes that have high densin-180 staining throughout the membrane surface, but no PSD-95 staining. One possibility is that this staining corresponds to the dendritic filopodial extensions viewed developing in “real time” in hippocampal slice cultures (Dailey and Smith, 1995). There is also electron microscopic evidence for similar dendritic extensions in the brain (Saito et al., 1990).

The CT245 anti-densin-180 antibody staining was more variable than the M2 anti-densin-180 staining, possibly due to sensitivity of the epitopes to fixative or incomplete permeabilization. However, I was able to detect synapse-like staining in the CA1 region of the 10 week old rat brain (Figure II.3). Also shown is process that extends through the molecular layer and contains both the high membrane surface staining and the punctate staining associated with synapses (Figure II.3, see left side of inset). A process that does not have the high membrane-associated densin-180 staining but does contain a number of

synapses along its length is shown for comparison (Figure II.3, see right side of inset). I hope to determine fixation and permeabilization conditions that give consistent specific staining with the CT245 antibody. Eventually, the mouse and rabbit anti-densin antibodies could be used for double-labeling to localize densin-180 at the synapse by electron microscopy and confirm the transmembrane orientation described in Chapter 3.

In Chapter 4, I put forward the hypothesis that densin-180 is expressed on the membrane surface of young neurons in culture where it may mediate adhesion and neurite outgrowth. During synapse formation in these neurons, the densin-180 cell body and membrane surface staining that is typical of younger neurons becomes clustered at synaptic sites. Interestingly, the anti-densin-180 staining of fixed rat brains is consistent with the staining we have seen in cultured neurons. Densin-180 antibodies reveal a punctate, synapse-like pattern of staining in the neuropil. Additionally, a subset of neurons have high cell body staining and membrane staining typical of immature neurons in culture. The similarities between the densin-180 staining of dissociated hippocampal cultures and of the adult rat hippocampus suggests that there may be dynamic mechanisms of neurite outgrowth and synapse formation that persist in the adult brain. Lastly, the high densin-180 staining of thin filopodia-like processes in the hippocampus suggests a role for densin-180 in the dynamics of synapse formation.

**REFERENCES**

Dailey, M. E. and Smith, S. J. (1996). The dynamics of dendritic structure in developing hippocampal slices. *J. Neurosci.*, *16*, 2983-2994.

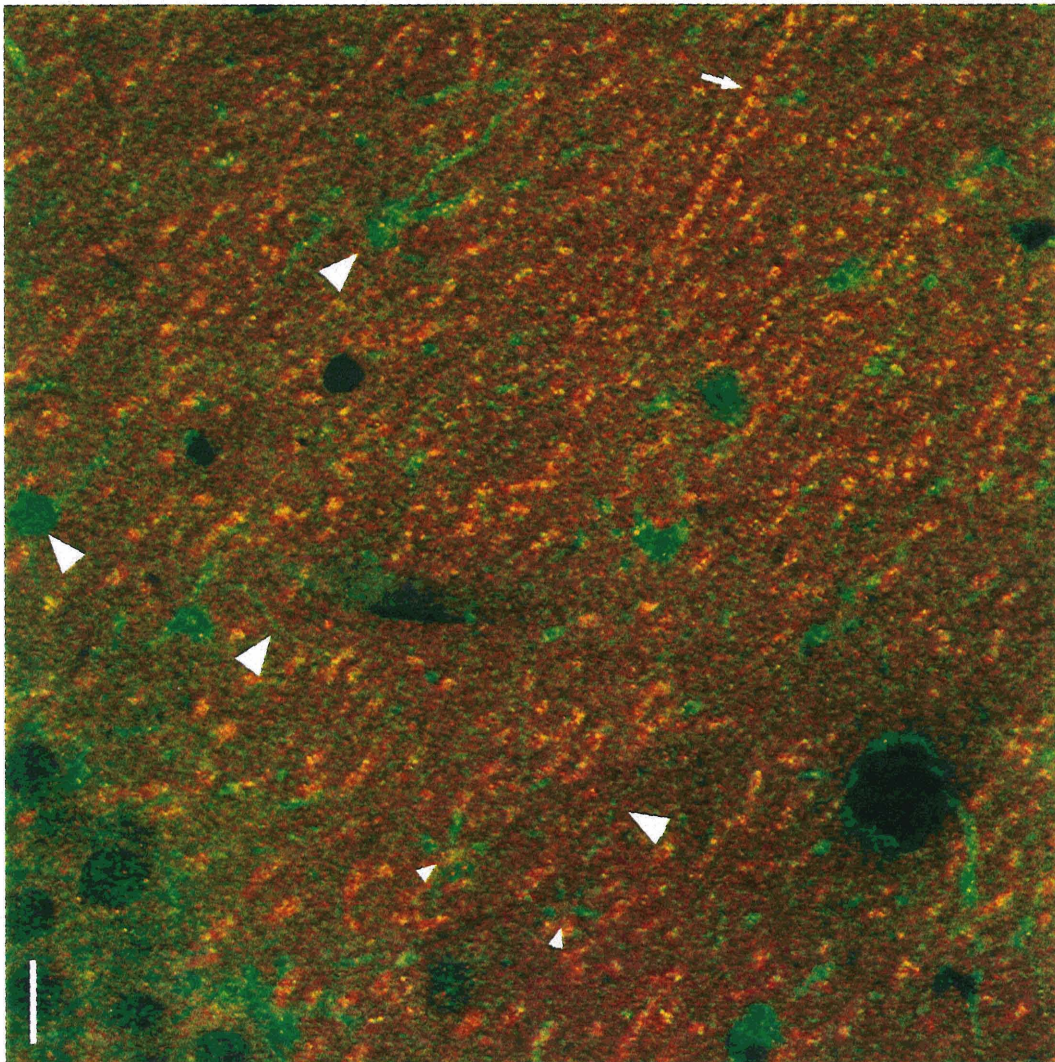
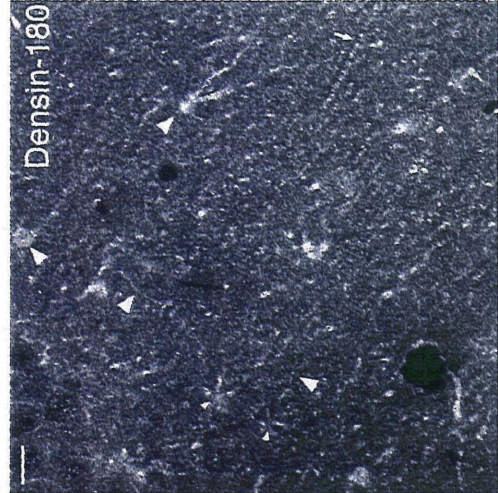
Saito, Y., Murakami, F., Song, W.-J., Okawa, K., Shimono, K., and Katsumaru, H. (1992). Developing corticorubral axons of the cat form synapses on filopodial dendritic protrusions. *Neurosci. Lett.* *147*, 81-84.

**FIGURE LEGENDS**

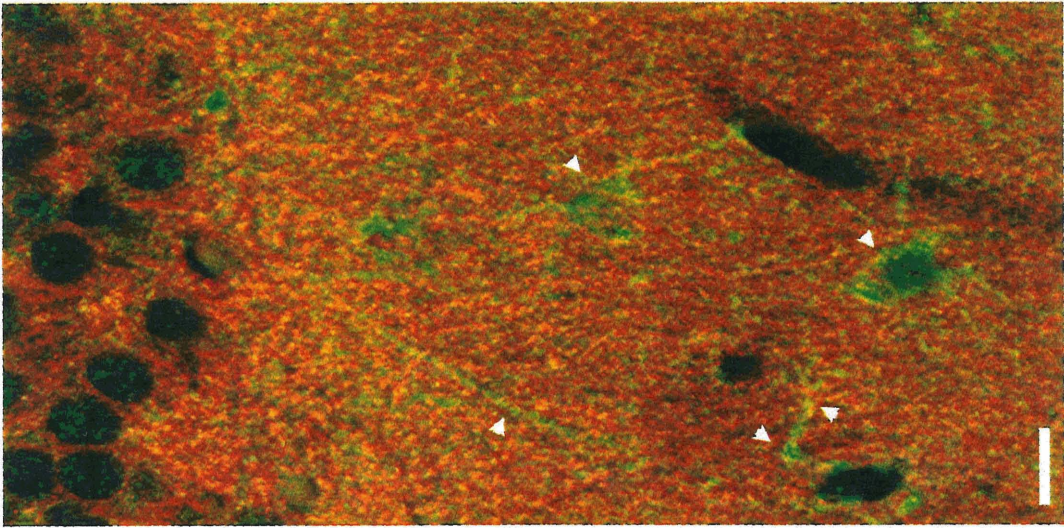
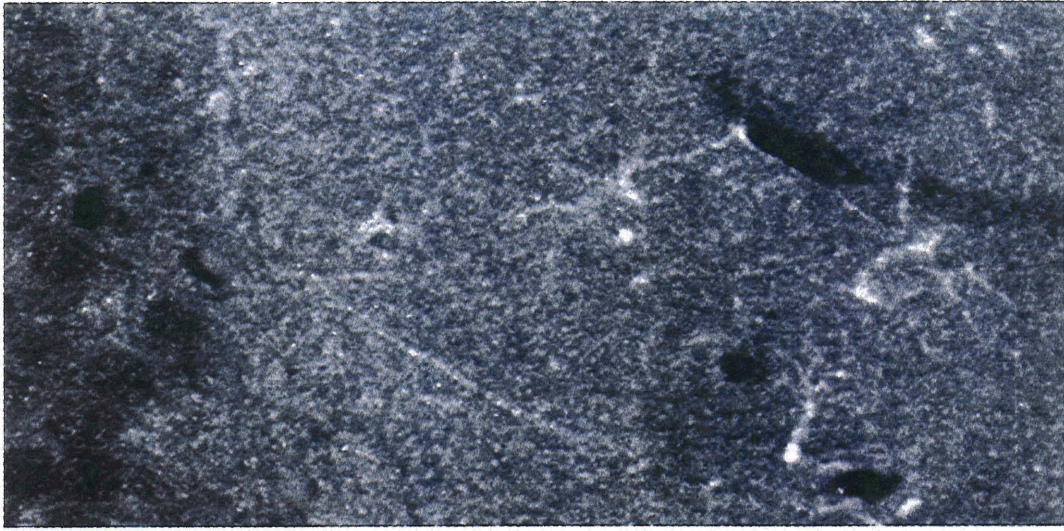
Figure II.1. Densin-180 (green) and PSD-95 (red) double labeling of the molecular layer in the CA3 region of the hippocampus. The cell body layer is at the upper left corner of the image. Cells and thin processes that stain for densin-180 and not for PSD-95 are shown with arrowheads. Star-shaped structures that are often stained with the M2 anti-densin-180 antibody are shown with smaller arrowheads. A dendrite that stains for both PSD-95 and densin-180 is indicated with an arrow. Scale bar, 15  $\mu\text{m}$ .

Figure II.2. Densin-180 (green) and PSD-95 (red) double-labeling of the molecular layer in the CA1 region of the hippocampus. Cells and processes that stain for densin-180 and not for PSD-95 are shown with arrowheads. Scale bar, 10  $\mu\text{m}$ .

Figure II.3. Montage of two 63X images of CT245 anti-densin-180 staining in the CA1 region of the hippocampus. A long “surface-staining” process is shown with arrows. The inset compares this process (left) with another dendrite (right) that lacks “surface-staining.” Synapse-like staining is shown with arrows and arrowheads on the inset. Scale bar, 15  $\mu\text{m}$ .

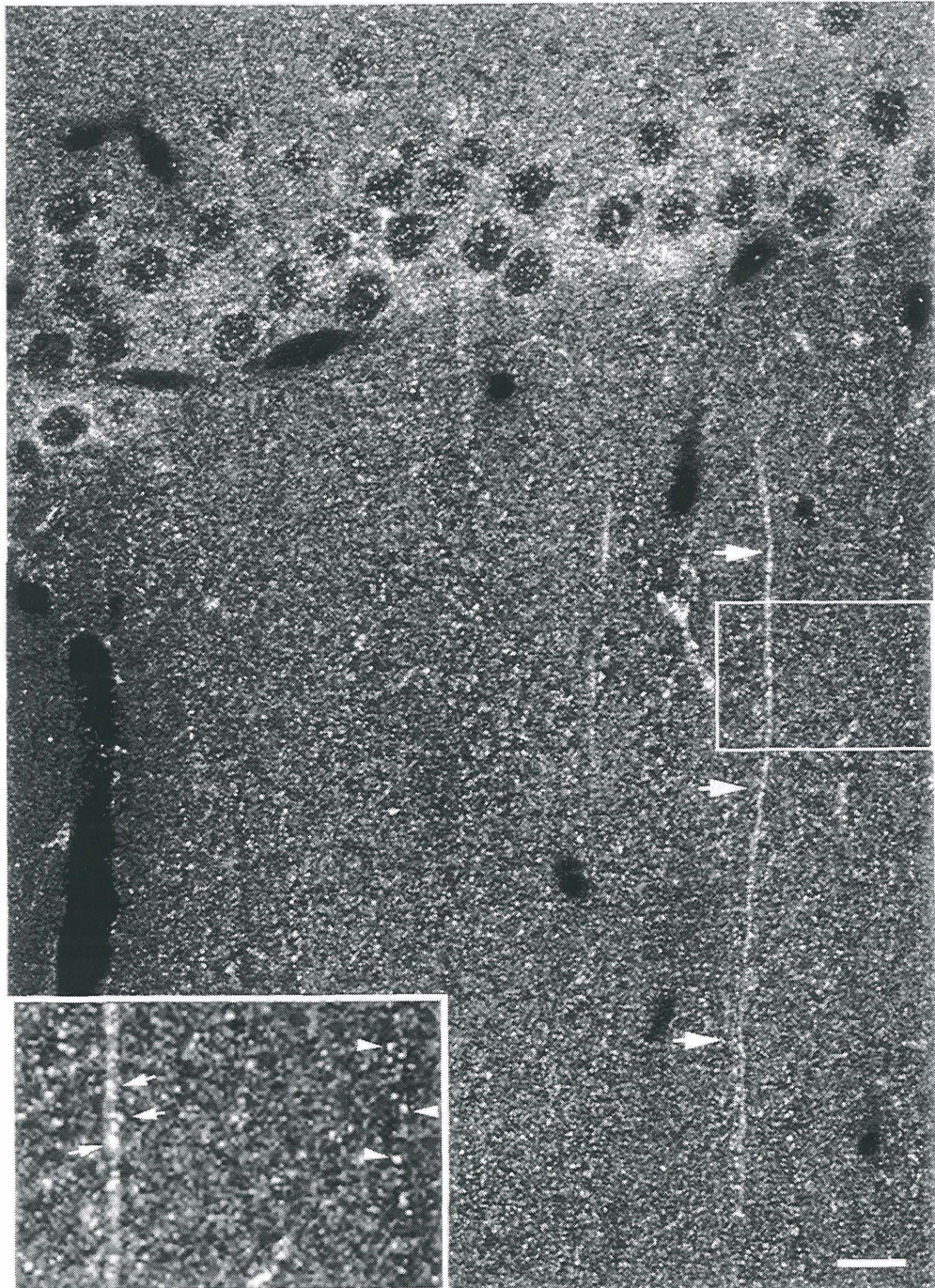


Densin-180 (green)



PSD-95 (red)





## **APPENDIX III**

### **Identification of citron in the PSD fraction**

In Chapter 3, I described the cloning of densin-180 based on peptide sequences obtained from the “PSD-up180” protein band in the PSD fraction (Chapter 2). However, only three out of seven peptide sequences obtained from the PSD-up180 band were found in the densin-180 peptide sequence. I recently performed a BLAST search of the database through the National Center for Biotechnology Information using the amino acid sequences of the other four PSD-up180 peptides (Fig. III.1). The BLAST search revealed that all four peptide sequences were identical to citron, a novel protein that binds to RhoA, RhoB, RhoC, and Rac1, members of the Ras-related small GTP-binding proteins.

Citron is a novel protein that was cloned using the yeast two-hybrid system with RhoC as bait (Madaule et al, 1995). Twenty clones from a mouse embryo cDNA library were obtained, but only one clone displayed strong reactivity with GTP-bound forms of RhoC and RhoA in overlay assays and was termed citron. Using polyhistidine or glutathione-S-transferase (GST) tagged proteins, Madaule et al. also found that citron binds to RhoA, RhoB, RhoC and Rac1 in a GTP-dependent manner *in vitro*.

The predicted amino acid sequence of citron contains several motifs found in signal transduction molecules and cytoskeletal elements. The N-terminal region of citron is made up of a large coiled-coil region that is distantly related to myosin and may mediate dimerization of citron. Next, a plekstrin-homology (PH) domain was identified in the citron sequence. PH domains are found in a number of proteins and are thought to mediate protein-protein and/or protein-membrane interactions (for reviews, see Shaw, 1996 and Gibson et al., 1994). PH sequences are found in a number of proteins thought to be involved in the regulation of small G proteins, including sos (Son of Sevenless), Ras-GAP (GTPase activator for Ras) and Ras-GRP (guanine nucleotide release factor for Ras) (for a list of other PH-containing proteins, see Shaw, 1996). Citron also contains a ring-H2

finger, a cysteine-rich motif similar to the zinc finger domain. Interestingly, protein kinase C also contains PH and ring-H2 finger domains and both motifs are thought to mediate binding to lipid second messengers. Lastly, at the C-terminus, there is a proline-rich SH3 binding motif and a terminal SXV (tSXV) motif (Kornau et al., 1995). The association of citron with the PSD fraction might be mediated by the binding of citron's proline-rich domain to the SH3 domain of PSD-95 and/or PSD-95 binding to the citron tSXV sequence.

I performed a BLAST network search using the published citron sequence to identify homologs. This identified some sequence similarities with three recently cloned Rho associated kinases: ROK $\alpha$  (RhoA-binding kinase, Leung et al., 1995), p160<sup>ROCK</sup> (Ishizaki et al., 1996) and Rho-kinase (Matsui et al, 1996). First, ROK $\alpha$  was cloned from a rat brain expression library probed with GTP-bound RhoA (Leung et al, 1995). ROK $\alpha$  is a 150 kDa protein that contains an N-terminal serine/threonine kinase domain that is most similar to the human myotonic dystrophy kinase. This domain is followed by a coiled-coil forming region and a PH domain that contains a ring-H2 domain insert in the loop between PH subdomains V and VI. Inserts in this position have also been identified in several PH domains of other proteins (Gibson et al., 1994). A comparison of the domain structures of ROK $\alpha$  and citron are shown in Figure III.2.

A second Rho-associated kinase has recently been cloned from mouse and termed p160<sup>ROCK</sup>. More recently, a third Rho binding kinase termed Rho-kinase was cloned from bovine brain (Matsui et al, 1996). Rho-kinase and ROK $\alpha$  are probably bovine and rat homologs of the same protein, as both are expressed in brain, migrate at the same apparent molecular weight on SDS-PAGE gels, and 96% of their amino acid sequences are identical. p160<sup>ROCK</sup> is probably an isoform of this family of proteins that is not

expressed in the brain.

The Rho binding domains in citron and ROK $\alpha$  were identified as the smallest positive cDNA clones identified in the initial cloning screens. These regions are shown in Figure III.2. In both cases, the Rho binding domain is partially overlapping with the C-terminal portion of the coiled-coil domain and the amino acid sequences of these domains were unlike any Rho binding domains previously identified in other proteins. I compared the sequences of citron and ROK $\alpha$  and found that the Rho binding domains are partially overlapping with 37% similarity and 21% identity over 70 amino acids (Fig. III.3a). The comparatively low overall homology between citron and ROK $\alpha$  suggests that the similarities in the Rho binding domains might reflect binding to the same brain-specific Rho-like protein. A comparison of the Rho binding domains of ROK $\alpha$  and the homologous region of p160<sup>ROCK</sup> is shown in Figure III.3b. Despite a high degree of homology in this region (73% similar and 59% identical residues), three gaps were placed in the sequences during the alignment. One possibility is that slight differences among these potential Rho-binding sequences are important for specificity of binding to particular Rho isoforms. The tissue-specific expression patterns of these proteins suggest that ROK $\alpha$ , Rho-kinase and citron bind to brain specific Rho-like proteins and p160<sup>ROCK</sup> binds to Rho proteins in other tissues.

## DISCUSSION

The Rho and Rac families of small GTPases control a variety of actin-dependent cellular processes in many different organisms (Hall, 1990). Some of these processes include tip growth of pollen tubes (Lin et al., 1996), budding in yeast (Mischke and Chant, 1995), and membrane ruffling in MDCK cells (Takaishi et al., 1995). Recently, transgenic mice were generated that expressed a constitutively active human Rac1 in Purkinje neurons that produces a dominant negative phenotype in *Drosophila* (Luo et al., 1996). One of the largest defects in these mutant mice was severe ataxia accompanied by a reduction in the size of spines formed in mutant Purkinje neurons. One possibility is that small GTP-binding proteins are important for the cytoskeletal rearrangements involved in the extension of spines from the dendritic shaft to meet the axon terminal.

In conclusion, I have identified citron as a component of the PSD fraction. Citron may be a target for the signal transduction mediated by small GTP-binding proteins at the synapse. Citron also contains motifs of a new class of Rho-binding proteins that includes the brain ROK $\alpha$  and Rho-kinase, as well as their homolog that is absent from brain, p160<sup>ROCK</sup>. The location of the Rho-binding domain near the end of a coiled-coil region raises the possibility that citron is a molecular motor that is coupled to GTP hydrolysis. Another possibility is that Rho binding translocates citron to the membrane as has been shown for ROK $\alpha$  and Rho-kinase in heterologous expression systems (see Leung et al., 1995 and Matsui et al., 1996).

In conclusion, the information presented here suggests a role for citron in synaptic functions mediated by Ras-like small GTPases, such as the proposed morphological changes that underlie spine formation and synaptic plasticity.

**REFERENCES**

- Gibson, T. J., Hyvonen, M., Musacchio, A., Saraste, M., and Birney, E. (1994). PH domain: the first anniversary. *TIBS* 19, 349-353.
- Hall, A. (1990). The cellular function of small GTP-binding proteins. *Science* 249, 635-637.
- Ishizaki, T., Maekawa, M., Fujisawa, K., Okawa, K., Iwamatsu, A., Fujita, A., Watanabe, N., Saito, Y., Kakizuka, A., Morii, N., and Narumiya, S. (1996). The small GTP binding protein Rho binds to and activates a 160 kDa Ser/Thr protein kinase homologous to myotonic dystrophy kinase. *EMBO J.* 15, 1885-1893.
- Leung, T., Manser, E., Tan, L., and Lim, L. (1995). A novel serine/threonine kinase binding the Ras-related RhoA GTPase which translocates the kinase to peripheral membranes. *J. Biol. Chem.* 270, 27-34.
- Lin, Y., Wang, Y., Zhu, J.-K., and Yang, Z. (1996). Localization of a Rho GTPase implies a role in tip growth and movement of the generative cell of pollen tubes. *The Plant Cell* 8, 293-303.
- Luo, L., Hensch, T.K., Ackerman, L., Barbel, S., Jan, L.Y., and Jan, Y.N. (1996). Differential effects of the Rac GTPase on Purkinje cell axons and dendritic trunks and spines. *Nature* 379, 837-840.

Matsui, T., Amano, M., Yamamoto, T., Chihara, K., Nakafuku, M., Ito M., Nakano, T., Okawa, K., Iwamatsu, A., and Kaibuchi, K. (1996). Rho-associated kinase, a novel serine-threonine kinase, as a putative target for the small GTP binding protein Rho. *EMBO J.* *15*, 2208-2216.

Madaule, P., Furuyashiki, T., Reid, T., Ishizaki, T., Watanabe, G., Morii, N., and Narumiya, S. (1995). A novel partner for the GTP-bound forms of *rho* and *rac*. *FEBS Lett.* *377*, 243-248.

Mischke, M.D. and Chant, J. (1995). The shape of things to come: morphogenesis in yeast and related patterns in other systems. *Can. J. Bot.* *73*, S234-S242.

Shaw, G. (1996). The pleckstrin homology domain: an intriguing multifunctional protein module. *BioEssays* *18*, 35-46.

Takaishi, K., Sasaki, T., Kameyama, T., Tsukita, S., Tsukita, S., and Takai, Y. (1995). Translocation of activated Rho from the cytoplasm to membrane ruffling area, cell-cell adhesion sites and cleavage furrows. *Oncogene* *11*, 39-48.

## FIGURE LEGENDS

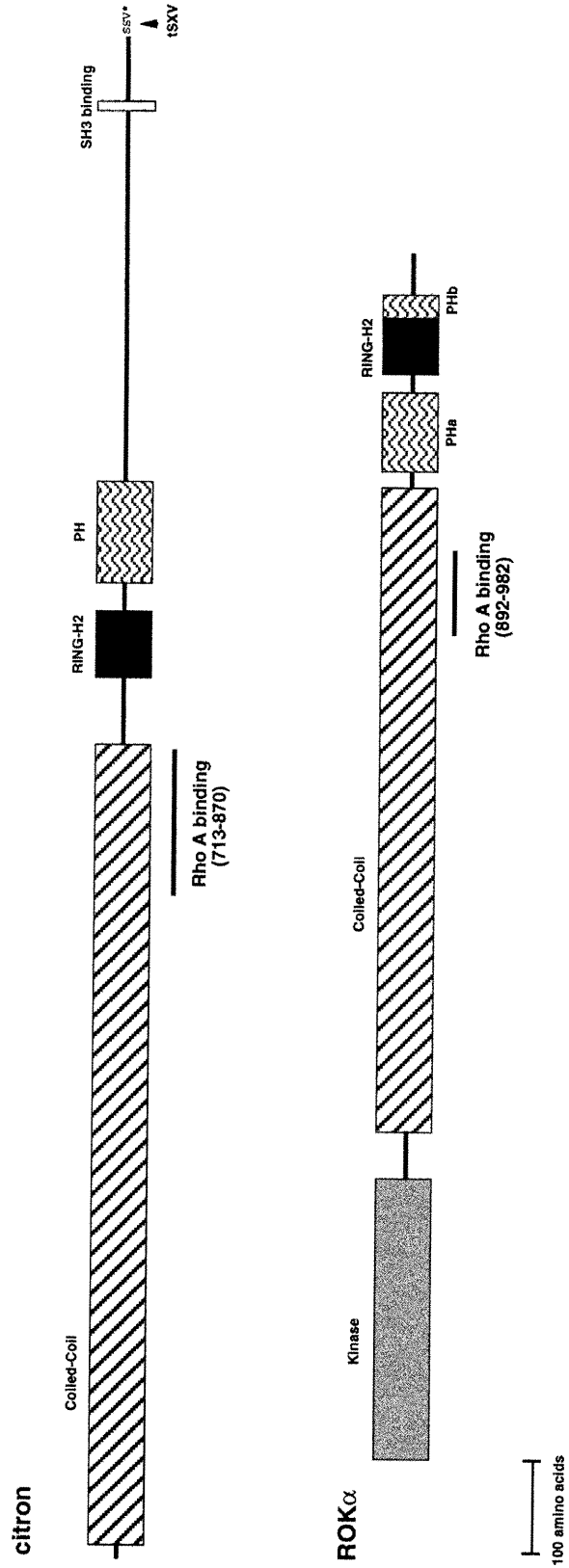
Figure III.1. Amino acid sequences of four PSD-up180 tryptic peptides are identical to citron. Twice-HPLC purified tryptic peptides were sequenced from peaks 12, 18, 24 and 27 of the second HPLC runs. Ambiguities in the peptide sequences are denoted by X. Initial yields of the first amino acid in each sequence were as follows: peak 18, 11.43 pmoles; peak 24, 8.07 pmoles; peak 27, 22.64 pmoles. Tube contamination resulted in ambiguities in the first four cycles in the sequence of peak 12, and the yield of the fifth amino acid (Val) was 1.06 pmoles. Shown below each PSD-up180 peptide sequence is the corresponding sequence in citron (amino acid numbers are shown at sides).

Figure III.2. Comparison of the domain structures of citron and ROK $\alpha$ . Coiled-coil forming regions (*boxes with diagonal lines*) and ring-H2 fingers (*black boxes*) are shown for both proteins. A complete pleckstrin homology (PH) domain is shown in citron and a broken PH domain is shown in ROK $\alpha$  (*boxes with wavy lines*). In citron, the SH3 binding motif is depicted as a *white box* and the terminal SXV motif is shown at the C-terminus. In ROK $\alpha$ , the serine/threonine kinase domain at the N-terminus is shown as a *gray box*. Unique sequences of each protein are shown by *thin black lines*.

Figure III.3. Sequence comparisons of Rho binding domains. A. Comparison of the overlapping sequences found in the Rho/Rac binding domain of citron and the Rho binding domain of ROK $\alpha$ . Black bars indicate the extent of the Rho binding domains mapped for each protein. B. The same region of ROK $\alpha$  is compared with Rho-kinase (Rho-K) and p160<sup>ROCK</sup>. ROK $\alpha$  and RhoK are identical except for a single amino acid in each (boxed

residue). Identical residues (black) and conservative substitutions (gray) are shown for the sequence alignments between citron and ROK $\alpha$  or between Rho-K and P160<sup>ROCK</sup>.





A

citron 709- **KKHAMLEMNARSIQQKLETERELKQRLEEQAQLQQQMDLQKNHIFRITQGLQALDRADLKERSDLEYQL**-781  
ROK $\alpha$  922- **DEEISAAAIKAQFEKQLL TERTLKTQAVNKLAEIMNRKE--PVKRGSDTVRRKEKENRKLHMEKSEREKL TQQM**-995

B

ROK $\alpha$  922- **DEEISAAAIKAQFEKQLL TERTLKTQAVNKLAEIMNRKE--PVKRGSDT--VRRKEKENRKLHMEKSEREKL TQQM**  
Rho-K 978- **DEEISAAAIKAQFEKQLL TERTLKTQAVNKLAEIMNRKE--PVKRGSDT--VRRKEKENRKLHMEKSEREKL TQQM**  
p160<sup>ROCK</sup> 978- **DEEISN--LKAQFEKNI TERTLKTQAVNKLAEIMNRKDFKIDRKKANTQDRRKEKENRKLQELNQEREKFNQM**